الجمهورية الجـزائـرية الديمـقـراطـيـة الـشـعـبـية
REPUBLIQUE ALGERIENNE DEMOCRATIQUE ET POPULAIRE
وزارة التـعـليـم العـالي و البـحث العـلـمـي
Ministère de l'Enseignement Supérieur et de la Recherche Scientifique
جـامعة أبي بـكـر بـلـقـا يـد– تـلمسان
Université Aboubakr Belkaïd– Tlemcen
كلية التكنلوجيا
Faculté de TECHNOLOGIE

THESE

Présentée pour l'obtention du **grade** de **DOCTEUR EN SCIENCES**

En : Electronique

Spécialité : Electronique

Par : BOUDKHIL Abdelhakim

Sujet

Computational Electromagnetic Characterization of Complex THz Antennas based on MEMS Technology

Soutenue publiquement le 03 Novembre 2018, devant le jury composé de :

Mr Meriah Sidi Mohammed	Professeur	Univ. Tlemcen	Président
Mr Benahmed Nasreddine	Professeur	Univ. Tlemcen	Directeur de thèse
Mme Benabdallah Nadia	MCA	ESSAT	Co-Directeur de thèse
Mr Merad Lotfi	Professeur	ESSAT	Examinateur 1
Mr Lasri Boumedienne	Professeur	Univ. Saida	Examinateur 2

Acknowledgements

First and foremost, praise is to Allah who granted me the faculty of reasoning and patience to achieve this research through which I wish my beloved family find the expression of my sincere gratitude for their support all along my career.

My thanks go also to my supervisors, jury members and colleagues who contributed to the success of this work…

...thank you all

Abstract

The very special demand for new integrated antennas with excellent performance for diverse terahertz (THz) frequency ranges grows for the foreseeable future, and requires effective electromagnetic (EM) optimization techniques of enhancing already established designs or developing newly proposed models. Recently, micro-electromechanical system (MEMS) processing has been identified as a very promising technology for revolutionizing a large class of antennas with THz waves by combining silicon-based microelectronics with advanced computer aided design (CAD) techniques to model accurately the physical behaviour of such three dimensional (3D) micro-devices, meet the very specific requirement of reducing the long and expensive development cycles, and reaching interesting characteristics including compact size, good radiation and wide bandwidth.

This research work provides for the THz wireless access systems novel designs of highly miniaturized helix antennas based on MEMS technology with particular emphasis on major optimization challenges facing the device structure complexity. The different antenna geometrical structures are developed using 3D high frequency structure simulator (HFSS) based on efficient computational techniques for modal analysis and active optimization. Each time, the optimization strategy aims to vary the antenna geometric structure and maximize its EM response with a high accuracy for the selective frequency band by training the samples and minimizing the error from Finite Element Method- (FEM) based simulation tool. Excellent antenna performance and high structure precision are finally achieved by modifying and rectifying different parameters embedded in silicon platform including the helix and feeding variables using reliable evolutionary optimizers, effective stochastic solvers and accurate automatic strategists for conceiving high-performance THz MEMS helix antennas.

Key words: Integrated antennas, Terahertz (THz) applications, Micro-electromechanical system (MEMS) technology, computational electromagnetic (EM) optimization, evolutionary/stochastic/automatic strategists.

List of Figures

List of Tables

List of Abbreviations

3D: Three Dimensional.

ADS: Advanced Design System.

ANN: Artificial Neural Network.

CAD: Computer Aided Design.

CPW: Coplanar Waveguide.

EM: Electromagnetic.

FEA: Finite Element Approximation.

FEM: Finite Element Method.

FIB: Focused Ion Beam.

GA: Genetic Algorithms.

GEO: Geostationary Orbit.

HFSS: High Frequency Structure Simulator.

LEO: Lower Earth Orbit.

MEMS: Micro-electromechanical System.

MIMO: Multiple Input Multiple Output.

ML: Mismatch Loss.

MLP: Multilayer Perceptron.

OFDM: Orthogonal Frequency Division Multiplexing.

Q-N: Quasi-Newton.

RF: Radiofrequency.

RL: Return Loss.

RS: Response Surface.

SEM: Scanning Electron Microscopy.

SNLP: Sequential Non Linear Programming.

THz: Terahertz.

UHF: Ultra High Frequency.

UWB: Ultra Wideband.

VSWR: Voltage Standing Wave Ratio.

Table of Contents

General Introduction

As new applications for the electromagnetic THz gap ranging from 0.1 to 10 THz [1] begin to emerge, a great deal of research has been performed to develop functional antennas to manipulate this unique band of waves and incorporate integrated radiators into high frequency systems, especially with the wide wireless technology demand in processing the increasing information capacity in various applications that has revived the usage of integrated antennas on very compact units as essential elements having always been an interesting but difficult subject for designing and modeling. It is now assured that the design of highly miniaturized antennas becomes more critical due to the needs in operating in several frequency bands occupying a large available area [2]. This has attracted the utilization of advanced integrating technologies, and driven requirements for accurate optimization procedures to establish a new class of compact integrated THz antennas to be mainly deployed in high frequency access systems. Micro-electromechanical system technology becomes therefore a very promising technology for revolutionizing such antennas with terahertz waves by combining silicon-based microelectronics with complex computer aided design techniques including evolutionary, stochastic and automatic methodologies to meet the very special demand of novel THz antennas for attractive applications [3].

Many new techniques of MEMS technology have started to gain a great deal of momentum from research, industry and standardization bodies to stimulate interest in the unique THz spectral and help manufacturing integrated antennas, enhancing their performance and achieving precise micro scale.

desucoFion beam (FIB) [4] is one of the significant techniques used for designing MEMS THz antennas, especially helix antennas. It consists of implementing silicon platforms as a very good solution for improving the antenna shape and performance. In very specific terms, helix antennas employing silicon-based microelectronics, have achieved over the last decade important characteristics including compact size, good radiation, and wide bandwidth, thus their implementation into planar forms seems to become easier due to the advanced micromachining techniques [5]. This has marked a major advancing in

the field of THz technology, leading to provide new models of THz antennas, especially with the use of accurate computer aided design tools and effective optimization techniques as excellent solutions for improvements in modeling, incorporation of analysis, and execution of repeated electromagnetic simulations until developing existing design models and achieving new design models with a very good accuracy [6]. Three-dimensional high frequency structure simulator [7] presents a good environment for excellent electromagnetic treatment based on evolutionary optimizers, stochastic solvers and automatic strategists to retain a high performance and good accuracy for the antenna structure as compared with finite element modelling, to improve the existing design models or develop new design models, based on reliable and fully functional approximations.

Interestingly, this research work provides for the THz wireless access systems, a novel category of integrated helix antennas based on MEMS technology, and explains the major optimization procedures used to treat the device structure complexity that offer fitness functions for excellent bandwidth learning and fast configuration evaluation. The proposed antenna designs are developed using HFSS software based on fast computational techniques for active electromagnetic investigation and optimization. The research study targets at maximize the antennas' electromagnetic performance for the selective band of frequencies through optimizing their geometrical configurations with a high accuracy based on finite element modeling. Excellent electromagnetic responses and high structure precisions are finally achieved by synthesizing different tunable parameters embedded in the silicon platform divided into the helix form variables and feeding line characteristics. The optimized antennas occupy highly miniaturized volumes of a micro scale having a etartbsus nocilis niht yrev. The proposed MEMS helix antenna designs are validated by demonstrating optimal results in terms of low return loss (RL) properties and excellent voltage standing wave ratios (VSWR) in comparison to the previous structures. This has afforded encouraging results due to the real progress of the different electromagnetic optimization techniques in providing a new class of antennas operating at various

THz frequency ranges covering attractive applications for different emerging fields [8-10].

Accordingly, this research work addresses fundamental concerns of newly integrated THz MEMS helix antenna designs and provides relevant representative developments in three chapters that present a balanced approach among various important technical issues pertinent to integrated THz antennas as follows:

- The first chapter describes how antennas have evolved historically, discusses the impact of antennas in various systems, and gives an idea of the range of their applications that include communications, remote sensing, radar, biomedicine, etc. This chapter introduces also the popular types of antennas, presents important advances made in their designs, and offers insight into integrated antennas which are incorporated into different modern wireless systems to transmit, collect and transfer information. Interestingly, understanding how these antennas are employed at different frequencies ranging from radio to terahertz requires a main focus into their design considerations and deep knowledge of the fundamental properties for their operation. Concepts such as efficiency, gain, bandwidth, radiation pattern, and others are covered in an evaluative manner.

- The second chapter exposes the characteristics of the electromagnetic THz gap to understand the serious technical challenges on the design of integrated antennas in this unique THz field, and master the use of submillimeter waves which are a fusion between microwaves and optics. Several THz antennas can be successfully integrated in different geometrical configurations using MEMS technology relying on silicon-based microelectronics processing. This has leaded to investigate the silicon-based microelectronics process, and study the

fundamentals of THz antennas on electrically thin and thick silicon substrates.

- Related to what has been reported in the first two chapters, the final chapter describes for the THz wireless access systems applications a variety of compact helix antenna designs embedded in silicon wafers, presenting a new class of high performance integrated antennas with uniform characteristics and optimal dimensions due to the right exploitation of effective MEMS processes, and sophisticated use of HFSS-based accurate computational electromagnetic optimization techniques. This chapter adds to the knowledge base provided by the previous chapters a particular emphasis on major optimization challenges facing the complex antenna structures developed to efficiently collect terahertz radiation for successful operations. Finally, the proposed helix antenna designs based on MEMS technology function in different THz ranges and find several applications in numerous areas such as sensing, radio astronomy, and space communications.

Finally, this research study attempts at the analysis and development of novel integrated antenna designs linking the well-known advantages of MEMS processing to the modular properties of the electromagnetic THz frequency field. It is the hope of this study to find in it the necessary prototypes and mechanisms that can help in manufacturing such a kind of antennas and realizing new wireless applications in the future research works.

Chapter One

Integrated **A**ntennas for **M**odern **W**ireless **S**ystems

1.1. Introduction

The dawn of the 21th century brought fundamental changes to modernize the first wireless systems due to the great advancement conceived by a series of relevant research studies. Electronic devices can be today integrated using highly precise manufacturing procedures that are very attractive to achieve a high quality, high power, and excellent handling capability for the miniaturized structures. As a new generation of modern wireless systems, integrated antennas have gained wide attention since their inception after having converted the bulky structures into corresponding compact forms, enabling the fabrication processing of those three-dimensional structures. Integrated antennas become very promising for high frequency links and gain a great worth in transmission, sensing, and imaging systems, etc. Accordingly, this introductory chapter offers insight into modern integrated antennas presenting:

- Historical perspective and applications of antennas;
- Popular types of antennas;
- Integrated antennas for modern systems.

1.2. Historical perspective and applications of antennas

1.2.1. History and development of antennas

Antennas present today an integral part of the daily-life requirements; they are employed to transmit and receive electromagnetic waves for a multitude of purposes; they serve as a transducer that converts guided waves into free-space waves in the transmitting mode, or vice-versa in the receiving mode. All antennas operate on the same basic principles founded by the electromagnetic theory of *J. C. Maxwell*. Numerous antenna designs began to emerge and find important applications over the entire electromagnetic frequency spectrum since 1901, the time of the time of Marconi's first experiments with transmitting electromagnetic waves.

In 1973, *Maxwell* published his famous book "*A Treatise on Electricity and Magnetism*" where incorporated all previously known results on electricity and magnetism to express the unified theory of the electromagnetics in what it is mathematically referred to *Maxwell*'s equations which hold over the entire electromagnetic frequency range [11]. *Maxwell*'s theory was met with much skepticism until it was validated by the father of radio *H. R. Hertz* with his experiments in 1886 [12] that aimed to demonstrate the existence of electromagnetic radiation.

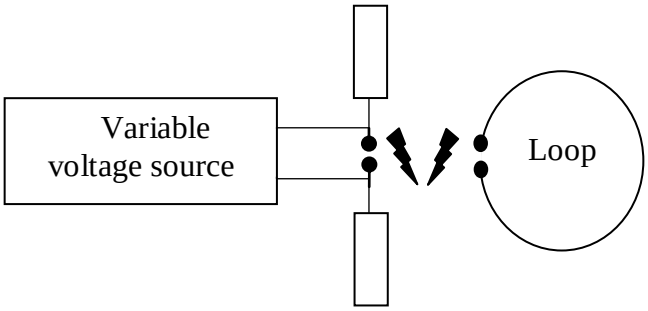

Figure 1.1 – Experimental set-up of *Hertz*'s apparatus

Hertz built the first radio system to produce and detect radio waves, consisting of a *λ/2* dipole (transmitting antenna) and a resonant loop (receiving antenna) at a wavelength of 4 m (figure 1.1). By turning on the induction coil, sparks were induced across the gap and detected at the receiving antenna .The information in Hertz's experiment was actually in binary digital form, by tuning the spark on and off. This could be considered the first digital wireless system composed of the best-known antennas: the dipole and the loop also called the *Hertz* antennas.

Almost a decade later in 1901, *G. Marconi* was able to receive signals across the Atlantic in *St. Johns, Newfoundland,* that were sent from a station he had built in *Poldhu, Cornwall, England. Marconi*'s transmitting antenna was a fan antenna with 50 vertical wires supported by two 6-m guyed wooden poles. The receiving antenna was a 200 m wire pulled up with a kite [13]. After, *Marconi* succeeded in commercializing wireless technology by introducing a

radiotelegraph system, which served as the foundation for the establishment of numerous affiliated companies worldwide. Monopole antennas were widely used in *Marconi*'s experiments; thus vertical monopole antennas are also called *Marconi* antennas.

For many years since *Marconi*'s experiment, antennas operated at low frequencies up to the ultra high frequency (UHF) region and were primarily wire-type antennas. The demands for effective communication systems during the second world war moved the field of antennas up into the higher frequencies, and led to the design of many new types of microwave antennas that were capable of producing highly directive beams with small-sized antennas. An excellent reference on the early work done in microwave antennas is the MIT Radiation Laboratory Series book by *Silver* [14].

Advances in computer architecture and technology moved the field into new directions and produced major advances, with microstrip antennas and arrays, in particular, being heavily investigated during the 1960–1980 period for a wide range of applications. In addition, the use of numerical techniques to analyze complex antenna systems became prevalent, making the issues of reduced computational time and computer memory storage requirements an important part of antenna design. Sophisticated simulation tools are now an integral part of antenna research, and several simulation packages are used extensively in reducing manufacturing costs and time.

Research during the latter part of the twentieth century led to the arena of wireless communications, and the role of antennas is becoming increasingly important. In some systems, the antenna is now no longer just a simple transmitting/receiving device, but a device which is integrated with other parts of the system to achieve better performance. This posed new and exciting challenges to antenna engineers, with stringent demands being placed on the size and performance of the antennas used for satellite and terrestrial communications. Research was directed toward the design of "smart" or

"adaptive" antennas that can perform well in a mobile environment [15]. More recently, micro-electromechanical system devices have emerged as an attractive option for high-frequency systems. MEMS phase shifters, with the advantages of low loss and fast actuation, have been investigated for use in fast-scanning phased arrays [16]. Reconfigurable antennas, where several antennas share the same physical aperture, cover different frequency bands, and perform different functions, have now caught the attention of researchers [17, 18].

Things have been changing quickly in the wireless world, and the applications of antennas range from communications to astronomy, to various deep-space applications but one thing has never changed since the very first antenna was made: the antenna is a practical engineering subject. It will remain an engineering subject. Once an antenna is designed and made, it must be tested. How well it works is not just determined by the antenna itself, it also depends on the other parts of the system and the environment. Elaborate antennas or antenna systems require careful design and a thorough understanding of the radiation mechanism involved. The selection of the type of antenna to be used for a given application is determined by electrical and mechanical constraints and operating costs. The electrical parameters of the antenna are the frequency of operation, gain, polarization, radiation pattern, impedance, etc. The mechanical parameters of importance are the size, weight, reliability, manufacturing process, etc. In addition, the environment under which the antenna is to be used also needs to be taken into consideration. Finally, the designers will have to meet all of these constraints, along with the standard antenna problems of polarization, scan rates, frequency agility, etc in order to provide a new class of high performance integrated antennas for the different modern systems [19].

1.2.2. Applications and impact of antennas on different systems

Today, antennas provide a very large range of applications in the military, civil and commercial fields. They enjoy extensive use in communication, biomedicine, sensing, imaging, astronomy, spectroscopy, collision avoidance, air

traffic control, global positioning systems, pagers, wireless networks, etc., and cover a very wide range of frequencies, as shown in figure1.2 [20].

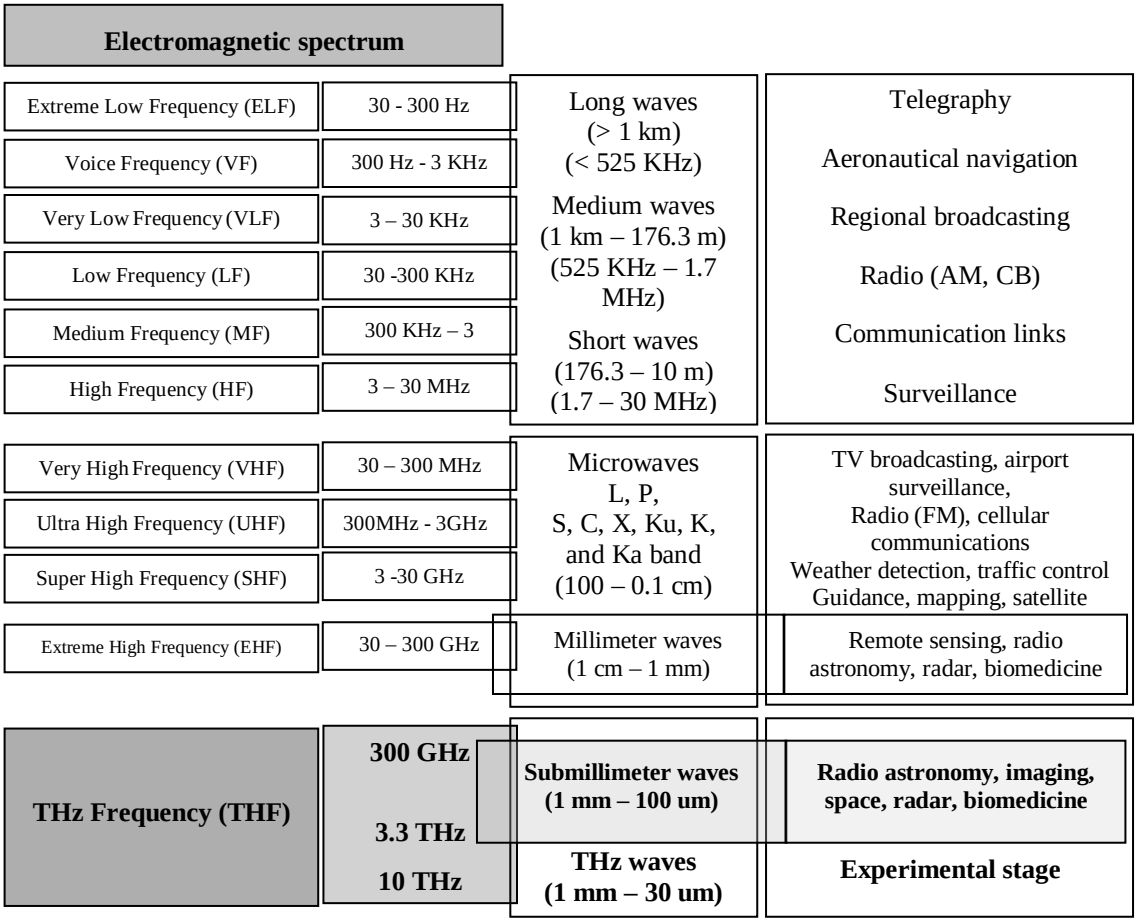

Figure 1.2 – Electromagnetic spectrum and general usage

1.2.2.1. Antennas for communication systems

Antennas are one of the most critical components in communication systems because they are responsible for the proper transmission and reception of electromagnetic waves. Effectively, a good antenna design help to relax the complex system requirements involved in a communication link and increase overall system performance. The choice of an antenna for a specific application (cellular, satellite-based, ground-based, etc.), depends on the platform to be used (car, ship, building, spacecraft, etc.), the environment (sea, space or land), the frequency of operation, and the nature of the application (video, picture, audio or data). Communication systems fall into several different categories [21]:

- Direct links: These are transmission links established between two highly directional antennas. The link can be between two land-based antennas (radio relays); between a tower and a mobile antenna (cellular communication); between a land-based antenna and a satellite antenna (satellite communication); between two satellite antennas (space communication). Usually these links operate at frequencies between 1 GHz and 25 GHz [22].
- Satellite communications: Antennas on orbiting satellites are used to provide communications between various locations around the earth. They are used either to form a large area-of-coverage beam for broadcasting, or spot beams for point-to-point communications [23]. In general, most telecommunication satellites are placed in geostationary orbit (GEO), about 22,235 miles above the earth. There are also some satellites at lower earth orbits (LEO) that are used for wireless communications. Modern satellites have several receiving and transmitting antennas that can offer services such as video, audio, and data transmission. The impact of antennas on satellite technology continues to grow. Most satellites operate at the L, S, or Ku band, but increasing demand for mobile telephony and high-speed interactive data exchange is pushing the antenna and satellite technology into higher operational frequencies.
- Personal and mobile communication systems: The vehicular antennas used with mobile satellite communications constitute the weak link of the system. If the antenna has high gain, then tracking of the satellite becomes necessary. If the vehicle antenna has low gain, the capacity of the communication system link is diminished. Moreover, handheld telephone units require ingenious design due to a lack of real estate on the portable device. There is more emphasis now on enhancing antenna technologies for wireless communications, especially in cellular communications, which will improve the link performance and reduce the undesirable visual impact of antenna towers. Techniques that utilize

smart antennas, fixed multiple beams, and neural networks are increasing the capacity of mobile communication systems, whether it is land-based or satellite-based. This will lead to the design of more compact and more sophisticated antennas [24].

1.2.2.2. Antennas for remote sensing systems

Remote sensing is the process of obtaining information about a certain object without coming into direct physical contact with it. Antennas such as horns, reflectors, helical phased arrays, and synthetic apertures are used in remote sensing from an airplane or a satellite to infer the physical properties of planetary atmosphere and surface, or to take images of objects [25]. The degree of resolution of a remote map depends on the ability of the antenna system to separate closely space objects in range and azimuth [26]. To increase the azimuth resolution, a technique called synthetic aperture is employed. Today, antennas are used for remote sensing applications in both military and civilian sectors.

1.2.2.3. Antennas for biomedical systems

The antenna used in many biological applications operates under very different conditions than do its more traditional free-space. Near fields and mutual interaction with the body dominate; also, the antenna radiates in a lossy environment rather than free space. Several antennas, from microstrip antennas to phased arrays, operating at various frequencies, have been developed to couple electromagnetic energy in or out of the body and enjoy several therapeutic and informational medical operations [27]. Antennas have also been used to stimulate certain nerves in the human body. The designers have to choose the right frequency, antenna size, and spot size that the beam has to cover in the body. Antennas such as helical-coils, ring capacitors, and dielectrically loaded waveguides are therefore very attractive because of their compactness. As the technology advances in the areas of materials and in the design of more compact antennas, more antenna applications will be found in the areas of biology and medicine [28].

1.2.2.4. Antennas for radio astronomy systems

Another field where antennas have made a significant impact is astronomy. A radio telescope is an antenna system that astronomers use to detect radiofrequency (RF) radiation emitted from extraterrestrial sources. Since radio wavelengths are much longer that those in the visible region, radio telescopes make use of very large antennas to obtain the resolution of optical telescopes. Antennas have also been used in constructing a different type of a radio telescope, called a radio interferometer, which consists of two or more separate antennas that are capable of receiving radio waves simultaneously but are connected to one receiver. The radio waves reach the antennas at different times and are used to measure the distance or angular position of an object with a very high degree of accuracy [29].

1.2.2.5. Antenna for radar systems

Modern civilian and military airplanes have several antennas on board that are used for altimetry, speed measurement, collision avoidance, communications, weather detection, navigation, and a variety of other functions. Each function requires a certain type of antenna and makes the operation of a radar system feasible. Scientists in 1930 observed that electromagnetic waves emitted by a radio source were reflected back by aircraft that could be detected by electronic equipment. Since then, several technological developments have emerged in the area of radar antennas, and the desire to operate at different frequencies has led to the development of several very versatile and sophisticated antennas. Radar antennas can be ground-based, mobile, satellite-based, or placed on any aircraft or spacecraft [30]. Today, radar antennas are used for coastal surveillance, air traffic control, weather prediction, surface detection, mine detection, tracking, air defense, speed detection, burglar alarms, missile guidance, mapping of the surface of the earth, reconnaissance, etc. Radar antennas are generally designed to be part of a very complex system that includes high-power klystrons, traveling wave tubes, solid-state devices, integrated circuits, computers, signal processing,

and a myriad of mechanical parts. The requirements vary depending on the application and the platform of operation [31].

1.3. Popular types of antennas

Since the start of radio communications, thousands of antennas have been developed. They can be categorized by various criteria [32]:

- ✓ In terms of the bandwidth, antennas can be divided into narrowband and broadband antennas;
- ✓ In terms of the polarization, they can be classified as linearly polarized or circularly polarized antennas;
- ✓ In terms of the resonance, they can be grouped as resonant or traveling wave antennas;
- ✓ In terms of the number of elements, they can be organized as element antennas or antenna arrays.
- ✓ In terms of physical structures, they can fall into wire-type antennas and aperture-type antennas.

Different types of antenna exhibit different features and can be analyzed using different methods and techniques. They have distinct characteristics that make them suitable for a variety of applications. Thus, they are very often used in array configurations to improve upon the characteristics of an individual antenna element [33].

1.3.1. Wire-type antennas

Wire-type antennas are made of conducting wires and are generally easy to construct, thus the cost is normally low. The most important examples include:

1.3.1.1. Dipoles

Dipoles (figure 1.3) are one of the simplest but most widely used types of antenna. A dipole can be considered a structure evolved from an open-end, two-

wire transmission line. A typical structure of a dipole consists of two metal wires which are normally of equal length. In reality, such kind of antennas cannot be found since the current is zero at the end of a line. For antenna analysis and design, it is all about the current distribution. Once the current distribution is known, other parameters, such as the radiation pattern and input impedance, can be obtained [20].

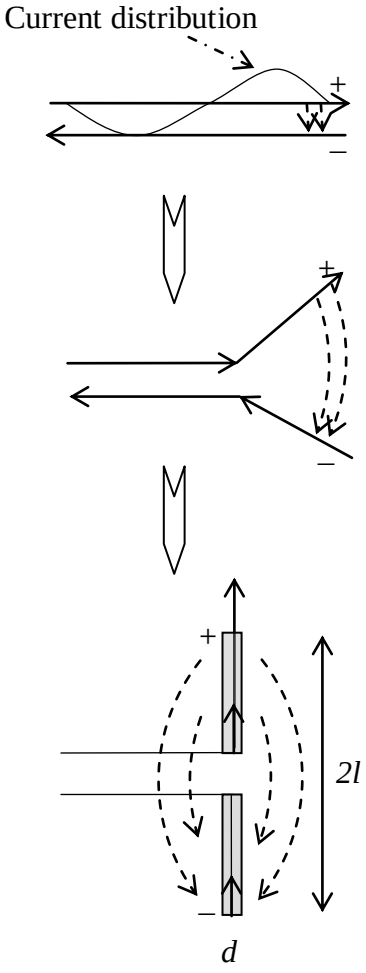

Figure 1.3 – Evolution of a dipole of total length *2l* and diameter *d*

Sometimes short dipoles are not employed for reception where signal-to-noise ratio is more important than the radiation efficiency. There are many other forms of dipoles developed for various applications. Biconical dipole offers a much wider bandwidth than the conventional cylindrical dipole; a bow-tie dipole has a broad bandwidth and low profile; while a sleeve dipole can be nicely fed by

a coaxial cable and exhibits a wide bandwidth. A *λ/2* folded dipole may be viewed as a superposition of two half-wavelength dipoles with an input impedance of around 280, which is close to the standard characteristic impedance of 300 for a two-wire transmission line. That is why it was widely used for TV reception in the good old days [34].

1.3.1.2. Monopoles

A monopole antenna (figure 1.4) is half of the dipole antenna. There are a lot of similarities between them, but there are also some differences. The best way to investigate the monopole is to apply the image theory [35] which convert the monopole to a dipole with length 2*l* in free space. The current distribution along the pole becomes the same as the dipole, thus the radiation pattern is the same above the ground plane. Since the power is only radiated to the upper half space and the power to the lower half space is reflected back to the upper space, this results in an increased directivity. The directivity of a monopole is therefore twice that of its dipole counterpart.

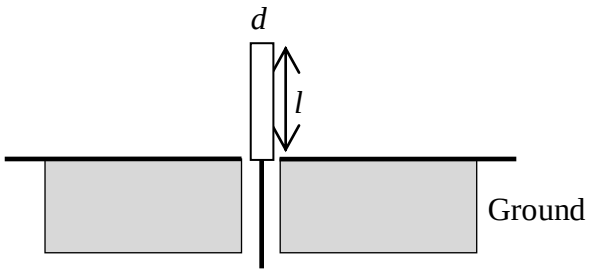

Figure 1.4 – A monopole antenna with a coaxial feed line

1.3.1.3. Loops

Loops [36] are another simple and versatile wire-type antenna. They take many different configurations, which include circular, square, rectangular, triangular, elliptical and other shapes. While the dipole is considered to be a configuration evolved from an open-end transmission line, the loop can be viewed as a configuration evolved from a short-end transmission line.

Thus, for a small loop, the current is large and the voltage is small – these results in small input impedance, which is very different from a short dipole whose impedance, more precisely the reactance, is very large If a loop cannot be considered small, the current distribution cannot be regarded as constant. As a result, many properties of the loop are changed and results obtained for a constant current cannot be applied to real antennas (figure 1.5).

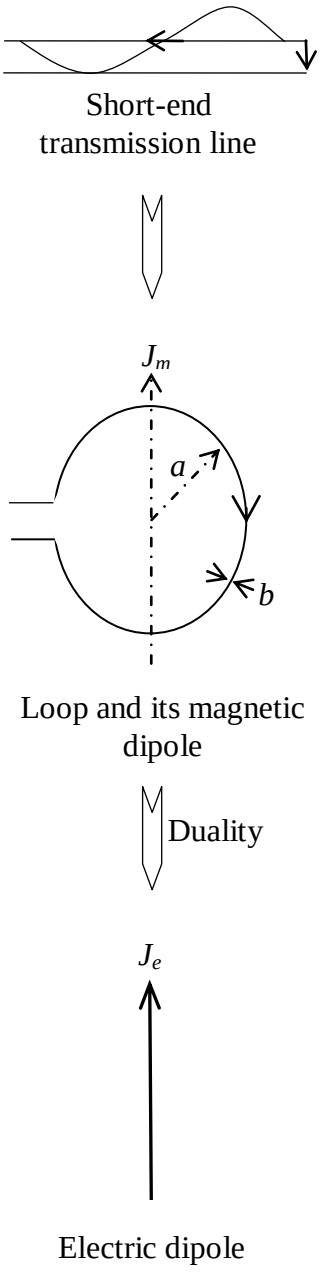

Figure 1.5 – Loop antenna and its corresponding dipoles

1.3.1.4. Helix antennas

Helix antennas [37] have very interesting and unique features. They may be viewed as a derivative of the dipole or monopole antenna, but it can also be considered a derivative of a loop antenna [32]. They have a nearly uniform resistive input over a wide bandwidth operate as a super-gain end-fire array over the same bandwidth. Furthermore, it is non-critical with respect to conductor size and turn spacing. It is easy to use in arrays because of almost negligible mutual impedance. Geometrically, a helical antenna consists of a conductor wound into a helical shape. It is a circularly/elliptically polarized antenna.

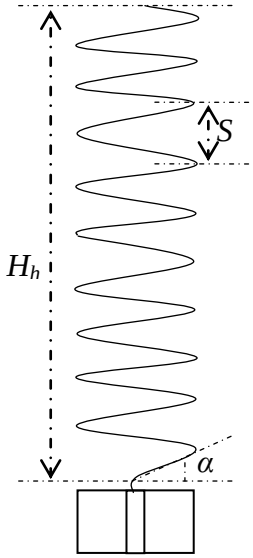

Figure 1.6 – Helix antenna geometrical structure

A helix wound like a right-hand (clockwise) screw radiates or receives right-hand circularly polarized waves, whereas a helix wound like a left-hand (anti-clockwise) screw radiates or receives left-hand circularly polarized waves. Although *a* helix can radiate in many modes, the axial (end-fire) mode and the normal (broadside) mode are the ones of most interest. The following notations are used for the analysis of helical antennas: Diameter of helix (D), spacing between turns also called pitch (S), number of turns (N), slent angle (α), change radius (R_c), circumference of helix ($C = \pi D$), and length of one helix (H_h) (figure 1.6).

1.3.2. Aperture-type antennas

This group of antennas is not made of metal wires but plates to form certain configurations that radiate and receive electromagnetic energy in an efficient and desired manner according the aperture type antennas. They are often used for higher frequency applications than wire-type antennas. Typical examples include:

1.3.2.1. Reflector antennas

Reflector antennas take various geometrical configurations, the most popular shape is the paraboloid – because of its excellent ability to produce a pencil beam with low side lobes and good cross-polarization characteristics in the radiation pattern. Reflector antennas [38] gained prominence due to their use with radar systems; they have played an important role in communication systems.

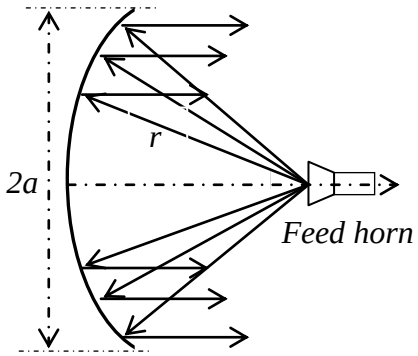

Figure 1.7 – Reflector antenna (paraboloidal shape)

They can have a variety of geometrical shapes and require careful design and a full characterization of the field system. *Silver* [14] presents the technique for their analysis based on aperture theory and physical optics. Other methods such as the geometrical theory of diffraction and the fast *Fourier* transform, along with various optimization techniques, are used more often for the accurate design of these antennas [39] (figure 1.7).

1.3.2.2. Lens antennas

At high frequencies, lens antennas [40] can be used to perform functions similar to reflector antennas. Both lenses and parabolic reflectors use free space as a feed network to excite a large aperture. The feed of a lens remains out of the aperture, eliminating aperture blockage and the resulting high sidelobe levels. Dielectric lens antennas are similar to the optical lens and the aperture of the antenna is equal to the projection of the rim shape (figure 1.8).

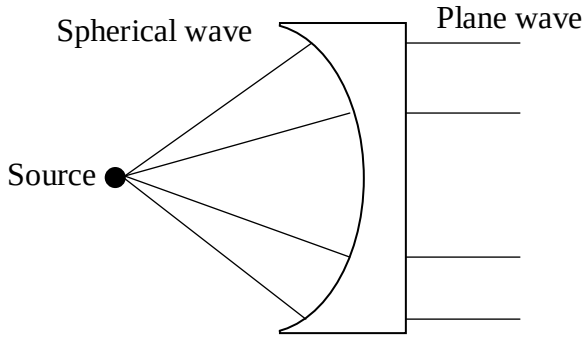

(a)

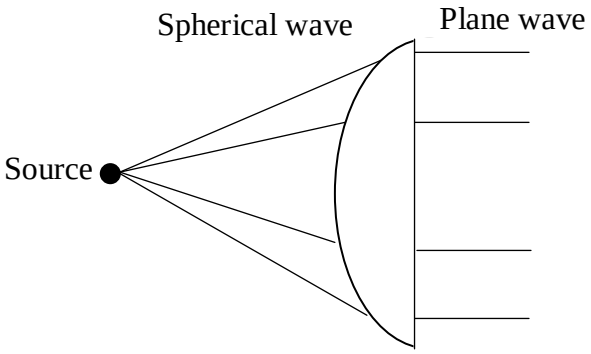

(b)

Figure 1.8 – Lens antennas, concave planar (a) and convex planar (b)

Lenses are divided into two categories: Single-surface lens which is an equiphase surface of the incident or emergent wave and the rays pass through normal to this surface without refraction, and dual-surface lens in which refraction occurs at both lens surfaces. Single-surface lenses convert either

cylindrical or spherical waves to plane waves. Cylindrical waves require a line source and a cylindrical lens surface, and spherical waves use a point source and a spherical lens surface. The far-field pattern is determined by diffraction from the aperture. Dual-surface lenses allow more control of the pattern characteristics. Both surfaces are used for focusing, and the second surface can be used to control the distribution in the aperture plane. Artificial dielectric lenses in which particles such as metal spheres, strips, disks, or rods are introduced in the dielectric have been investigated by *Kock* [41]. The size of the particles has to be small compared to the wavelength. Metal plate lenses using spaced conducting plates are used at microwave frequencies. Since the index of refraction of a metal plate medium depends on the ratio of wavelength to the spacing between the plates, these lenses are frequency sensitive.

1.3.2.3. Horn antennas

The electromagnetic horn antenna (figure 1.9) is characterized by attractive qualities such as unidirectional pattern, high gain, and purity of polarization. Horn antennas are used as feeds for reflector and lenses antennas and as a laboratory standard for the calibration of other antennas [42]. Horn antennas can be of rectangular or circular type. Circular horns derived from circular waveguides, can be conical, biconical, or exponentially tapered. Rectangular horns derived from a rectangular waveguide can be pyramidal or sectoral E-plane and H-plane horns.

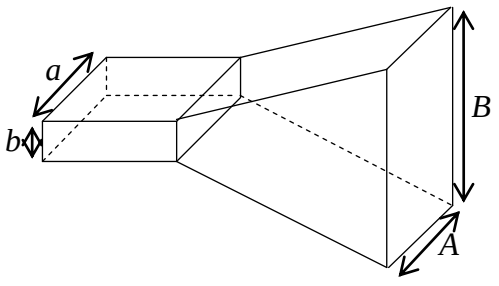

Figure 1.9 – Horn antenna (pyramidal geometric structure)

The E-planes sectoral horn has a flare in the direction of the field of the dominant TE_{10} mode in the rectangular wave guide and the H-plane sectoral horn has a flare in the direction of the H-field. The pyramidal horn has a flare in both directions. The radiation pattern of the horn antenna can be determined from a knowledge of the aperture dimensions and the aperture field distribution. The large aperture and single-mode excitation can be achieved by gradually flaring the waveguide to form a horn. Higher order modes are generated at the throat of the horn (the region between the waveguide and the horn). However, these will be attenuated in the throat region if the flare angle is not large. The flare angle of the horn and its dimension affect its radiation pattern and directivity. Maximum directivity can be achieved by optimizing the horn length and the flare angle. The need for feed systems that provide low cross polarization and edge diffraction and more symmetrical patterns led to the design of the corrugated horn. These horns have corrugations or grooves along the walls that are *λ/4* to *λ/2* deep. The conical corrugated horn, referred to as a scalar horn, has a larger bandwidth than its small flare angle corrugated horn. This horn is very suitable as a feed for reflector antennas [43].

1.3.2.4. Microstrip antennas

Microstrip patch antennas (figure 1.10) appear in a variety of shapes, including rectangular, circular, elliptical, and triangular. They are planar and conformal structures that are also lightweight and can be used with integrated circuits [44, 45]. Microstrip or printed antennas are used in several applications, including radar, GPS, mobile communications, aeronautical applications, medical applications, etc. Microstrip antennas employ several feed mechanisms. Each feed configuration has its advantages and disadvantages. For impedance matching purposes, the offset microstrip line feed is the easiest to use since the offset depth controls the input impedance of the antenna. Moreover, this configuration is simple to fabricate and analyze as well. However, the feed line radiates and causes pattern and polarization degradation.

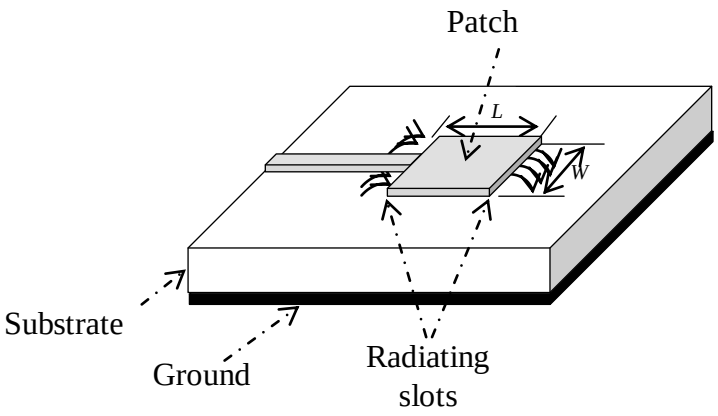

Figure 1.10 – Microstrip antenna structure

The coaxial probe feed reduces spurious feed radiation, it is fairly easy to construct and match, but it tends to have a narrow bandwidth. The aperture-coupled feed isolates the feed mechanism from the radiating element through the use of a ground plane. Energy from the feed line is coupled to the element patch through the aperture slot. Finally, the proximity-coupled feed removes the ground plane so it is easier to manufacture than the aperture-coupled feed. It also exhibits low spurious radiation and provides the largest bandwidth of the feed configurations [46].

1.4. Integrated Antennas for modern systems

In today's environment of connectivity, wireless devices are ubiquitous. As the radiofrequency electronics technology for these wireless devices continues to decrease in size, there is a corresponding demand for a similar decrease in size for the antenna element. Unfortunately, the performance requirements for the antenna are rarely relaxed with the demand for smaller size. In fact, the performance requirements generally become more complex and more difficult to achieve as the wireless infrastructure evolves but with the deployment of advanced MEMS processes, challenges outperform the significant limitations associated with the design of such radiating structures, and make possible the fabrication of highly miniaturized antennas operating over multiple frequency.

1.4.1. Design considerations of integrated antennas

In general, antennas are designed in well-defined environments, over either infinite or large ground planes, however, integrated antenna for modern wireless systems have to operate on an electrically small device, which will cause a distortion of its radiation characteristics. It is thus important to determine how the fact of integrating an antenna in an electrically small device will affect its actual behavior regarding both input and radiation characteristics [47]. Indeed, designing an integrated antenna is not an easy task, as this type of antenna is subject to very stringent specifications. Small size, light weight, compact structure, low profile, robustness, and flexibility are the prime considerations conventionally taken into account in small antenna design. In addition, as modern wireless systems are required to operate at multiple standards, their antennas are expected to grab as much spectrum as possible, so they may provide multiband or broadband operation [48].

Although the progression in microelectronics has resulted in striking reductions in the size of the device, the size of the antenna cannot be shrunk so easily, as it is determined not only by technological, but mostly by physical factors. Extensive research has been carried out in the past decades to find ways of reducing the size of resonant antennas so that they will fit within a given volume. This implies that either the antenna has to be electrically small or conformed to a certain shape adapted to a small volume available. However, this gives rise to restrictions regarding polarization, radiation efficiency, and bandwidth, and furthermore increases the sensitivity to manufacturing tolerances. In the past, some compromises were adopted regarding the performance of the antenna, and certain degradation in its matching and efficiency characteristics was accepted, if the aims of integration and cost were accepted. Yet, the pressure of wireless systems is changing the trend, and now new efforts should be provided to obtain antennas with more efficient radiating characteristics. A key challenge for the industry is reducing the presence of noise affects and the baseband electromagnetic occurring when converting magnetic energy of a

varying magnetic field to electrical energy, retaining the original information contained in the magnetic field around the integrated antenna. This has been recently amended, to reflect new requirements for manufacturing processes to surpass the problems related to antenna design and master the measurement setups to improve the behavior of such miniaturized devices due to advanced technology such as MEMS processing technology [49].

1.4.2. Fundamental properties of integrated antennas

The performance of single and multiband integrated antennas is characterized by a number of electrical properties, which include input impedance, efficiency, voltage standing wave ration, return loss gain, bandwidth, quality factor (*Q*), and radiation pattern [20].

1.4.2.1. Input impedance, efficiency, VSWR, RL and gain

The complex, frequency-dependent input impedance of the small antennas is given by:

$$Z_A(\omega) = R_A(\omega) + jX_A(\omega) \tag{1.1}$$

Where $R_A(\omega)$ and $X_A(\omega)$ are the antenna's frequency-dependent resistance and reactance, respectively, ω is the radian frequency, and f is the frequency in Hz. The antenna's frequency dependent radiation efficiency is given by:

$$\eta_r(\omega) = \frac{R_r(\omega)}{R_A(\omega)} \tag{1.2}$$

Where $R_r(\omega)$ is the antenna radiation resistance. Any small antenna that behaves as a series RLC circuit is dipole- or monopole like from an impedance perspective and can be identified by the fact that there is not a DC short anywhere within the antenna structure that connects the center conductor of the feed cable to its shield or ground. Any small antenna that behaves as a parallel RLC circuit is loop from an impedance perspective and can be identified by the

fact that there is a DC short somewhere within the antenna structure that connects the center conductor of the feed cable to its shield or ground. Dipole- and monopole antennas behave as a series RLC circuit, where their radiation and loss resistances are in series from very small values of ω through their first series resonant frequency. Loop antennas behave as a series RLC circuit for very small values of ω. However, as ω approaches the loop's first resonant frequency, the antenna behaves as a parallel RLC circuit and the radiation and loss resistances are in parallel. For all antennas, the input voltage standing wave ratio is given by:

$$VSWR(\omega) = \frac{1 + |\Gamma(\omega)|}{1 - |\Gamma(\omega)|} \tag{1.3}$$

Where $\Gamma(\omega)$ is the frequency-dependent complex reflection coefficient given by:

$$\Gamma(\omega) = \frac{Z_A(\omega) - Z_{CH}}{Z_A(\omega) + Z_{CH}} \tag{1.4}$$

Where Z_{CH} is the real characteristic impedance of the transmission line connecting the antenna to a transmitter. While voltage standing wave ratio provides a quantitative indication of the level of mismatch between the antenna's impedance and the transmission line's characteristic impedance, a more direct measure relating the amount of power reflected at the antenna's feed point terminal to the incident or forward power is the mismatch loss (ML) defined by:

$$ML(\omega) = 1 - |\Gamma(\omega)|^2 \tag{1.5}$$

In practice, the voltage standing wave ratio and mismatch loss are often characterized by the return loss, which is defined as:

$$RL(\omega) = 20log\left(|\Gamma(\omega)|\right) \tag{1.6}$$

For most wireless, integrated antennas, the voltage standing wave ratio is required to be less than 3 throughout the designated operating band. This is

equivalent to a return loss requirement of 6 dB. If the antenna's pattern directivity (*D*) is defined, then the antenna's overall or realized gain (*G*) is defined:

$$G(\omega) = \eta_r(\omega)\left(1 - \left|\Gamma(\omega)\right|^2\right) \tag{1.7}$$

n the case of the device integrated monopole (or other small device integrated antenna), the ground plane is small in extent and may have dimensions approaching or less than the value of the operating wavelength. In this case, the directivity is typically less than 3 (4.8 dB) and the maximum realized gain of the antenna is less than 4.8 dBi. The typical value of realized gain for efficient antennas ranges between 2 and 4 dBi.

1.4.2.2. Bandwidth and quality factor

One of the challenges associated with the design of integrated antennas is achieving the desired voltage standing wave ratio over one or multiple operating bands. From a practical perspective, the designer is usually interested in the VSWR bandwidth, defined by a specific value of voltage standing wave ratio, relative to the characteristic impedance of a transmission line (typically 50/70Ω) or the output impedance of a transmit amplifier or receive circuit. This VSWR bandwidth can easily be determined through simulation or measurement. The quality factor allows also the designer to determine how well the antenna design performs relative to theoretical limits. For a small antenna, there are established, fundamental limits for the minimum value *of* quality factor that can be achieved. Often, the definition of bandwidth can be ambiguous; however, it is defined according two specific ways [50].

For the antenna that exhibits a single impedance resonance, VSWR bandwidth in terms of the fractional bandwidth as:

$$FBW = \frac{f_h - f_l}{f_0} \tag{1.8}$$

Where f_h and f_l are the frequencies for an arbitrary VSWR, above and below, the frequency of minimum VSWR, f_0, respectively.

For the antenna that exhibits multiple impedance resonances or a single wideband resonance within its defined VSWR bandwidth, and where the bandwidth is relatively large (a wideband antenna), it is defined in terms of the bandwidth ratio as:

$$FBW = \frac{f_h}{f_l} \tag{1.9}$$

Where f_U and f_D are the upper and down frequencies defining the full extent of the operating band for a defined VSWR. For wideband antennas, the value of the bandwidth ratio, *BWR*, is assumed to be greater than approximately 1.25. The antenna may have one region of VSWR bandwidth that simultaneously covers multiple operating bands.

The definition for the quality factor of an antenna is not ambiguous. There is only one definition for exact quality factor, which is defined for the resonant or tuned antenna as:

$$Q(\omega_0) = \frac{\omega_0 W(\omega_0)}{P_A(\omega_0)} \tag{1.10}$$

Where ω_0 is the resonant or tuned frequency, $W(\omega_0)$ is internal energy, and $P_A(\omega_0)$ is the power accepted by the antenna, including the powers associated with radiation and loss.

1.4.2.3. Radiation pattern

The radiation pattern [50] is defined as the spatial distribution of a quantity that characterizes the electromagnetic field generated by the antenna. The field intensity of the propagating wave decreases by $1/R$ with distance R from the source. To understand how an antenna radiates, consider a pulse of electric charge moving along a straight conductor. A static electric charge or a charge

moving with a uniform velocity does not radiate. However, when charges are accelerated along a conductor and are decelerated upon reflection from its end, radiated fields are produced along the wire and at each end.

The 3D spatial distribution of the radiated energy is displayed as a function of the observer's position along a constant radius. Power patterns and field patterns are commonly used. The power pattern is a plot of the received power at a constant radius, and the field pattern is the spatial variation of the electric and magnetic fields at a constant radius. The space surrounding an antenna is divided radially into three regions:

- The near-field (reactive region) which is the portion of the near-field region immediately surrounding the antenna where the reactive field dominates.
- The near-field (radiating/*Fresnel* region) which is the portion of the near field of an antenna between the reactive near-field region and the far-field region, where the angular field distribution is dependent on the distance from the antenna.
- The far-field (*Fraunhofer* region) which is the region of the field of an antenna where the angular field distribution is essentially independent of the distance from a specified point in the antenna region.

The radiation pattern is commonly described in terms of its principal E-plane (xoy) and H-plane (yoz) patterns. For a linearly polarized antenna, the E-plane pattern is defined as the plane containing the electric field vector and the direction of maximum radiation, and the H-plane pattern is the plane containing the magnetic field vector and the direction of the maximum radiation.

Figure 1.11 shows a rectangular and a polar plot of a radiation pattern. The major lobe contains the direction of maximum radiation, and between the lobes there are nulls or directions of minimum radiation. Some patterns may have more

than one major lobe. Minor lobes levels are expressed relative to the major lobes level.

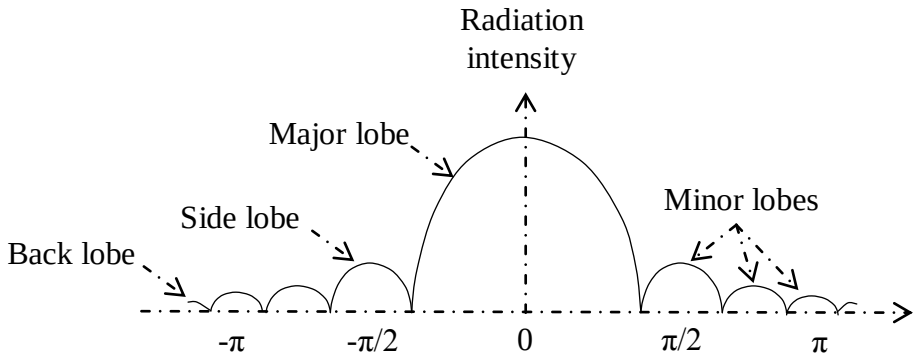

(a)

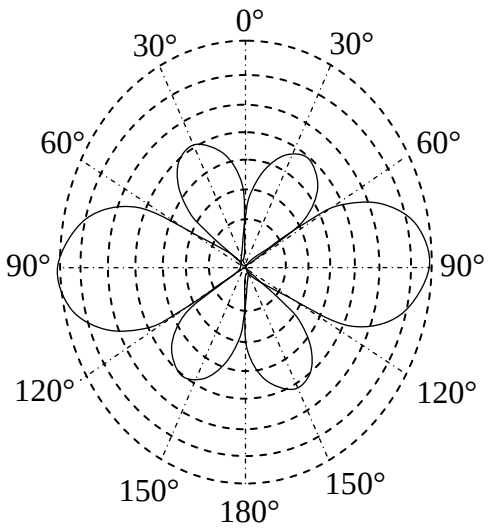

(b)

Figure 1.11 – Radiation patterns in rectangular (a) and polar (b) forms

Practical antennas are designed to have directional radiation patterns; they will radiate or receive radiation more effectively in one specified direction than in others. An isotropic radiator, often used as a reference for expressing an antenna's directional properties, is a hypothetical lossless antenna radiating equally in all directions. An omni-directional pattern is a special case of a directional pattern where the radiation is non-directional in the azimuthal plane and directional in the elevation plane.

Chapter Two

MEMS **A**ntennas for **T**Hz **W**ireless **S**ystems

2.1. Introduction

Electromagnetic THz gap occupies an extremely large regime ranging from microwaves to infrared band and offers a large field for modern wireless systems. In the last two decades, micro-electromechanical technology has grown exponentially and its effect on the research in this unique band of the electromagnetic spectrum has been noticed, and with the sustaining progress in integration with silicon-based microelectronics processing, various potential design of integrated antenna operating at THz wave band have been reported in the field of science and technology [51]. Interestingly, this descriptive chapter presents mainly exhaustive illustrations of:

- Electromagnetic THz gap.
- THz integrated antennas.
- Micro-electromechanical systems for THz integrated antennas.

2.2. Electromagnetic THz gap

The electromagnetic THz gap presents a main portion of the electromagnetic frequency spectrum which extends from 0.1 to 10 THz, and shows the ray of hope to the modern wireless systems to meet the future need and carter the exponential growth in the data rates required by such a kind of high performance systems. This presents a potential challenge to the scientific community to increase the operating frequencies, the wireless systems may fetch a high data rate to the target customers. This becomes possible with the increasing of operating frequencies to the terahertz band ranging from microwave band to infrared band of the electromagnetic frequency spectrum as illustrated in figure 2.1 [52, 53]. Indeed, due to its unique position, as this gap is situated between these two already well-explored regimes of the spectrum, it is possible to use electronic as well as photonic route to pave the way in the terahertz spectrum. However, with the increase in the operating frequency, the

device characteristics changes that needs a thorough analysis of various THz system components, and requires advanced technologies to integrate these components in micro and nanometer scales such as MEMS technology which presents a convincing technology to model functional and high performance devices for diverse THz systems [54-56].

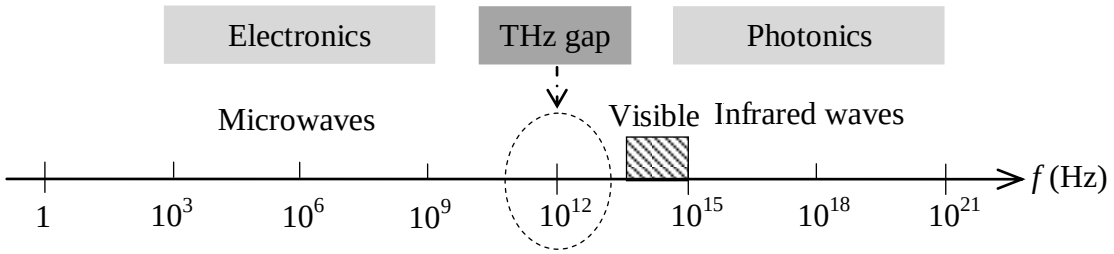

Figure 2.1 – Position of electromagnetic THz gap in the frequency spectrum

Categorically, electromagnetic THz gap finds its applications in various areas including communication and defense applications, radio astronomy and space instrumentations, medical and agriculture sciences, imaging and sensing of concealed items, time-domain spectroscopy, defense applications, earth and basic sciences. The broad application area of THz gap is due to its unique radiation characteristics which [57]:

- Penetration: The terahertz wave can pass through the different materials with different levels of the attenuation.
- Resolution: The resolution of an image increases with the decrease in the wavelength, and the resolution in the terahertz band is better than that of the microwave regime of the spectrum.
- Spectroscopy: Various solid and gaseous materials exhibit terahertz signature in 0.5–3-THz band and can be used for the detection.
- Non-ionization: Due to the low-power levels, terahertz exhibits low ionization effect on the biological tissues.

- Scattering: The scattering is inversely proportional to the wavelength, and it is low in the terahertz band in comparison with the light wave.

- Intensity: The collimation of the wave is easier in the terahertz regime of the spectrum in comparison with that of the microwave.

Interestingly, terahertz waves provide other important advantages comparing to the microwave and infrared waves, especially in the present systems [58]:

- THz band offers a wider bandwidth.

- The diffraction of the THz waves is low in comparison with that of the microwaves and millimeter waves, which is the advantageous in the line-of-sight and point-to-point links.

- The licenses have been presently allocated up to 250 GHz, and thereafter, it is license free.

- This band offers high degree of information security, especially in the spread spectrum technology.

- In comparison with infrared, THz has low attenuation of the signal in certain atmospheric conditions like fog.

- The time-varying refractive index of the atmospheric path increases the scintillation effect in the infrared links, and it can be reduced in the THz links.

- The significant development to enhance the data rate in the THz wireless systems is rapid due to the possibility of implementing advanced modulation techniques (orthogonal frequency division multiplexing (OFDM), multiple-input multiple-output (MIMO)...).

These interesting properties of the terahertz waves make the electromagnetic THz gap potential candidate for the various scientific and industrial applications.

2.3. Integrated antennas for THz systems

To overcome the limitation caused due to the high loss of the signal in THz wireless systems, different hardware parameters need to be optimized. Among them, there is the need of the further research and development in high performance integrated antennas with light profiles to provide low-loss interconnections and inexpensive terahertz wireless systems.

THz has remained a bandgap due to the scarcity of high power devices but with the fast progress in the field of technology, various THz integrated antennas have been reported to be widely used in wireless systems as a valid alternative solution to the photonic devices which need a more complex photomixing techniques in generating the terahertz waves above 1 THz [59], or the excessively large oscillators generating terahertz signals below 1 THz due to the requirement of high magnetic field [60]. Likewise, the role of the THz integrated antenna in modern wireless systems has gradually increased and found relevant applications in different fields especially sensing and imaging systems. The role of the THz integrated antenna in wireless systems is easily understood with the help of *Friis* and Brown analysis [61, 62]. The power supplied to the load of a receiving antenna is given by:

$$P_{out} = P_{in}\left(\frac{\lambda}{4\pi d}\right) G_r G_t F_r\left(\theta_r, \Phi_r\right) F_t\left(\theta_t, \Phi_t\right) \tau \varepsilon_p \qquad (2.1)$$

Where P_{out}, P_{in}, k, d, G_t, G_r, $F_r(\theta_r, \Phi_t)$, $F_t(\theta, \Phi_t)$, τ, and ε_p are the output power, input power to the transmitting antenna, wavelength, distance between the transmitter and receiver, gain of the transmitting antenna, gain of the receiving antenna, position in spherical coordinate system of the receiving antenna, position of the transmitting antenna, path power transmission factor, and

polarization coupling efficiency, respectively. From this equation, it is noticed that the output power to the load is directly proportional to the gain of the transmitting and receiving antenna. With the help of the reciprocity theorem, the antenna can be used for the transmission and reception purpose at the same time [61]. Under this condition, the output power is proportional to the square of the antenna gain. The antenna gain and directivity are related by the following equation where subscript indicates the transmitting condition.

$$G_t = \frac{P_{rad}}{P_{in}} D_t \tag{2.2}$$

From the second equation, it is obvious that the directivity of the antenna is proportional to the gain and the terahertz link must be directional to penetrate through the hostile environmental effect. It is interesting to mention that even before the conceiving the idea of terahertz communication, due to the potential advantages of this band of the spectrum, various terahertz antennas were developed for the other scientific applications.

Integrated lens and helix antennas embedded in silicon wafers [62] are the most popular at terahertz frequencies. These kinds of antennas have been essentially used for the detection of terahertz signals, and can be easily fed by different primary sources, thus their analysis reveals two main things:

- The directivity of the antenna increases with the increase in the extension length and the size of the lens.
- The directivity also depends on the relative dielectric permittivity of the material used in the lens.

In general, silicon (ε_r = 11.9) is used as the dielectric material in such kinds of antennas, which behaves as a collimator and theoretically any kind of the primary source may be attached to it. However, with the increase in the extension length, the compactness of the antenna is disturbed and it is difficult to integrate all kinds of the primary sources to the antenna based on silicon substrate. Due to

the use of the high-dielectric permittivity material, the shock wave which occurs due to the difference between the dielectric permittivity of the air and substrate cannot be ruled out. The analysis of an antenna based on a low-dielectric permittivity material has been demonstrated that the length of the extension must be increased to meet the specific directivity requirement. The high directivity of the antenna can also be achieved by using the low-relative dielectric permittivity material, but it is at the cost of the compactness. Further, due to the less density, low-permittivity substrate antenna offers the low payload to the system in comparison with the antenna designed on the high-relative dielectric permittivity substrate. The main feature of these kinds of antennas is the same plane feeding mechanism. The feeding may be given by the coplanar waveguide (CPW) [63].

The integrated horn antenna [64] has also been reported in which the horn consists of two stacked wafers. The horn cavity is formed on the first wafer, and a dipole is placed at its back. The second wafer behaves as a reflecting surface. In spite of the existence of the various forms of terahertz antenna, Koch [65] is in the opinion of the use of waveguide-fed horn and planar antennas for the future wireless systems. The waveguide-fed horn antenna offers excellent performance and low loss. However, the planar antenna structure offers a greater potential, which have integration compatibility with the planar devices.

The simplicity in design, low cost, and low profile of the planar antenna motivates the designers to develop the methodology to enhance the directivity of the microstrip antenna to meet the future wireless requirements. Various microstrip terahertz antennas have also been studied in recent past in which design issues of this kind of the antenna have been addressed. In most of the cases, the directivity of the antenna remains low; however, it can be increased by using the array of antennas in place of single patch. Microstrip antennas may find suitable applications in the surveillance and systems [66, 67].

Finally, THz integrated antennas need an important design attention due to their compactness to make them suitable to operate above 1 THz frequency and

find potential applications in THz signal generation where THz links are feasible. For this, it is better to employ effective manufacturing processes to enhance their efficiency, sensitivity, and power-generating capability. MEMS processing constitute a very attractive technology for developing high performance integrated antennas operating in higher frequencies lying in the terahertz regime of the electromagnetic spectrum [68].

2.4. Micro-electromechanical systems for THz integrated antennas

As the size of radiators is reduced to enhance the performance of THz frequency links, they cannot collect much of the terahertz radiation, and, therefore, the detection of such radiation becomes difficult. MEMS antennas provide in fact efficient radiation elements of large coverage that are highly recommended to manipulate THz waves due to their low profile, excellent electromagnetic response and the fact that they can be softly integrated with electronics. They are realized in a single-crystal silicon substrate and can be fabricated using conventional bulk micromachining relying on available focused ion beam technique, and it is usual practice to integrate the feeding into the dielectric substrate. MEMS antennas have been used in many applications. They have been used in the design of high receivers for astronomical, atmospheric, and imaging arrays. In general, the size of MEMS antennas is comparable to the wavelength of the THz radiation being detected to achieve a fast response. The antenna collects the radiation and supplies an electrical signal to be processed. So far, several antenna geometrical configurations have been used to serve THz wireless systems [69, 70].

2.4.1. Investigation of silicon-based microelectronics process

With the emergence of new applications for wireless systems operating in the electromagnetic THz gap, a new generation of reliable MEMS antennas is developed to meet the specific requirements of this unique spectral. Many new

processes of silicon-based microelectronics become therefore very useful for designing such compact antennas by implementing silicon wafers to widely preserve the well-known advantages of micromachining technologies such as high precision, high performance, and self consistency [71].

Therefore, MEMS technology after several years of scaling is approaching a number of fundamental limitations that can only be addressed by the use of silicon-based processes. To meet the challenging MEMS technology requirements as well as staying cost effective, major efforts have been expended to combine the low cost and well-established silicon-based processing attributes, enable performance superior to that achievable with compound semiconductors such as sapphires (SiC, InP, or GaAs), and realize many advantages for silicon substrates summarized in:

- Silicon substrate has high thermal and electrical conductivity, and mechanical hardness, which is better for very large-scale device integration.
- Silicon substrate would significantly reduce manufacturing costs compared to sapphire substrates.
- Silicon substrate has potential wafer-size expansion, which would further reduce the manufacturing process costs.
- Silicon substrate has excellent low-field and high-field electron transport properties.
- Silicon substrate has ultrahigh-speed switching at very low supplied voltages.
- Silicon substrate has realized the ultimate vision of high switching activity factor low voltage and high speed with the functional density advantages.

The lack of large area of the substrates and the high price, e.g. sapphires, create a high cost and throughput chokehold on compound semiconductor foundries. In many cases, a superior compound semiconductor technology has little or no commercial market simply based on the high cost of manufacturing. Silicon substrate offers in fact a low price as compared to sapphire substrates, high crystalline perfection, availability of large size substrates, and all types of conductivity. Large-area silicon substrates can simply act as a building block to further lower the fabrication process cost of integrated devices. However, there are still many issues that deal with integration of MEMS structures with silicon-based microelectronics:

- Lattice mismatch causes a high-density dislocation in the substrate, which may reduce significantly usable area and decrease its quality.

- Thermal mismatch is a major problem, which causes strain, defects, and even cracks during the preparation and operation of the substrate: The thick epilayers on silicon substrates for device fabrication is difficult to be achieved without cracks.

- Lack of semi-insulating silicon substrate, which may lead to parasitic capacitance effects during high-frequency operation.

Many different techniques have been developed to overcome these major mismatches with great success, the fact that excellent device performance has been achieved, and are starting to become commercially available. Accordingly, FIB stress-introducing technique is now coming to fruition after years of promise as excellent solution to further fabricate high quality MEMS structures. With an approach that directly integrates the MEMS structures in the silicon wafer, only one wafer is processed to achieve a finished chip.

FIB process enables an easy etching of MEMS structures which are formed under thin silicon layers that take place well below the silicon melting point, and undergo a transformation with high growth temperatures. MEMS structures

grown on silicon using FIB technique gain numerous advantages divided mainly into, a diminution in the absorption effect, enhancement in the operation quality, and expansion in the voltage yield that gained big interest in recent years [72].

2.4.2. Study of THz antennas on electrically thin and thick silicon substrates

At microwave frequencies, because the wavelength is relatively large, it is easy to fabricate antennas with thin dielectric substrates. However, at terahertz frequencies, the substrate thickness becomes too small to handle. The silicon substrate tends to be too fragile to support the antenna device for reliable operation. Indeed, THz antennas are different than microwave ones in that the surface impedance of the metals is much higher at very high frequencies due to the skin effect. This fundamental difference causes losses that can slow the antenna currents so that the antenna does not radiate very efficiently. The high surface impedance is not a constant, but depends on the characteristics of the incident waves, antenna section shape, and silicon substrate thickness. Accordingly, the antenna should be chosen as a compromise between bandwidth and efficiency in order to take the advantages of the large radiation and fast response. For this, the antenna can be realized by using electrically thick silicon substrate to keep a fast detection. However, for good radiation, the silicon substrate thickness must be much smaller than the operating wavelength ($\leq \lambda/20$) to avoid substrate losses [73].

Interestingly, antennas deposited on silicon wafers couple energy primarily into the dielectric platform rather than into the air. When compared to a wave in air, the wave on the antenna is a slow wave and excites evanescent modes. Compared to a wave in the dielectric, it is a fast wave and excites radiation fields. Therefore, for silicon substrates with high dielectric constants (11.9), most of the energy ($\geq$ 90%) is confined in the dielectric wafer instead of being radiated in free space. Also, the efficiency of the antenna is limited by the amount of power lost to surface waves. As the silicon substrate becomes electrically thicker, more

surface modes can exist, which can have a detrimental effect on antenna performance. Moreover, the finite size of the silicon substrate diffracts these surface waves from the substrate edges, and this affects the sidelobe level, polarization, and main beam shape [74].

Another crucial aspect for a good design is to reduce loss due to dielectric heating that requires special substrate geometry to achieve high efficiency. Several techniques have been employed over the years to reduce losses and enhance coupling of radiation from the antenna to free space. One of the earliest approaches is to utilize a lens of the same dielectric constant attached to the silicon substrate, called substrate lens. This technique completely reduces substrate mode losses and diffraction at the edges [75]. In order to reduce reflection losses at the air/dielectric interface, a matching layer is required with the design of the substrate lens. Numerous antenna structures have been studied and used with a substrate lens, including helical antennas, offering an attractive alternative to bowtie antennas particularly for wideband applications [76]. Thereafter, other approaches are used to handle the substrate mode problem by removing the substrate and integrating the antenna on a thin dielectric membrane. The membrane is so thin compared to the free-space wavelength that the antenna effectively radiates as if it were in free space. Other techniques have also been developed to reduce or even eliminate surface waves. One of these techniques is based on the use of photonic bandgap substrates. According to this technique, holes in certain arrangements are drilled in the substrate to create certain periodic patterns that result in an increased efficiency and directivity [77].

2.4.3. MEMS helix antennas for THz applications

The proficient use of different MEMS processes has recently provided a new class of integrated antennas for THz applications, especially helix antennas embedded in silicon wafers which have generally inherent bandwidth properties, and firm structural characteristics. Helix antennas of circular or square section based on MEMS technology can be applied in many ways, the example described

below in figure 2.2 illustrates a practical case of a helix antenna successfully designed for the 0.1 to 2.7 THz range [73] presenting a great achievement that promotes the different theoretical aspects of modeling MEMS helix antennas for THz wireless systems.

Figure 2.2 – Scanning electron microscopy (SEM) photograph of THz helix antenna structure consisting of *40-um* square spirals around a center post

The terahertz antenna structure is fabricated by forming fibers that can be grown into complex three-dimensional structures directly on the substrate. Terahertz radiation detection device can be realized with MEMS micro-bolometers that convert received terahertz radiation into a change in resistance. Arrays of these antenna-bolometer pairs can be also fabricated on the same substrate to realize a terahertz imaging device. The antenna conductor can be coiled in the clockwise or counterclockwise direction depending on the polarization requirements. The slent angle, α, provides a measure of how tightly the helix is wound. For a given circumference, smaller values of α imply closer turn spacing. The operation of the THz helix antenna can be described in terms of transmission and radiation modes. Transmission modes describe how an

electromagnetic wave propagates along the helix. At low frequencies, where the wavelength is much longer than the helix circumference, regions of positive and negative charge in the current distribution are separated by many turns. Because of this separation, the electric field becomes directed mainly along the axis of the helix.

At frequencies where the wavelength approaches the value of the helix circumference, higher order transmission modes occur. The radiation field pattern depends on the radiation modes excited. There are mainly two modes: The normal mode and the axial mode. The axial mode antenna is the most widely used mode. Actually, the axial mode helical antenna is the most widely used circularly polarized antenna, either in space or on the ground. For the axial mode to occur, the frequency of operation must be such that the helix circumference is within the range 0.75 to 1.33 λ. The axial mode is characterized by a symmetric main lobe directed along the axis of the helix.

On the other hand, for the normal mode the maximum field strength occurs in the direction perpendicular (normal) to the helix axis. The radiation resistance in this case is very low and hence the normal mode helix is not a very efficient antenna. For this discussion, only the axial mode helical antenna is considered. The input impedance of the axial mode antenna is mostly resistive and is given by:

$$R = 140\left(\frac{X}{\lambda}\right)\Omega \tag{2.2}$$

This is an empirical formula used for calculating the impedance of a helix antenna. It does not take into account the effect of skin depth, but since no closed-form solution exists, it is a reasonable approximation. It is this impedance that can be used for matching purposes with a waveguide or bolometer. More specifically, the dimensions of the helix at 1 THz (λ *=300* μm) are: *D = 15 um, S = 81.3 um, N = 5,* α *= 13°,* R_c *= 0 um, C =* 47.12 um, and H_h *=406.5 um.*

Finally, the dimensions providing the most uniform characteristics over the greatest frequency range of a THz MEMS helix antenna will be referred to as optimal dimensions. This presents the purpose of many research works over the past decades as well as constitutes the subject of this work which aims to develop the MEMS helix antenna design in a way it provides high performance and interesting properties for wide or multiband THz applications.

Chapter Three

Computational **E**lectromagnetic **T**echniques for **O**ptimizing **T**Hz **M**EMS **H**elix **A**ntennas

3.1. Introduction

The very special demand for novel integrated antennas with excellent performance for diverse THz frequency ranges grows for the foreseeable future, and requires effective electromagnetic optimization processes of enhancing already established designs or developing newly proposed models. Recently, micro-electromechanical systems processing has been identified as a very promising technology for revolutionizing a large class of antennas with THz waves by combining silicon-based microelectronics with complex computer aided design tools to model accurately the physical behaviour of such 3D micro-devices, and meet the very specific requirement of reducing the long and expensive development cycles, and reaching interesting characteristics including compact size, low profile, good directivity, wide bandwidth, and attractive applications thanks to the advanced electromagnetic optimization techniques [78].

The final chapter describes for the THz wireless access systems novel designs of highly miniaturized helix antennas based on MEMS technology with particular emphasis on major optimization challenges facing the device structure complexity. The different antenna geometric structures are developed using 3D HFSS for modal electromagnetic analysis, and accurate CAD techniques for active electromagnetic optimization. Each time, the optimization strategy aims to vary the antenna geometric structure and maximize its electromagnetic response with a high accuracy for the selective band of frequencies by training the samples and minimizing the error from FEM based simulation tool. Excellent antenna performance and high structure precision are finally achieved by modifying and rectifying different tunable parameters embedded in silicon platform including the helix form parameters, and feeding line variables. This technical chapter presents with details:

- Evolutionary optimizers for developing THz MEMS helix antennas.
- Stochastic solvers for designing THz MEMS helix antennas.

- Automatic strategists for modeling THz MEMS helix antennas.

3.2. Evolutionary Optimizers for developing THz MEMS helix antennas

MEMS processing becomes a promising micromachining technology for conceiving complex antenna designs with excellent performance, and a high μm-level precision to offer very good applications for different frequency ranges of the electromagnetic THz field, relying on advanced software tools and fast optimization techniques. Accordingly, HFSS-based Quasi-Newton (Q-N) and Sequential Non Linear Programming (SNLP) approaches lead to excellent electromagnetic solutions with high accuracy and good response.

In the first section, a novel geometrical configuration of an ultra wideband (UWB) MEMS helix antenna using HFSS software is described. The optimization procedure relies on Q-N and SNLP algorithms to offer fitness functions for excellent bandwidth learning and fast configuration evaluating. The antenna occupies a very compact volume of 79×80×152 μm ($0.960\ 10^{-3}$ mm^3) including the silicon substrate having a thickness of 9.3 μm and a dielectric constant of 11.9. The explored MEMS helix antenna design is validated by demonstrating optimal results in terms of return loss properties in comparison to the previous optimized structures [79, 80].

The antenna with optimized parameters operates in a wide bandwidth from 2.5 to 5 THz and shows good radiation patterns, very low reflection coefficients with less than -20dB to -88dB, and excellent voltage standing wave ratios of less than 1.15 to 1.00 over the entire bandwidth. The compact optimized MEMS antenna is finally simulated by covering an ultra wide range of frequencies of 8.7 THz extending from 1.2 to 9.9 THz and shows very good performance resulting in a low reflection coefficient of less than -15dB for the entire bandwidth, offering a large field for THz wireless applications.

3.2.1. Geometric structure of the UWB MEMS helix antenna

Electromagnetic THz gap remains one of the least explored regions of the frequency spectrum for diverse applications, for the reason that it claims a deep knowledge of radiofrequency engineering and semiconductor physics. The size of a THz antenna is expected to closely relate to wavelength, which is about 30 μm (10 THz) to 3 mm (0.1THz) [81].

Micro-electromechanical systems therefore present a suitable technology for manufacturing compact THz antennas with low profile, wide bandwidth, and large radiation. Several processes to fabricate THz antennas employing MEMS technology have been reported in recent years, in which the fabrication process is highly precise and antennas with compact size become soft to be integrated with other devices [82].

FIB process provides a great flexibility to explore such MEMS antennas in micrometer scale and makes possible to fabricate 3D structures with low cost by employing a large irradiation area of FIB on suspended film structures with the advantages of high controllability and repeatability [83, 84].

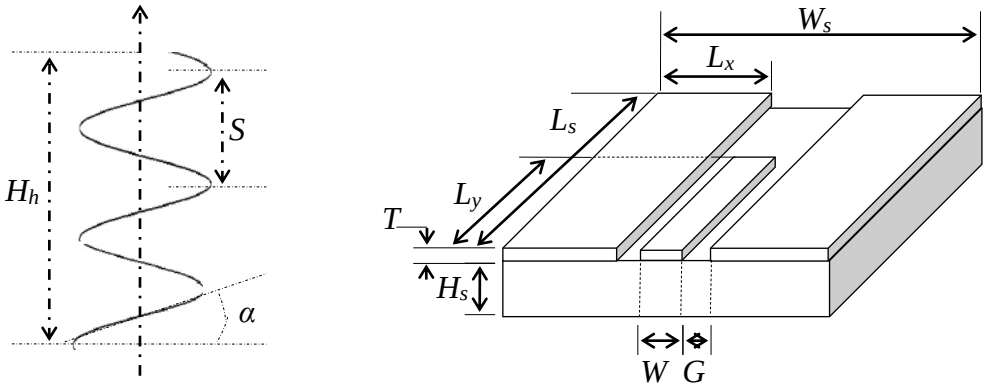

(a) **(b)**

Figure 3.1 - Geometric structure of the THz UWB MEMS helix antenna, (a) schematic diagram of the helix, (b) 3D model of the CPW feeding

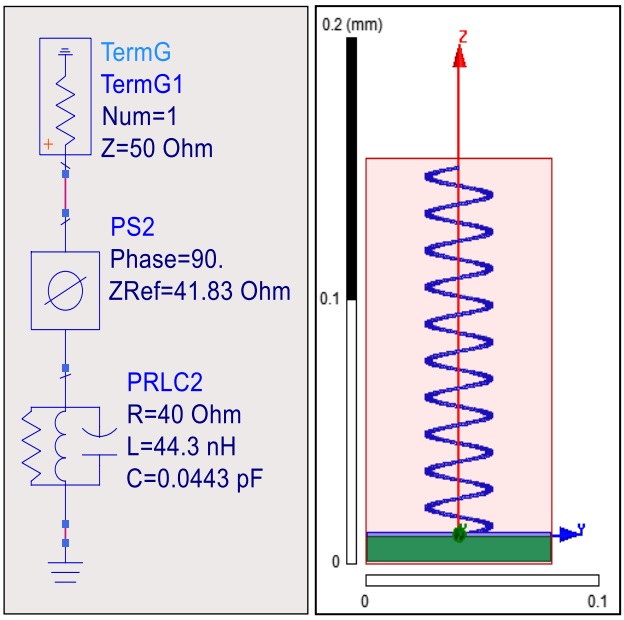

(a) **(b)**

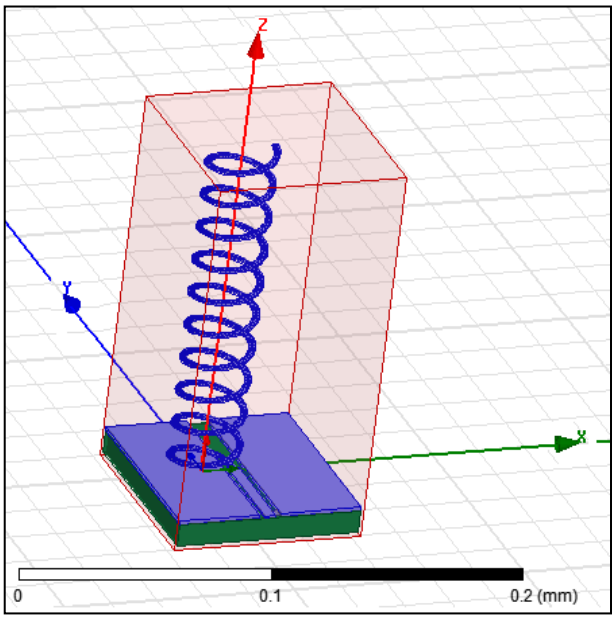

(c)

Figure 3.2 – THz UWB MEMS helix antenna equivalent circuit (a) in ADS, 2D (b) and 3D (c) models in HFSS

The proposed MEMS antenna is realized in a single-crystal silicon substrate and can be fabricated using conventional bulk micromachining relying on available FIB stress-introducing technique [85]. Figure 3.1 illustrates the

geometric structure of the UWB MEMS helix antenna proposed for the optimization and development. Figure 3.2 shows the equivalent circuit (a) of the optimized UWB MEMS helix antenna implemented using advanced design system (ADS) simulator, the two-dimensional cross-section (b) and three-dimensional view (c) of the antenna using HFSS software which clearly indicates that the antenna reaches a high level of precision leading to interesting characteristics including large bandwidth and low reflection coefficient. The proposed structure uses mainly the set of equations demonstrated in [79] to calculate the helix parameters. The antenna is fed with a coplanar waveguide and working in transmission mode.

3.2.2. Antenna optimization and development

The proposed antenna design is firstly simulated by HFSS software which constitutes an interactive tool for computing the basic electromagnetic field quantities and analyzing the electromagnetic behavior of the structure within FEM [7] to understand the physical problem to be optimized.

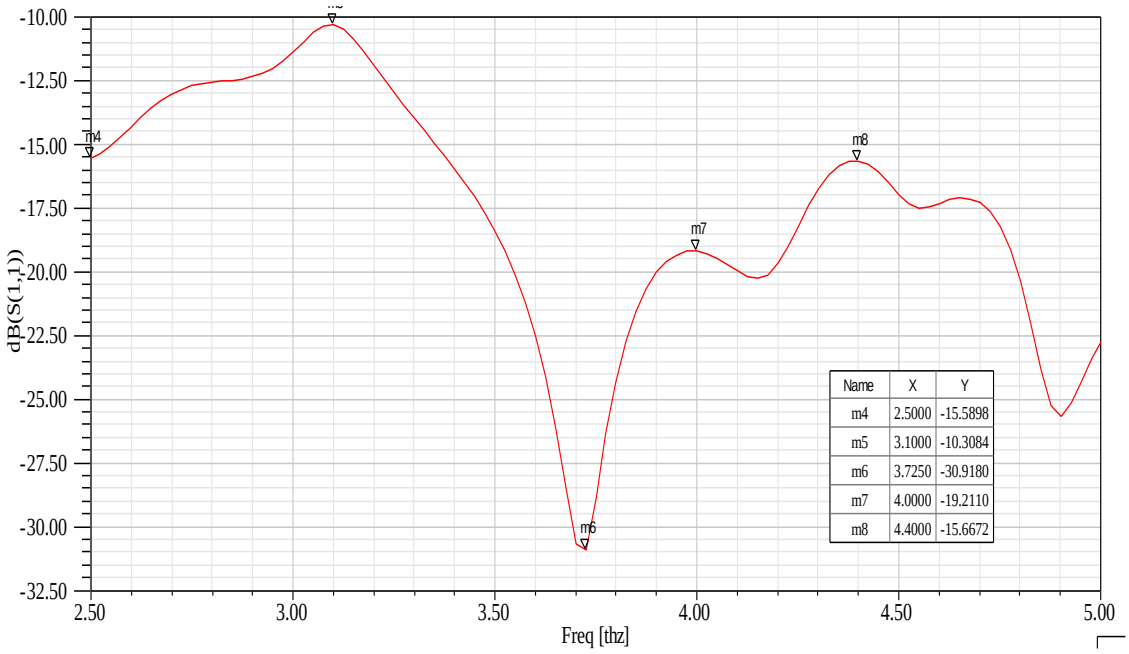

Figure 3.3 – Simulated RL graph of the proposed UWB MEMS helix antenna with initial parameters in 2.5 – 5 THz

Figure 3.3 presents the simulated return losses of the proposed geometrical configuration for a frequency range from 2.5 to 5 THz. As it is observed, geometric parameters initially proposed for the analysis show less acceptable performance which needs to be more enhanced. The structure is then optimized by coupling Q-N and SNLP methods in order to improve the antenna performance, and achieve a high μm-level precision of the helix form parameters, CPW feeding characteristics and silicon platform dimensions.

3.2.2.1. Quasi-Newton optimization

First, Quasi-Newton optimizer is employed to find a minimum or maximum of the cost function which relates three basic parameters in the model, including the helix diameter (D), CPW width (W), and silicon thickness (H_s) to the return loss properties. This choice is mainly based on selecting parameters exhibiting a smooth characteristic and little numerical noise.

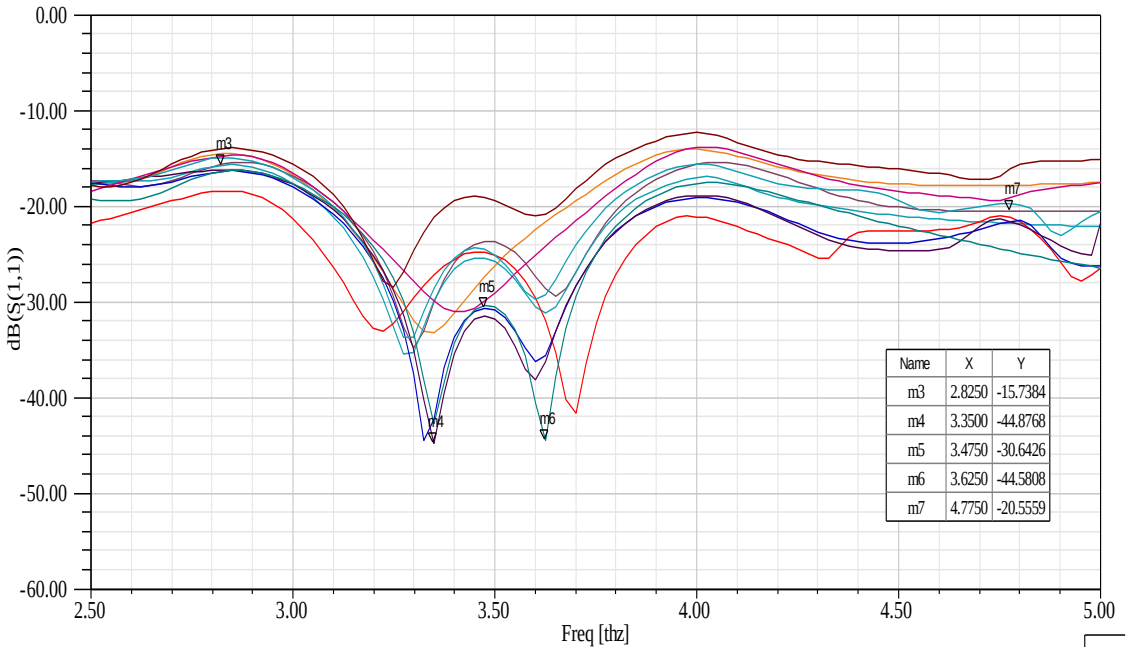

Figure 3.4 – Simulated RL graph of the optimized MEMS helix antenna using HFSS-based Q-N optimizer in 2.5 – 5 THz

This technique works to approximate locally the optimization parameter values that will be placed back into the original function and used to calculate a gradient which provides a step direction and size for determining the next best

values in the iteration process. However, this approach suffers from two fundamental problems: The first issue is the possible presence of local minima; once the Q-N optimizer has located a minimum, this technique will locate the bottom and will not search further for other possible minima and not a good global solution to the problem. The second issue is numerical noise; the calculation of the parameter values involves taking the differences of numbers that get progressively smaller.

At some point, the numerical imprecision in the parameter calculations becomes greater and the solution will oscillate and may never reach convergence. For this, to use the Q-N optimizer effectively, the starting point of each parameter optimization is chosen close to the expected minimum displayed by the primary simulation based on the understanding of the physical problem being optimized. The Q-N optimizer begins then to vary the value of the selected parameters on the basis of getting a minimum or maximum of the cost function to overall simulation goals. Figure 3.4 shows the simulated return losses of the optimized antenna design using Q-N technique which shows that the antenna configuration begins to present good performance for the same frequency range with low return losses of less than -15dB to -44dB.

3.2.2.2. Sequential Non Linear Programming optimization

Next, in order to achieve a high level of performance of the antenna design, Sequential Non Linear Programming optimizer is further added to analyze four additional parameters including the helix pitch (S), helix turn number (N), CPW gap (G), and CPW thickness (T). The antenna height (H_A) and the substrate width (W_s) will be automatically optimized relating into these parameters. The main advantage of SNLP optimizer over Q-N optimizer is that it handles the optimization problem in more depth, and assumes that the optimization variables span a continuous space and take any value within the allowable constraints and within the numerical precision limits of the simulator. The SNLP optimizer estimates the location of improving points with an accurate finite element approximation (FEA) with response surfaces (RS) and light evaluation of the cost

function. This allows a faster practical convergence speed than that of Q-N optimizer.

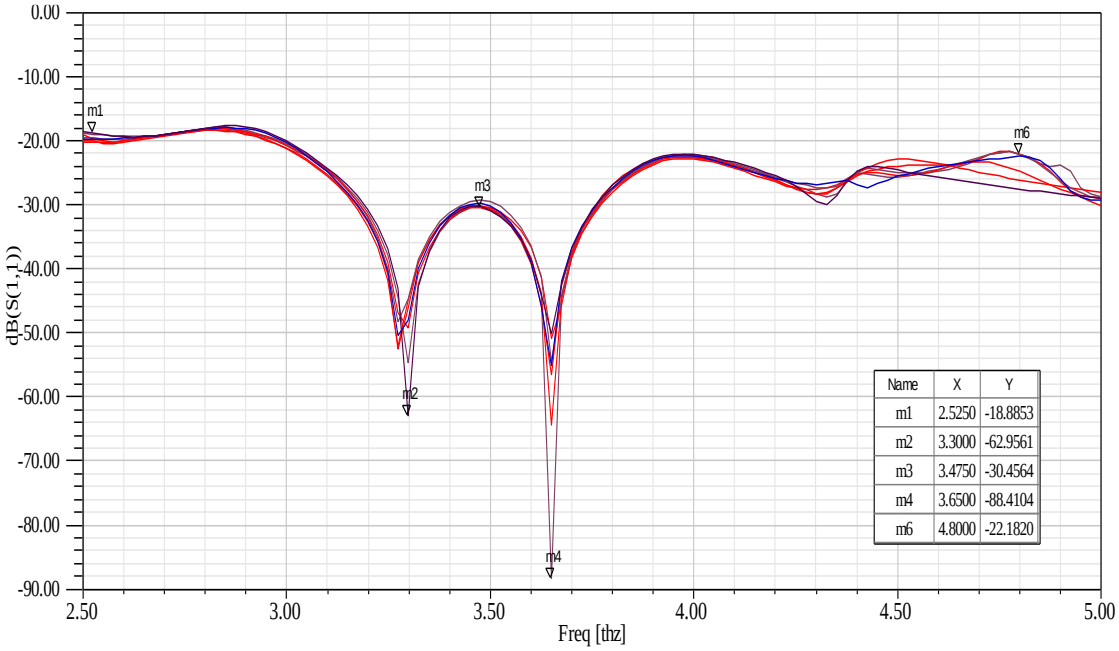

Figure 3.5 – Simulated RL graph of the optimized MEMS helix antenna using HFSS-based SNLP optimizer in 2.5 – 5 THz

Another advantage is that SNLP optimizer allows the use of nonlinear constraints, making it much more general than Q-N optimizer. The SNLP optimizer creates the response surface using a polynomial approximation from the FEA simulation results available from past solutions. The response surface is most accurate in the local vicinity. The response surface is used in the optimization loop to determine the gradients and calculate the next step direction and distance. The response surface acts as a surrogate for the FEA simulation, reducing the number of FEA simulations required and greatly speeding the problem. Convergence improves as more FEA solutions are created and the response surface approximation improves. As illustrated in Figure 3.5, the antenna geometry obtained from the SNLP technique presents very low reflection coefficients with less than -18dB to -88dB, resulting in a significantly high performance for the selected band of frequencies.

Figure 3.6 shows the simulated return loss (a), radiation pattern (b), and voltage standing wave ratio (c) graphs of the optimized MEMS helix antenna design finally obtained using HFSS based on Q-N and SNLP solvers [86] that indicates excellent performance for the developed antenna design interpreted by very low return losses of less than -30 over the central frequency band.

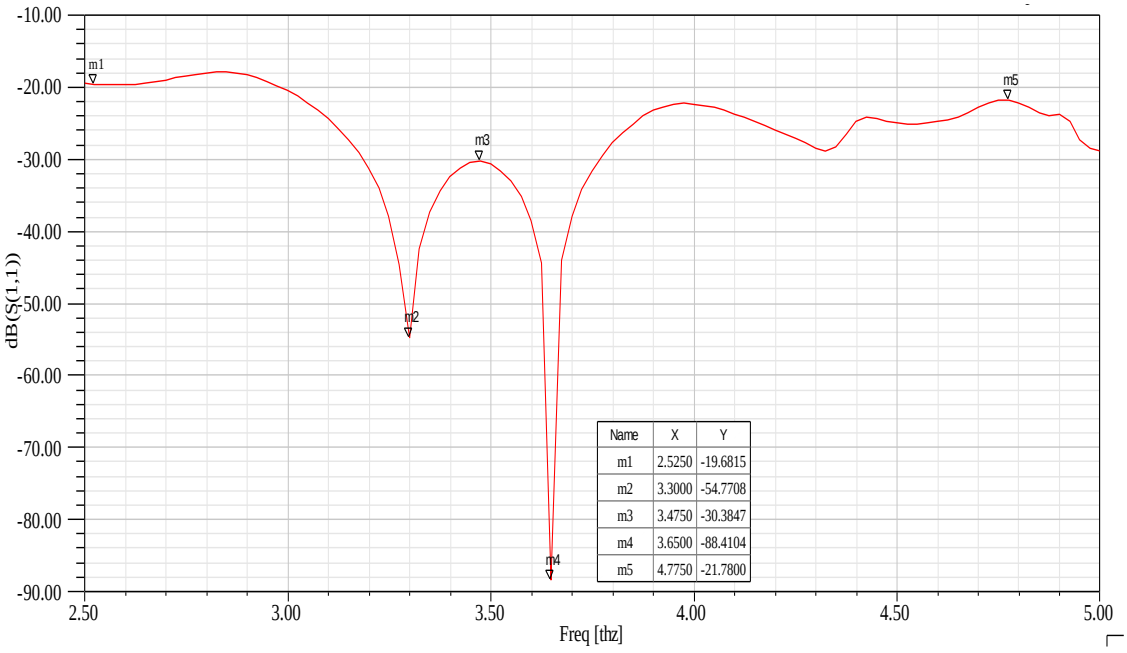

(a)

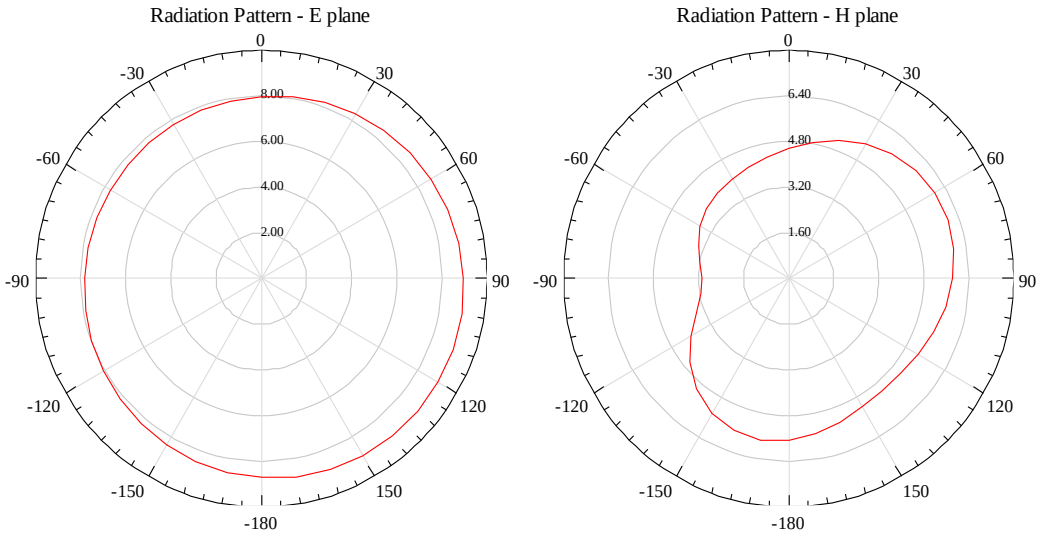

(b)

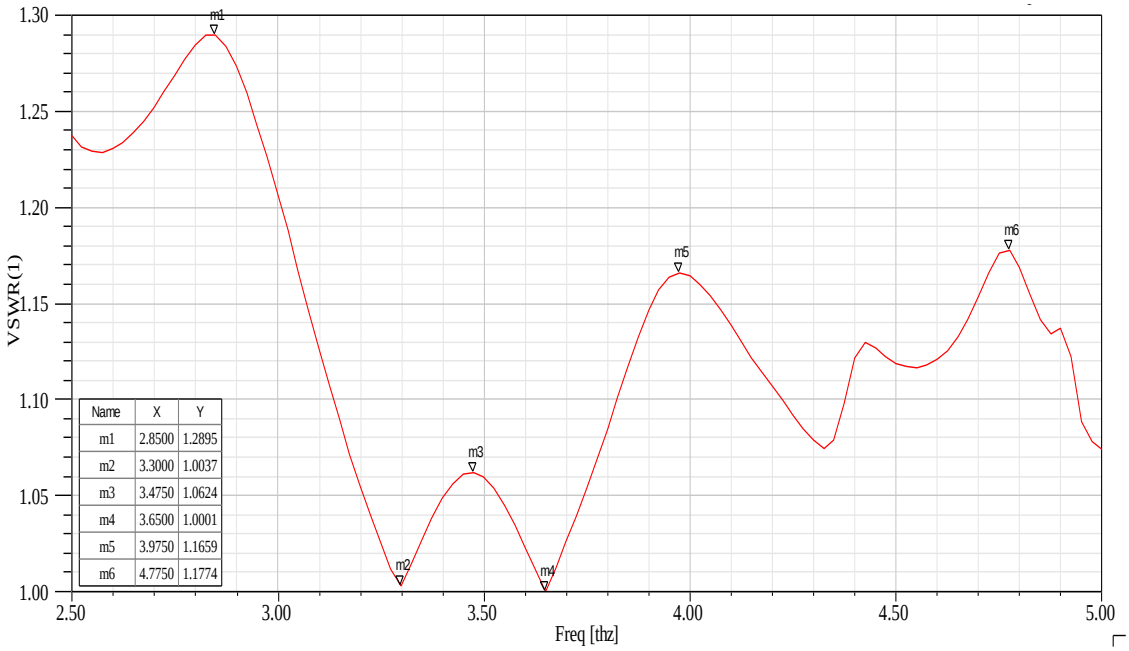

(c)

Figure 3.6 – Simulated RL (a), radiation pattern (b), and VSWR (c) graphs of the optimized THz MEMS helix antenna using HFSS-based evolutionary optimizers

Thus, the radiation patterns, both in E-plane (xoz-plane) and H-plane (yoz-plane) of the antenna transmission mode at the central frequency (3.5 THz), keeps good directivity with slightly bending in the side lobes of yoz-plane due to the fine modeling process. This demonstrates the high efficiency of the applied optimization strategy to provide a good geometrical accuracy and excellent electromagnetic response for the developed antenna design for a very wide THz comparing to previous research works. The promising results obtained from the efficient electromagnetic optimization are then compared to the results previously achieved in [79, 80].

As shown in figure 3.7, it is clearly observed that the new THz MEMS helix antenna geometric characterization developed by HFSS based on efficient electromagnetic optimization comes with very low return losses with closely less than -20dB over the entire frequency band, and less than -30dB over the central frequencies from 3.2 to 3.7 THz, and approximately -55dB and -89dB at 3.20

THz and 3.80 THz respectively, this significantly validates the excellent performance for the proposed THz MEMS helix antenna design improved by Q-N and SNLP optimizers comparing to the previous attempts.

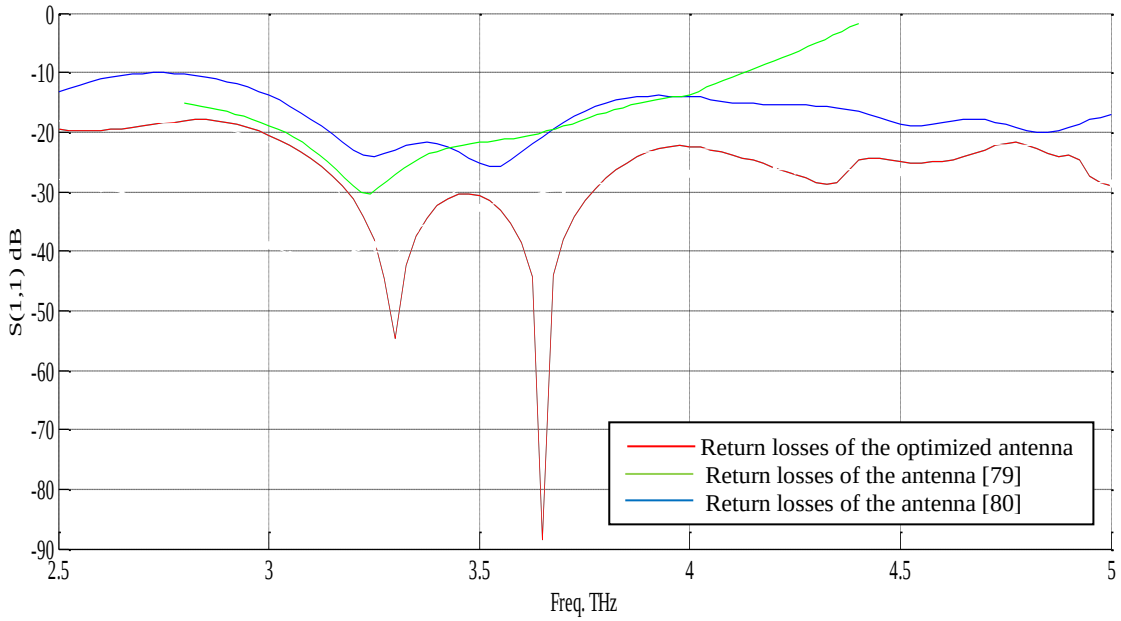

Figure 3.7 - Comparison of RL of the optimized antenna to the antennas [79, 80]

The compact THz antenna design optimized using Q-N and SNLP methods has been tested and simulated covering an ultra wide range of frequencies of 8.7 THz extending from 1.2 to 9.9 THz as presented in figure 3.8. The antenna shows very low return losses of closely less than -15dB for the entire bandwidth presenting a great success in finding useful design with very good performance for UWB wireless products. This demonstrates the advantage of HFSS optimization techniques in offering a more degree of freedom in developing new structures, supporting multiple resonance modes distributed across a large THz spectrum, based on the proposed THz UWB MEMS helix antenna design which offers very good applications for an ultra wide range of frequencies covering more than 87.87% of the electromagnetic THz gap that is highly attractive to support several THz systems such as radar, biomedical, sensing, imaging, space, radio astronomy, and spectroscopy systems. Details of geometrical configuration of the THz MEMS helix antenna optimized in HFSS-based evolutionary optimizers are presented in table 3.1.

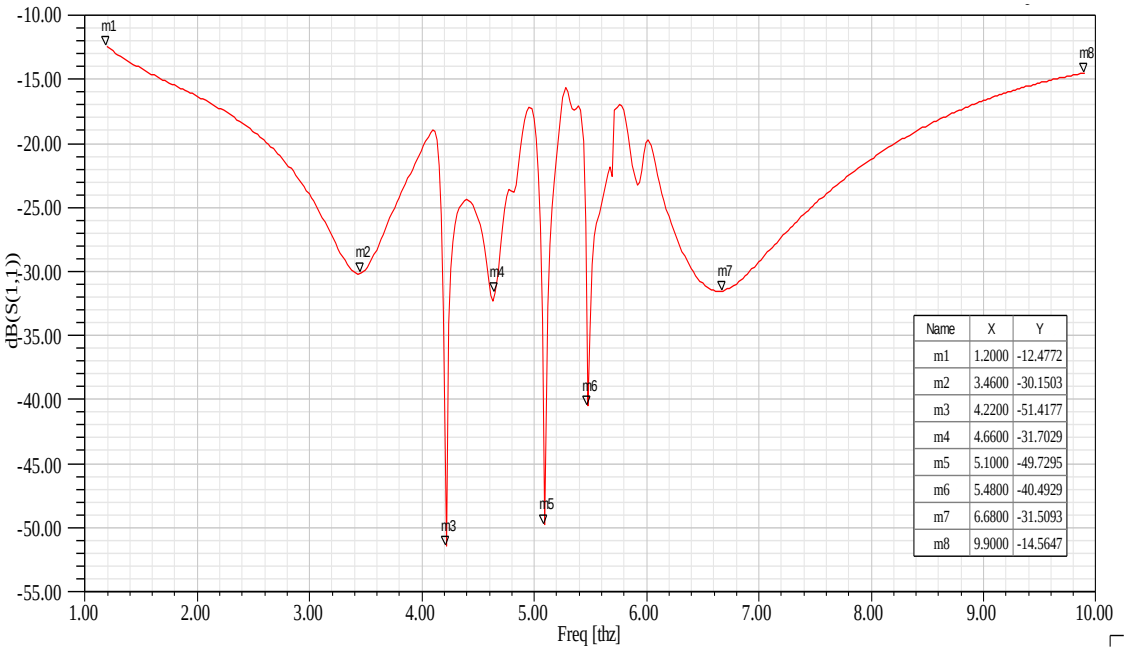

Figure 3.8 – Simulated RL graph of the proposed UWB MEMS helix antenna optimized by HFSS-based evolutionary optimizers in 1.2 to 9.9 THz

Table 3.1 - Characterization of the THz UWB MEMS helix antenna optimized in HFSS using evolutionary optimizers

Section	Parameter	Value (µm)	Specification
Helix form	Diameter (D)	27.3661	Q-N optimization
	Pitch (S)	14.1409	SNLP optimization
	Turn number (N)	10	SNLP optimization
	Slent angle (α)	9.340°	$S = \pi.D.tan\ \alpha$
	Height (H_h)	141.4090	$H_h = S.N$
CPW feeding	Width (W)	4.8659	Q-N optimization
	Gap (G)	2.0937	SNLP optimization
	Width (L_x)	35	/
	Longer (L_y)	40	/
	Thickness (T)	1.5674	SNLP optimization
Silicon platform	Thickness (H_s)	9.2952	Q-N optimization
	Longer (L_s)	80	/
	Width (W_s)	79.0533	$W_s = W + 2(L_x + G)$
Antenna	Height (H_A)	152.2721	$H_A = H_s + T + H_h$

3.3. Stochastic solvers for designing THz MEMS helix antennas

THz MEMS helix antennas employing silicon substrates, have effectively achieved interesting properties including compact volume, light profile, wide bandwidth, high directional gain, and soft integration due to the use of effective CAD tools and accurate automatic techniques that offer excellent solutions to bring the CAD for such high frequency structures to its current state of the art. Accordingly, Genetic Algorithms (GA) [87, 88] present an important class of stochastic optimization technique used to develop new designs and find excellent modeling solutions by imitating the biological processes of reproduction and natural selection to solve for the fittest problems.

Based on the optimized THz UWB MEMS helix antenna design developed using evolutionary optimizers, the second section describes in the fisrt stage a new design of a MEMS horn-shaped helix antenna. The antenna geometry is optimized using GA technique for excellent bandwidth learning and fast configuration evaluating. The MEMS antenna occupies a very compact volume of 79×80×188 μm (1.1881 10^{-3} mm^3) including the silicon substrate having a thickness of 8.5 μm and a dielectric constant of 11.9. The optimized horn-shaped helix antenna design based on MEMS technology has been evaluated using HFSS software; the antenna has been found to resonate at 4.05 THz and show very low return losses less than -20dB to -70dB and excellent voltage standing wave ratios of closely less than 1.20 to 1.00 for a wide frequency band ranging from 3.5 to 4.5 THz, resulting in excellent electromagnetic response and good directivity due to the high geometrical accuracy achieved using effective stochastic solvers in rectifying the antenna parameters.

In the second stage, a novel design of a compact MEMS pyramidal helix antenna is proposed for the wireless access systems using for modal electromagnetic analysis automatic stochastic solvers. In this case, the antenna occupies a highly miniaturized volume of 80×80×217 μm (1.3888 10^{-3} mm^3)

including the silicon substrate having a thickness of 8.14 μm, and a dielectric constant of 11.9. The explored MEMS pyramidal helix antenna design shows good radiation patterns, low return losses with closely less than -15dB to -35dB, and excellent voltage standing wave ratios of less than 1.20 to 1.03. The antenna demonstrates very good performance for a wide range of frequencies covering more than 150 GHz presenting a large area for wireless applications.

3.3.1. Adaptive Genetic Algorithms optimization process

In Genetic Algorithms optimization [89] as illustrated in figure 3.9, the random selection of evaluations to proceed to the next generation has the advantage of allowing the optimizer to jump out of a local minima at the expense of many random solutions which do not provide improvement toward the optimization goal.

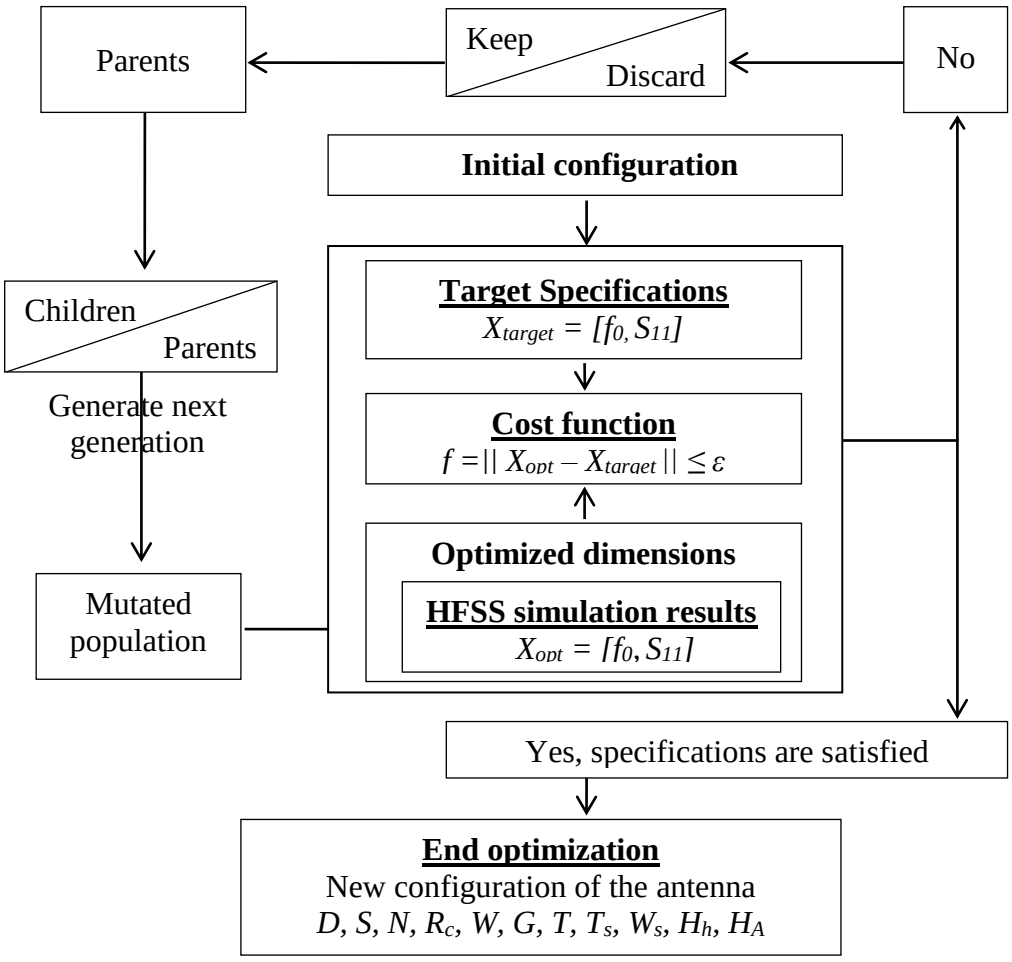

Figure 3.9 - Adaptive GA optimization process

GA optimizer performs the search via a population to population presenting an iterative process that goes through a number of generations to vary the values of the antenna parameters initially selected for the optimization on the basis of finding a minimum or maximum of a cost function parameters to overall simulation goals.

In each generation some new individuals (children) are created and the grown population participates in a natural selection process that in turn reduces the size of the population to a desired level (next generation). When a smaller set of individuals must be created from a bigger set, the GA optimizer selects individuals from the original set.

An iterative process starts then selecting the individuals and fills up the resulting set, but instead of selecting the best so many, using a roulette wheel that has for each selection-candidate divisions made proportional to the fitness level relative to the cost function of the candidate to force the standard formula obtain the physical characteristics, using robust numerical approximations in finding the optimized dimensions. The GA optimizer becomes more effective if the starting point of the parameter optimization is chosen close to the expected minimum displayed by the primary simulation.

3.3.2. MEMS horn-shaped helix antenna

The proposed MEMS horn-shaped antenna is also realized in a silicon platform and fabricated using conventional bulk micromachining based on FIB stress-introducing process. Figures 3.10 and 3.11 present respectively the geometrical structure and the HFSS models of the novel MEMS antenna developed by GA solvers. The initial parameters selected for the MEMS pyramidal helix antenna proposed for the analysis and optimization are those of the UWB MEMS helix antenna developed in the previous section. Figure 3.12 presents the simulated return losses of the initial geometrical configuration of the antenna for a wide frequency range from 0.6 to 1.3 THz.

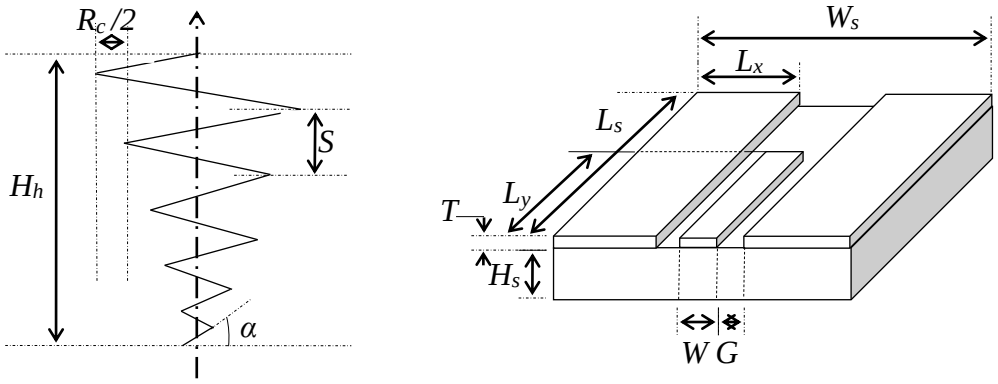

(a) **(b)**

Figure 3.10 – THz MEMS horn-shaped helix antenna geometric structure, (a) schematic diagram of the helix, (b) 3D model of the CPW feeding

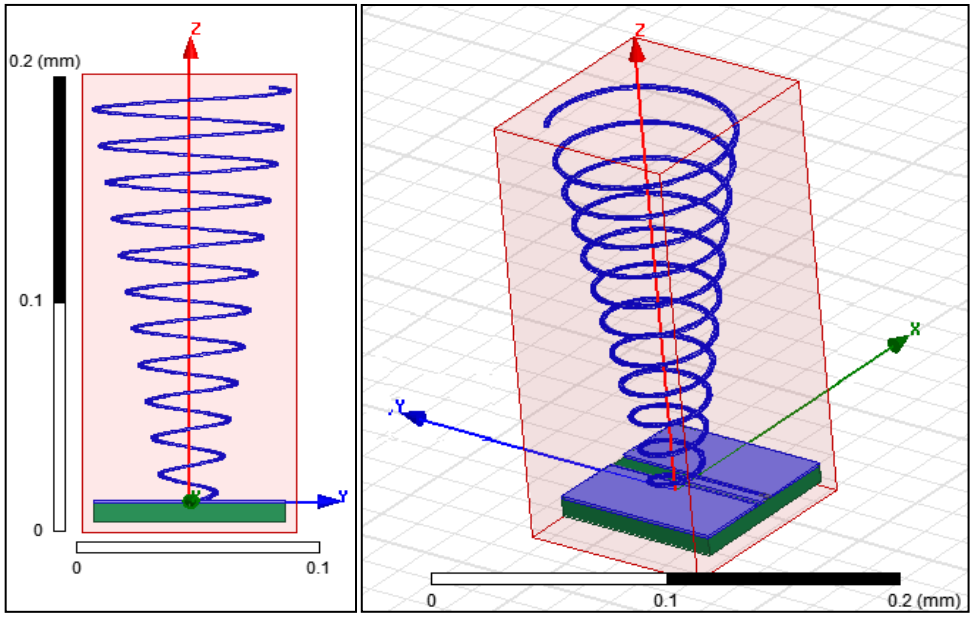

(a) **(b)**

Figure 3.11 - 2D (a) and 3D (b) HFSS models of the optimized THz MEMS horn-shaped helix antenna

The initial antenna parameters show inacceptable performance that needs to be deeply improved using effective stochastic search techniques for the production of a new antenna configuration providing simulation results close to the target design specifications. GA optimizer is used to optimize the antenna

performance due to its parallel architecture and probabilistic nature that uses a type of random selection and applies it in a structured manner.

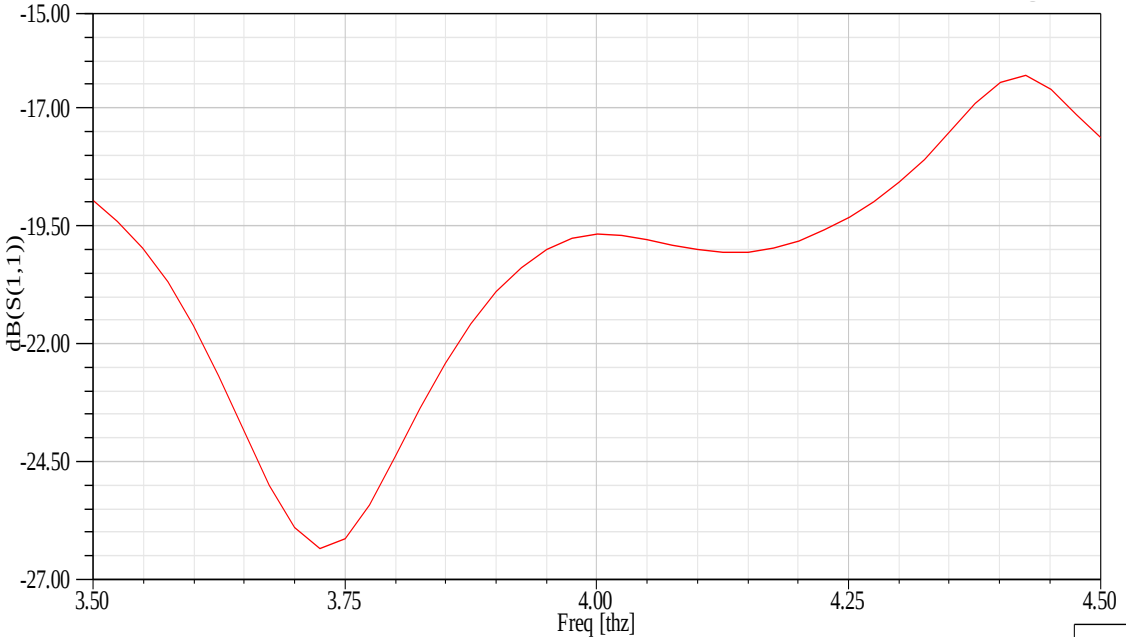

Figure 3.12 - Simulated RL graph of the proposed MEMS horn-shaped helix antenna with initial parameters in 3.5 – 4.5 THz

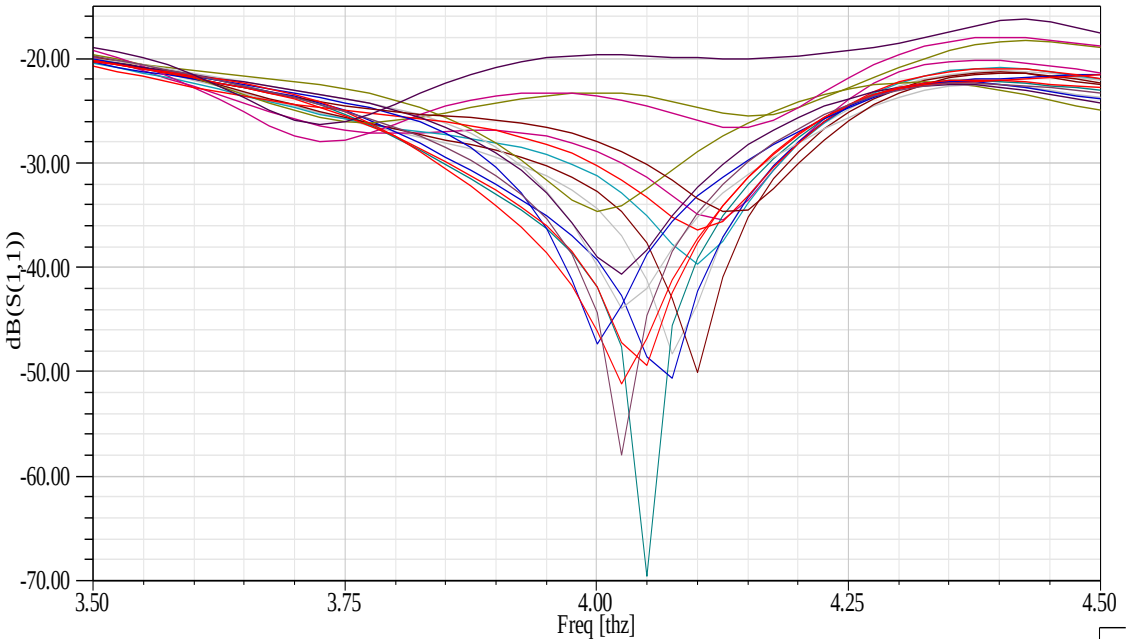

Figure 3.13 - Simulated RL graph of the MEMS horn-shaped helix antenna using HFSS-based GA solvers in 3.5 – 4.5 THz

Figure 3.13 shows the simulated return the MEMS horn-shaped antenna design during the optimization using HFSS-based GA optimizer. The new antenna configuration begins to present very low reflection coefficients after each iteration with less than -20dB to -70dB, resulting in a significantly high good performance for the selected band of frequencies. As illustrated in Figure 3.14 (a, b, c), the optimized antenna finally obtained resonates at 4.05 THz and presents a wide bandwidth of more than 0.8 THz (800 GHz).

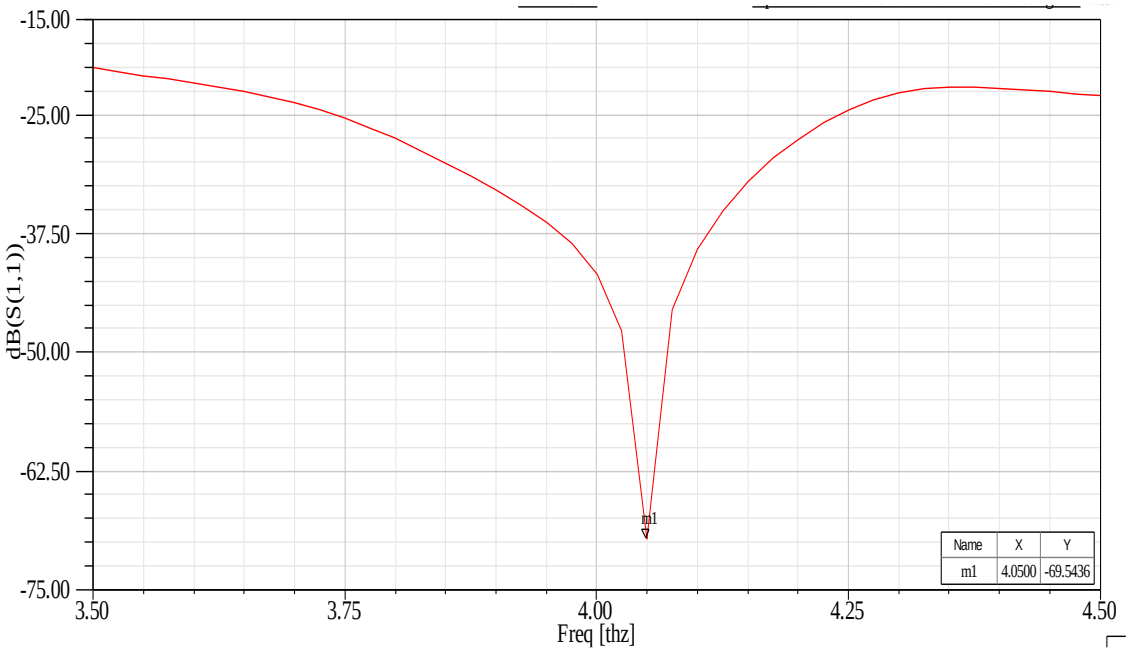

(a)

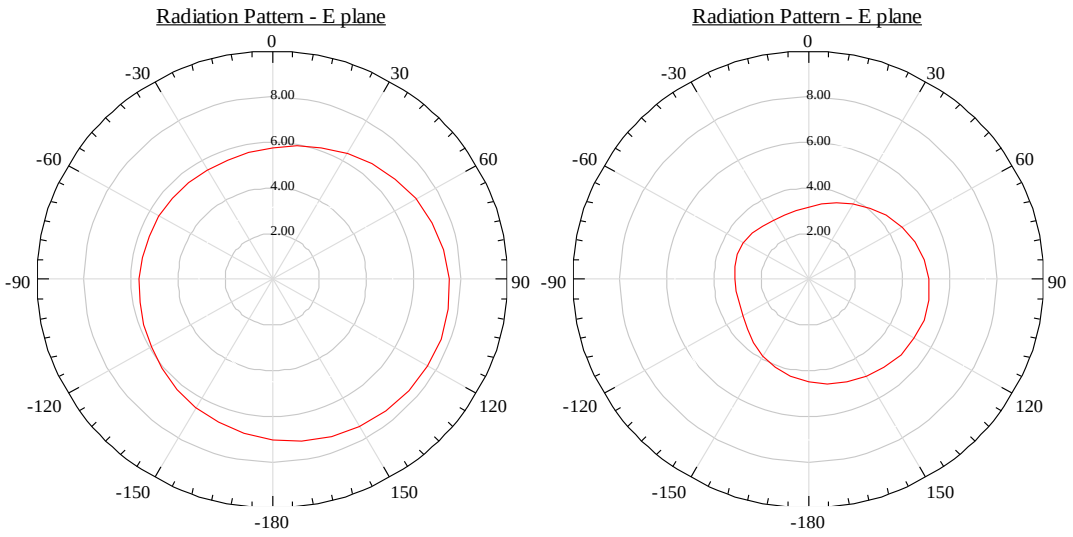

(b)

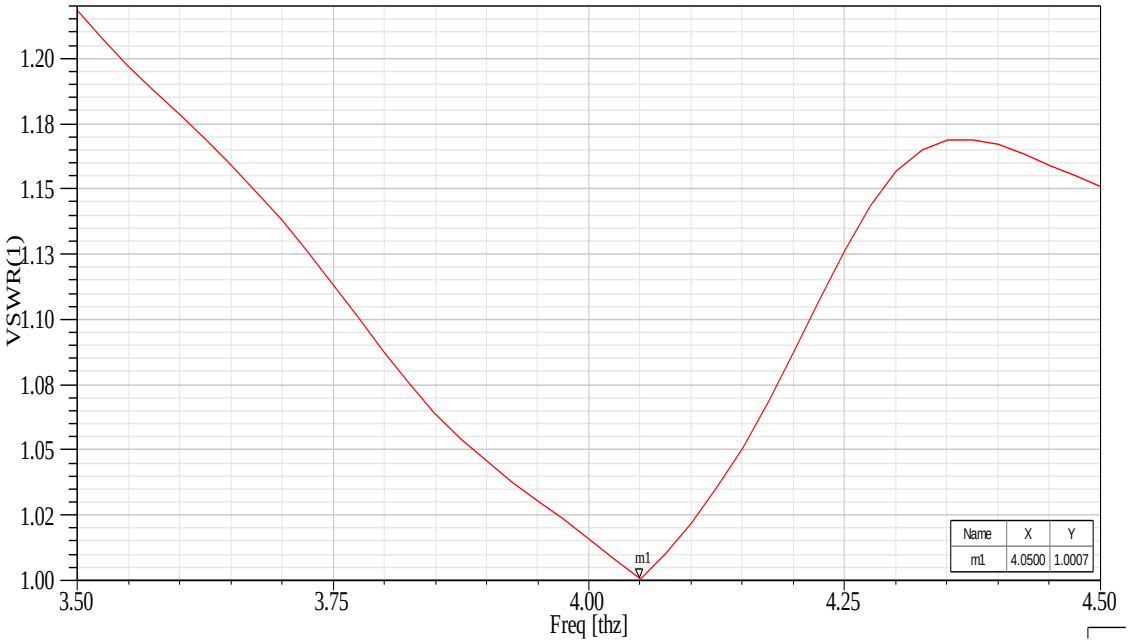

(c)

Figure 3.14 - Simulated RL (a), radiation pattern (b), and VSWR (c) graphs of the optimized THz MEMS horn-shaped helix antenna using HFSS-based stochastic solvers

Table 3.2 - Characterization of the THz MEMS horn-shaped helix antenna optimized in HFSS using stochastic solvers

Section	Parameter	Value (µm)
Helix form	Diameter (D)	20.4166
	Pitch (S)	16.3062
	Turn number (N)	11.3403
	Radius Change (R_c)	2.7798
	Slent angle (α)	14.2638°
	Height (H_h)	184.9171
CPW feeding	Width (W)	4.8946
	Gap (G)	2.3860
	Thickness (T)	1.1895
Silicon platform	Thickness (H_s)	8.4954
	Width (W_s)	79.6666
Antenna	Height (H_A)	194.6020

The novel MEMS conical helix antenna geometric characterization developed by HFSS-based on stochastic solvers comes with very low return loss with approximately -69.54dB and excellent voltage standing wave ratio with ideal value which is equal to 1.0007 at the resonance frequency. The radiation pattern at the resonance frequency, keeps very good directivity in both xoz-plane and yoz-plane due to the active modeling process. Details of the geometrical configuration of the new MEMS horn-shaped helix antenna optimized in HFSS based on Genetic Algorithms are presented in Table 3.2.

Finally, it is very important to mention that the size of the helix aperture (pitch *S*, and radius change R_c) presents a very significant parameter in improving the helix antenna performance and making it very beneficial to the THz applications. The optimized antenna design presents in fact a potential candidate for THz wireless products due to GA optimization technique presenting a global search technique that is particularly very effective in a high-dimension multimodal function due to their versatility and ease of implementation [21].

3.3.3. MEMS pyramidal helix antenna

A novel MEMS pyramidal helix antenna design [90] operating in THz frequency range from 2.29 to 2.63 THz has been also found using GA solvers

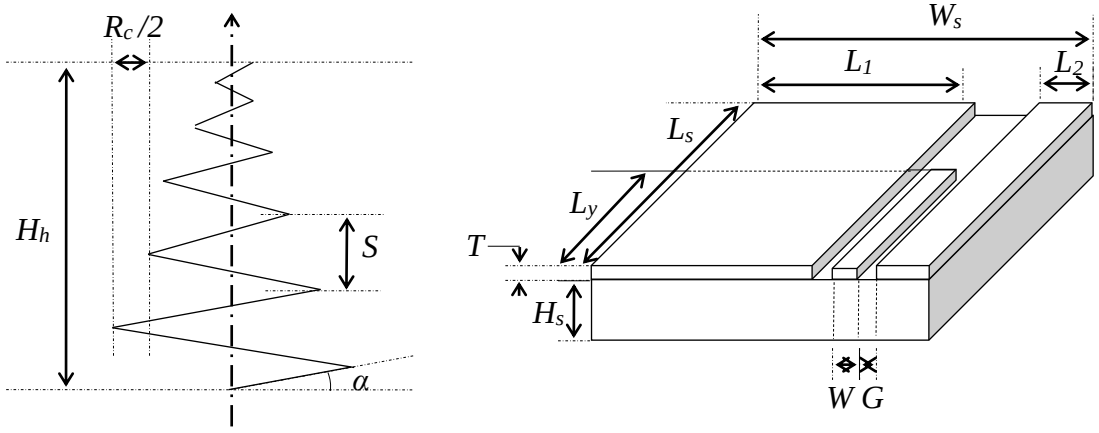

(a) **(b)**

Figure 3.15 – THz MEMS pyramidal helix antenna geometric structure, (a) schematic diagram of the helix, (b) 3D model of the CPW feeding

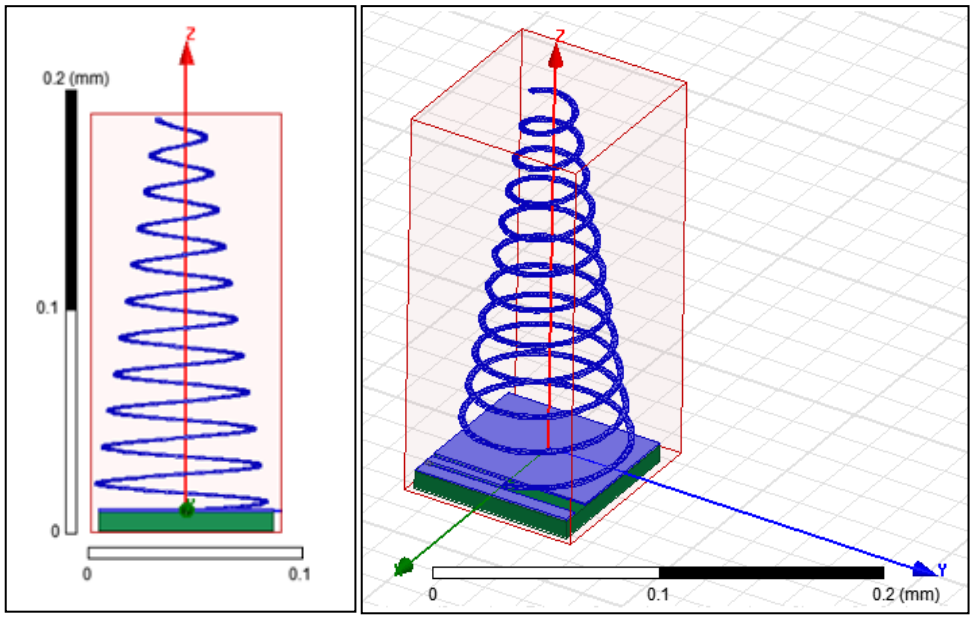

(a) **(b)**

Figure 3.16 - 2D (a) and 3D (b) HFSS models of the THz MEMS pyramidal helix antenna

relying on the THz UWB MEMS helix antenna design already developed in the section (3.3). The new compact geometrical configuration of the proposed antenna has been evaluated using HFSS software; very low return losses and excellent voltage standing wave ratios have been obtained. The proposed MEMS pyramidal helix antenna is realized in a silicon platform using FIB stress-introducing technique as presented in figures 3.15 and 3.16 that show the geometric structure, and HFSS models.

The simulated return losses of the initial geometrical configuration selected for the proposed antenna - as displayed in figure 3.17 - has been deeply improved using HFSS on based effective stochastic search solvers [13, 14] which are automatically employed to handle the optimization in more depth due to their parallel architecture and probabilistic nature that use a type of random selection and applies it in a structured manner to vary the values of the parameters selected for the optimization including the CPW width (W), gap (G) and thickness (T), the silicon thickness (H_s) and width (W_s), the helix diameter (D), pitch (S), turn

number (N), slent angle (α), Λ-shaped radius change (R_A), and height (H_h) on the basis of finding a minimum or maximum of a fitness function.

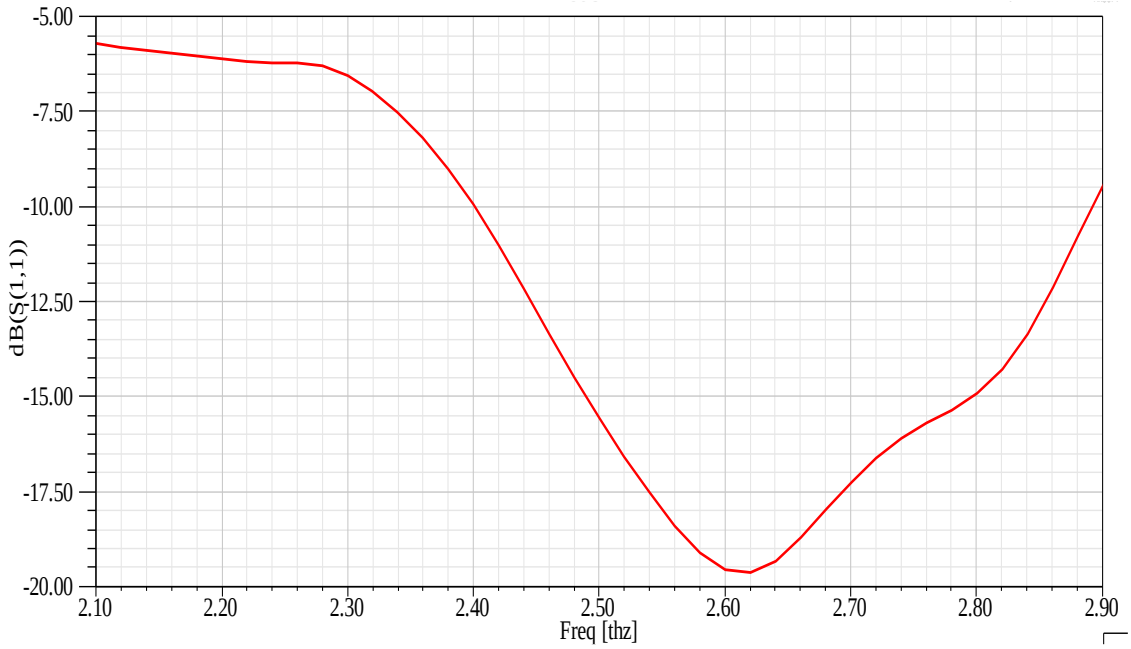

Figure 3.17 - Simulated RL graph of the proposed MEMS pyramidal helix antenna with initial parameters in 2.1 – 2.9 THz

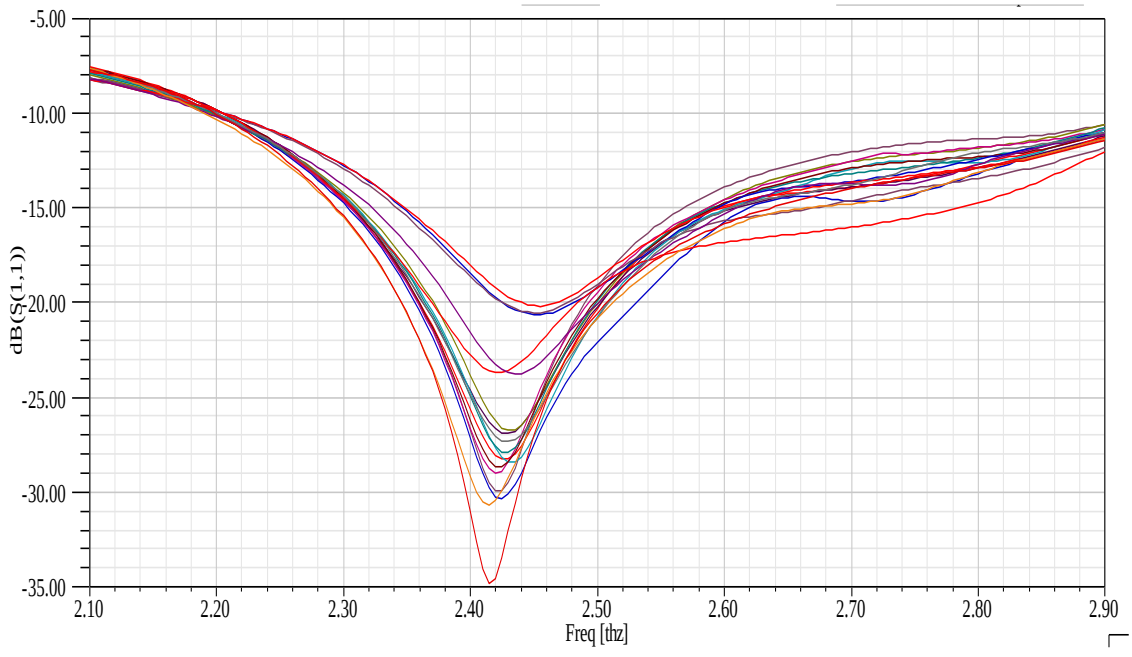

Figure 3.18 - Simulated RL graph of the MEMS pyramidal helix antenna using HFSS-based GA solvers in 2.1 – 2.9 THz

Figures 3.17 shows the simulated return losses (a), radiation patterns (b), and voltage standing wave ratios (c) of the optimized antenna geometry finally obtained which presents a very low reflection coefficient and excellent ratios due to the good adaptation of the feeding line to the helix antenna, and the high precision achieved by optimization techniques, resulting in high performance for the selected band of frequencies.

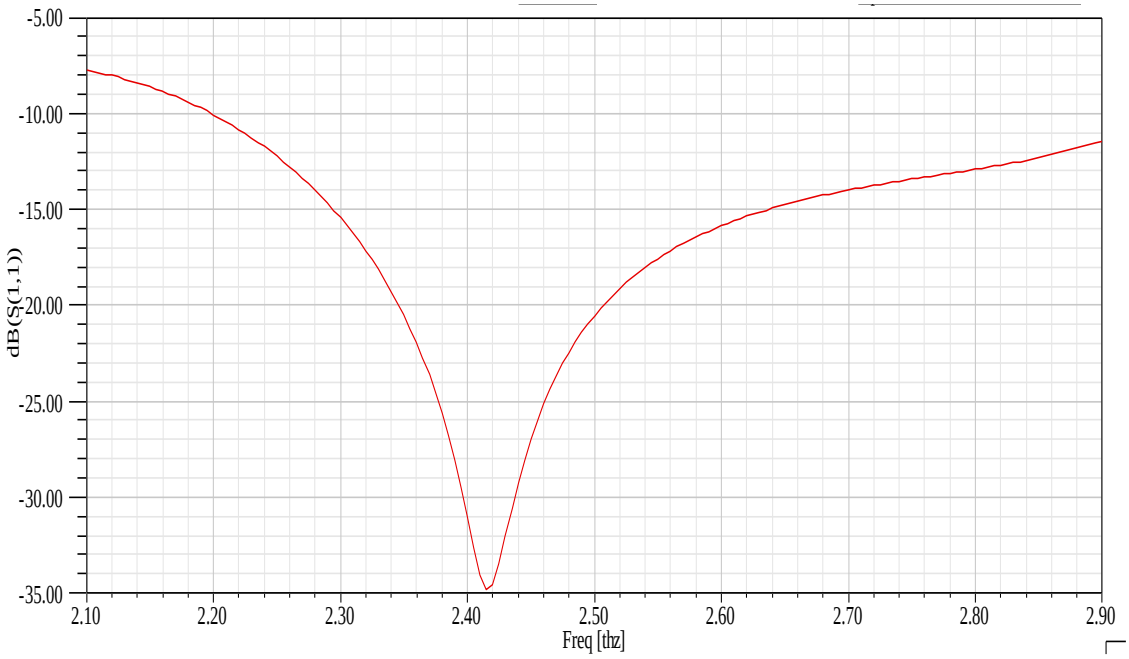

(a)

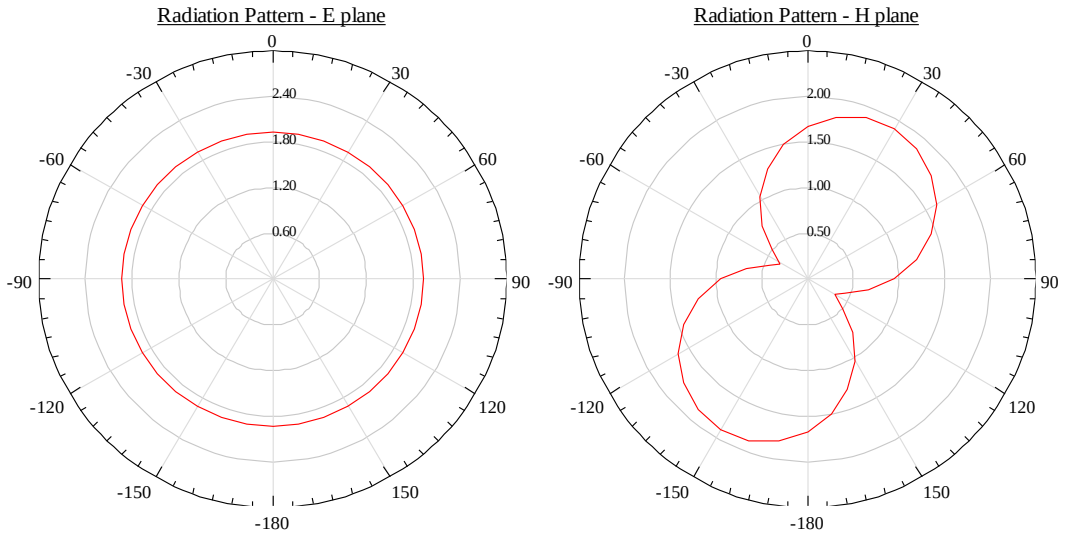

(b)

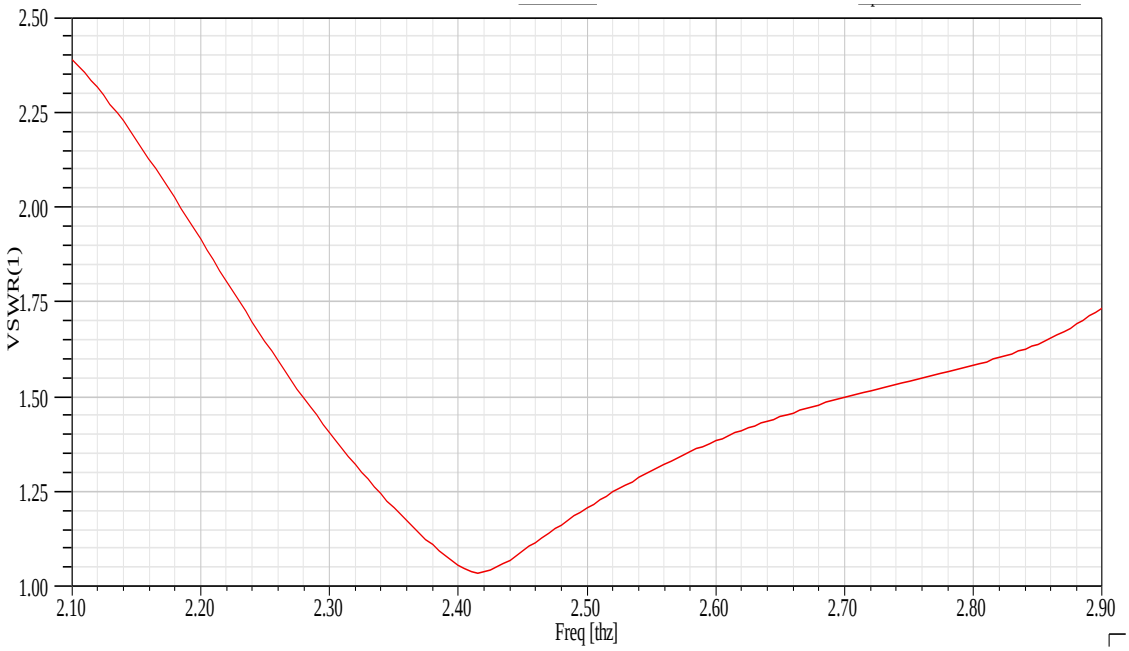

(c)

Figure 3.19 - Simulated RL (a), radiation pattern (b), and VSWR (c) graphs of the optimized THz MEMS pyramidal helix antenna using HFSS-based stochastic solvers

The novel MEMS pyramidal helix antenna geometric characterization developed by HFSS based on high automatic GA solvers comes with very low return losses with closely less than -15dB from 2.29 to 2.63 THz, and less than -20dB over the central frequencies to achieve less than -34dB at f_0 = 2.41 THz. The voltage standing wave ratios present also excellent values of less than 1.25 from 2.34 to 2.52 THz to achieve the value of 1.03 at the resonate frequency f_0 = 2.41 THz. Thus, the radiation patterns in E-plane and H-plane keeps good directivity with slightly bending in the side lobes of yoz-plane due to the fine modeling process. This validates the excellent performance of the proposed MEMS pyramidal helix antenna design. HFSS software constitutes therefore relevant device for the improvement of THz technology due to its efficient optimization techniques. Details of geometrical configuration of the novel MEMS pyramidal helix antenna optimized in HFSS based on effective stochastic solvers are presented in Table 3.3.

Table 3.3 - Characterization of the THz MEMS pyramidal antenna optimized in HFSS using stochastic solvers

Section	Parameter	Value (µm)
Helix form	Diameter (D)	19.3601
	Pitch (S)	16.0064
	Turn number (N)	10.7333
	Radius Change (R_Δ)	-2.5327
	Slent angle (α)	14.7442^o
	Height (H_h)	171.8014
CPW feeding	Width (W)	4.9644
	Width (L_1)	63
	Width (L_2)	7
	Gap (G)	2.6110
	Thickness (T)	1.1821
Silicon platform	Thickness (H_s)	8.1415
	Width (W_s)	80.1864
Antenna	Height (H_A)	181.1250

3.4. Automatic strategists for modeling THz MEMS helix antennas

Microelectromechanical systems become very useful for designing THz antennas operating in the electromagnetic THz field through implementing silicon-based microelectronic devices that widely preserve the well-known advantages of micromachining technologies such as high precision, high performance, and self consistency. MEMS helix antennas employing silicon substrates, have achieved over the past decade interesting characteristics after having used automatic modeling techniques to provide complex THz antennas with numerous wireless access applications. Accordingly, Artificial Neural Networks (ANN) [91, 92] present a very popular class of automatic search techniques leading to novel design models and optimal solutions,

consisting of complex information processing systems inspired by the studies of the ability of the human brain to learn from observations and generalize by abstraction.

Based on the set of antennas developed using stochastic solvers, the final section describes first a new compact geometric configuration of a MEMS horn-shaped helix antenna using Artificial Neural Networks which are employed for the modeling of antenna design problems to obtain a surrogate based model instead of a computationally intensive three dimensional electromagnetic simulation in design. The optimized antenna occupies a very compact volume of 79×80×162 μm (1.02×10^{-3} mm^3), including the silicon substrate having a thickness of 9.3 μm and a dielectric constant of 11.9. The proposed MEMS helix antenna design is validated by demonstrating optimal results in terms of low return loss properties and voltage standing wave ratios. The antenna has been also found to resonate at 3.59THz and operate in a wide bandwidth from 3.12 to 4 THz with a very low reflection coefficient with less than -20dB over the entire bandwidth.

Second, a novel design of MEMS pyramidal helix antenna using accurate Artificial Neural Networks model is proposed for dualband wireless applications. The antenna geometry is optimized in a way it resonates at 0.93 THz and 2.39 THz and shows low reflection coefficient of less than -43dB and ideal simulated voltage standing wave ratio of 1.01 for the resonace frequencies, resulting in excellent performance. The new MEMS antenna design is validated by presenting optimal results in terms of low return losses of closely less than -15dB to -43dB, and excellent simulated voltage standing wave ratios of less than 1.5 to 1.01 for the down and upper frequency bands ranging from 0.8 to 1 THz and from 2.3 to 2.5 THz respectively. The optimized MEMS pyaramidal helix antenna occupies a highly miniaturized volume of 79×80×189 μm ($1.1944\ 10^{-3}$ mm^3) including the silicon substrate having a thickness of 9.3 μm and a dielectric constant of 11.9.

3.4.1. ANN modeling of the MEMS helix antenna

Geometrical parameters of the proposed MEMS helix antenna have been optimized by introducing an accurate ANN model using MATLAB programming [93-95], in order to enhance the accuracy of the existing structure - already developed by stochastic solvers in the section (3.4 – figures 3.10 and 3.11) - through an automated data training process having the ability to capture multi-dimensional arbitrary nonlinear relationships in a very fast way to finally provide a high-level antenna design.

In this work, a multilayer perceptron (MLP) network structure has been adopted for the calculation of the resonant frequencies and return losses of the antenna using for training standard, back propagation algorithms [96], in which neurons are grouped into three layers divided into: first layer which consists of input neurons, output layer which contains the output neurons, and remaining layer presenting the hidden layer.

After having defined the antenna's input and output variables as a first stage known as neurons process, training data are generated using multi-HFSS simulations to provide a neural network model that will be incorporated into the simulator again for fast and accurate optimization as a second stage of the overall device called network training process. Likewise, the training error is automatically calculated, and network weights are being updated after each cycle in order to minimize the training error. The aim of the network training process is then to teach the network to produce valid response for inputs from outside the training data that is simply called generalization [97].

After, the optimization operation will be launched aiming to determine a new configuration of the MEMS helix providing simulation results (X_{HFSS}) close to the target design specifications (X_{target}) initially proposed. The key technique used in this adaptive CAD procedure is explained in details in figure 3.19 which presents the set of the design process steps. Parameters outputted by the trained ANN model have been implemented by HFSS software to compare the antenna

response with the target response. ANN model developed for the optimization offers the advantage of superior computational ability to provide optimal geometric configurations due to its high efficiency and interconnectivity to solve design problems.

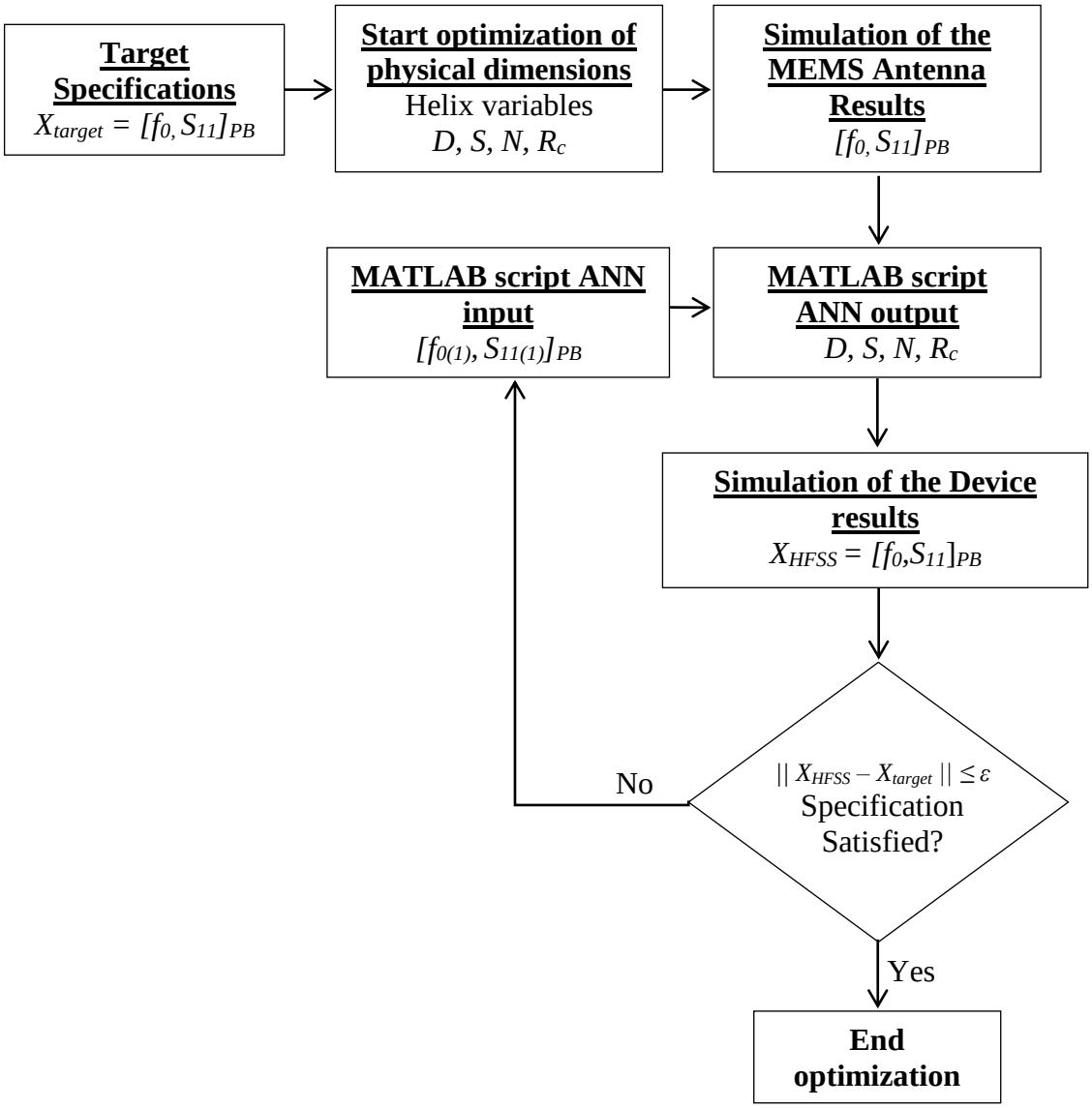

Figure 3.20 - Adaptive CAD procedure for the ANN optimization process

3.4.2. MEMS horn-shaped helix antenna

The size of the THz MEMS horn-shaped helix antenna (section 3.4.2 - figures 3.10 and 3.11) is expected to closely relate to wavelength as occupying the electromagnetic spectrum that spans between 3 and 4.2 THz. In fact, micro-electromechanical systems present the suitable technology for manufacturing the

proposed THz MEMS horn-shaped helix antenna [98] in which the fabrication process is highly precise and antennas become soft to be integrated with other devices.

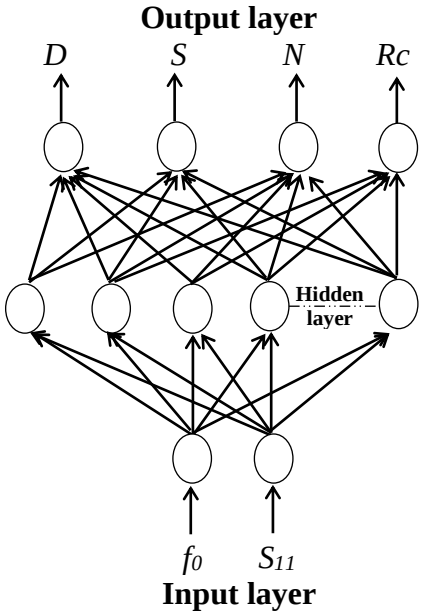

Figure 3.21 - MLP-ANN architecture selected for the optimization

Table 3.4 - ANN parameters of the MEMS horn-shaped helix antenna

Parameter	**Optimized values**			
Training algorithm	Feed-forward MLP/ Backpropagation			
Number of neurons	Number of input neurons / Number of output neurons		2	4
	Number of hidden neurons		11	
Transfer function	Hidden levels		Sigmoïde	
	Hidden levels		Lineair	
Inputs definition		***f0 (THz)***	***S11 (dB)***	
	Max	3	-35	
	Min	4.2	-70	
Learning rate	0.02			
The number of epochs	1000			

Figure 3.20 illustrates the MLP-ANN architecture used for the simulation and optimization. For the considered MEMS horn-shaped helix antenna, the developed neural model is designed to produce output parameters divided into

the helix diameter (D), pitch (S), turn number (N), and radius change (R_c) having resonance frequency (f_o) and return loss (S_{11}) as inputs. The antenna height, the helix height, and the helix slent angle and height will be automatically optimized related into the output parameters. The neural network parameters used for the optimization are indicated in Table 3.4.

Figure 3.21 shows the simulated return losses of the antenna design, optimized using the accurate ANN model. It is clearly observed that the geometric configuration begins to provide low return losses from iteration to other that become very close to the target return losses in the 8th iteration. Figure (5-i) shows that the antenna structure comes with very low return losses over the entire bands of resonance. The antenna has been found to resonate at 3.59 THz with a return loss of less than -63dB.The values obtained from ANN are very close to target values. The difference between the ANN outputs against target is measured in terms of performance which is very close to set goal to be achieved in testing for better performance of the network model.

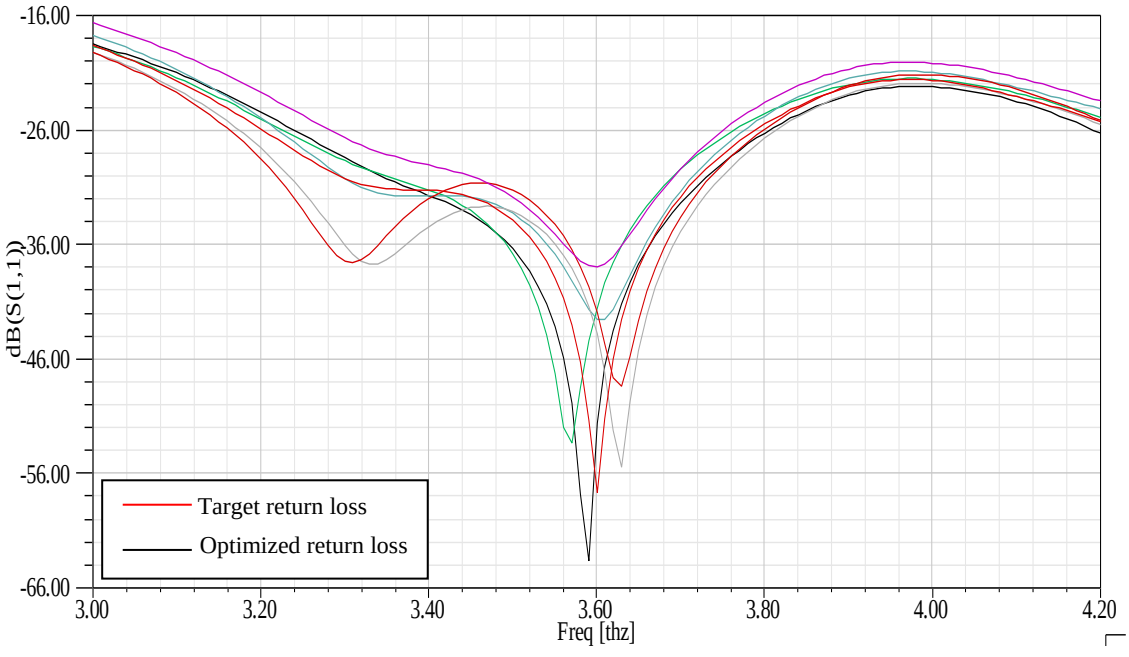

Figure 3.22 – Simulated RL graph of the MEMS horn-shaped helix antenna in 3 – 4.2 THz during the optimization for 8th iterations

Similarly, figure 3.22 illustrates the simulated return losses (a), radiation patterns (b), and voltage standing wave ratios (c) of the optimized antenna design finally obtained using HFSS based on ANN modeling. It is clearly observed that the optimized antenna geometry presents very low reflection coefficients with less than -17dB to -63dB, and excellent voltage standing wave ratios from 1.35 to 1.00, resulting in a significantly high performance for the selected band of

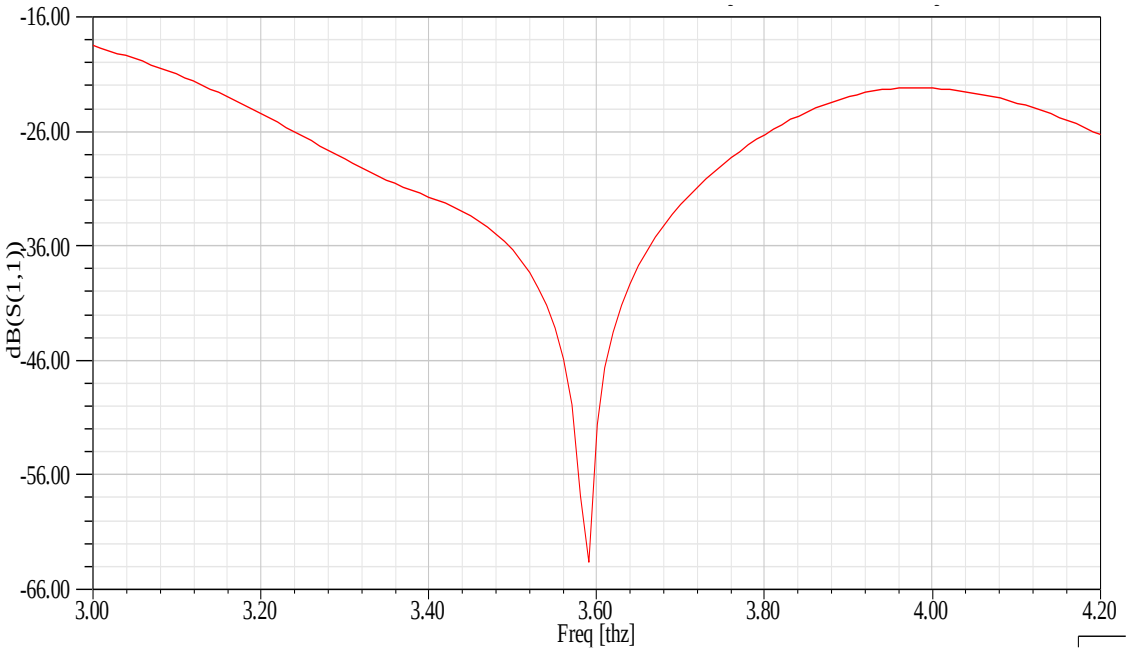

(a)

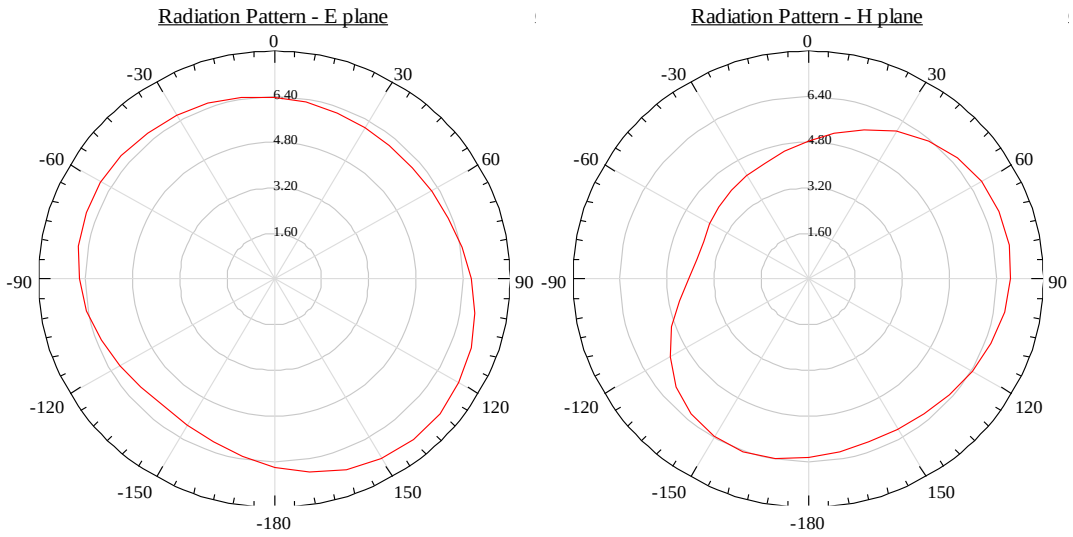

(b)

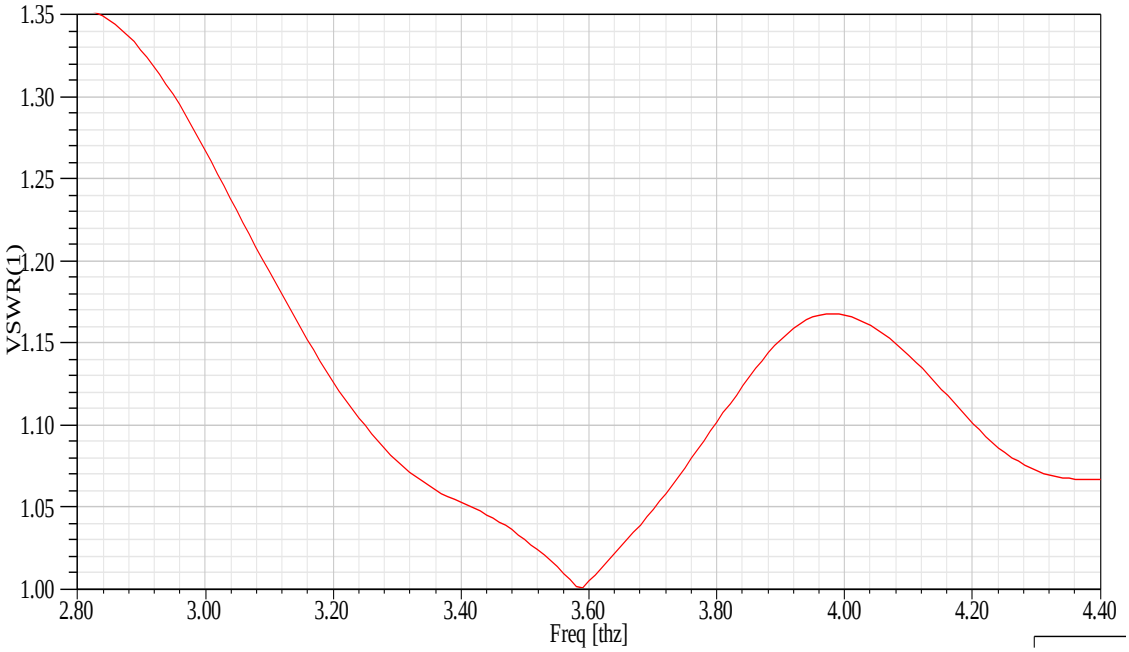

(c)

Figure 3.23 - Simulated RL (a), radiation pattern (b), and VSWR (c) graphs of the optimized THz MEMS horn-shaped helix antenna using HFSS-based ANN modeling

Table 3.5 - Characterization of the THz MEMS horn-shaped helix antenna optimized in HFSS using ANN modeling

Section	Parameter	Value (µm)
Helix form	Diameter (D)	25.4565
	Pitch (S)	14.3676
	Turn number (N)	10.5738
	Radius Change (R_c)	2.6483
	Slent angle (α)	10.184°
	Height (H_h)	151.9201
Antenna	Height (H_A)	161.6050

frequencies. Thus, the radiation pattern keeps good directivity with slightly deterioration in the side lobes of yoz-plane due to the fine modeling process. This demonstrates the high efficiency of the applied optimization strategy to provide a

good geometrical accuracy and excellent electromagnetic response. Table 3.5 shows the final geometric configuration reported from the 8th iteration, selected for the MEMS horn-shaped helix antenna design after optimization.

3.4.3. MEMS pyramidal helix antenna

In this step, geometrical parameters of the THz MEMS pyramidal helix antenna design [99] already optimized using GA technique (section 3.4.3 - figures 3.15 and 3.16), have been analyzed by an efficient MLP network which uses for the automated data training process, back propagation algorithms in which neurons are grouped into: input neurons including down and upper return losses (S_{11D} and S_{11U}), and down and upper resonance frequencies (f_D and f_U). The output neurons contain the helix variables (D, S, N and R_A) as illustrated in figure 3.23. Table 3.6 displays the neural network parameters employed in the optimization process. Likewise, a suitable network is generated for a set of data training process to produce valid response for inputs from outside the training data. After being successfully trained, the network will learn the input-output relation among the helix parameters, return losses, and resonance frequencies to be used as the objective function in calculating the optimized dimensions.

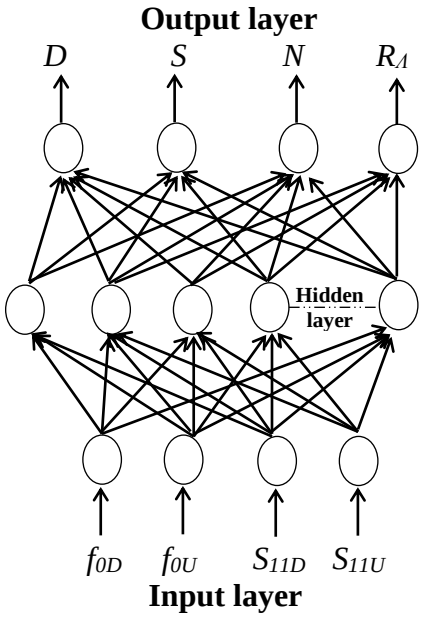

Figure 3.24 - MLP-ANN architecture selected for the optimization

Table 3.6 - ANN parameters of the MEMS pyramidal helix antenna

Parameter	Optimized values				
Training algorithm	Feed-forward MLP/ Backpropagation				
Number of neurons	Number of input neurons / Number of output neurons			4	4
	Number of hidden neurons			14	
Transfer function	Hidden levels			Sigmoïde	
	Hidden levels			Lineair	
Inputs definition		f_{0D} (THz)	f_{0U} (THz)	S_{11D} (dB)	S_{11U} (dB)
	Max	0.5	1.75	-35	-35
	Min	1.75	3.0	-55	-55
Learning rate	0.01				
The number of epochs	1200				

The network will automatically get the ability to capture multidimensional arbitrary nonlinear relationships in a very fast way to enhance the accuracy of the existing antenna design and provide a high performance level. After each cycle, the network weights are being updated and the cost function parameters are being minimized or maximized to overall the simulation goals.

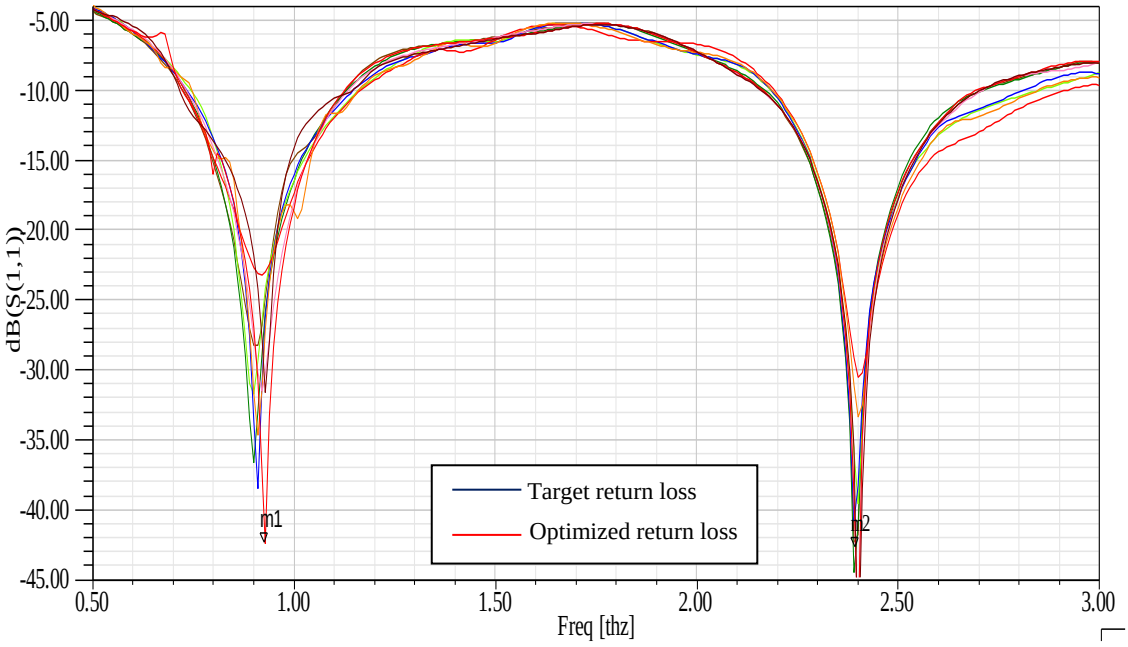

Figure 3.25 – Simulated RL graph of the MEMS pyramidal helix antenna in 0.5 – 3 THz during the optimization for 6th iterations

Figure 3.25 shows the simulated return losses of the MEMS pyramidal helix antenna during the optimization: The antenna resonates at 0.93 THz and also at 2.39 THz, and presents an equitable bandwidth of 0.2 THz for the down and upper frequency bands, and excellent performance demonstrated by very low return losses from -15dB to -45dB.

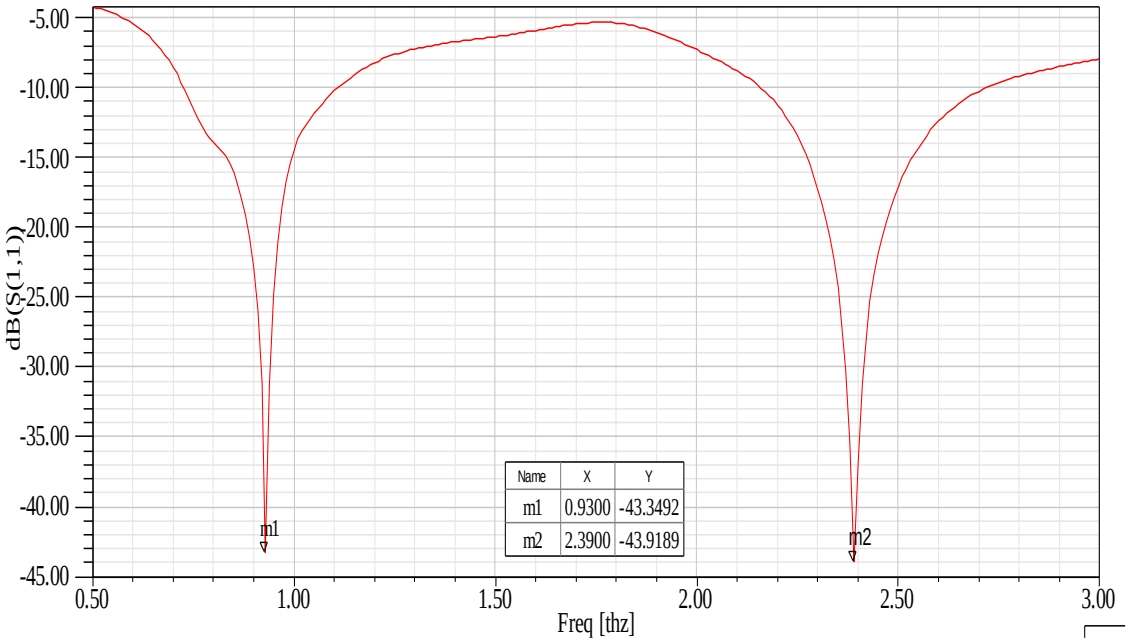

(a)

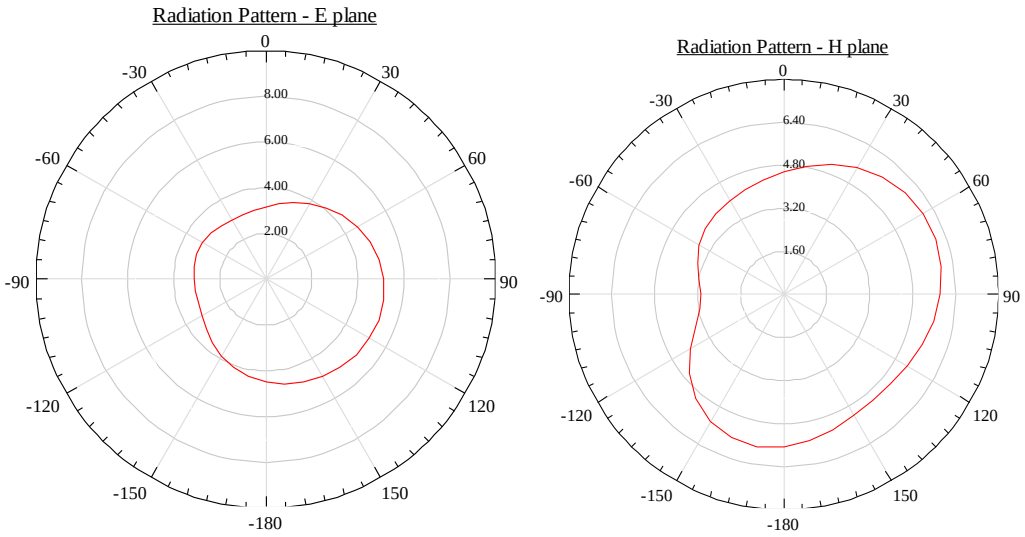

f_{0D} = 0.93 THz

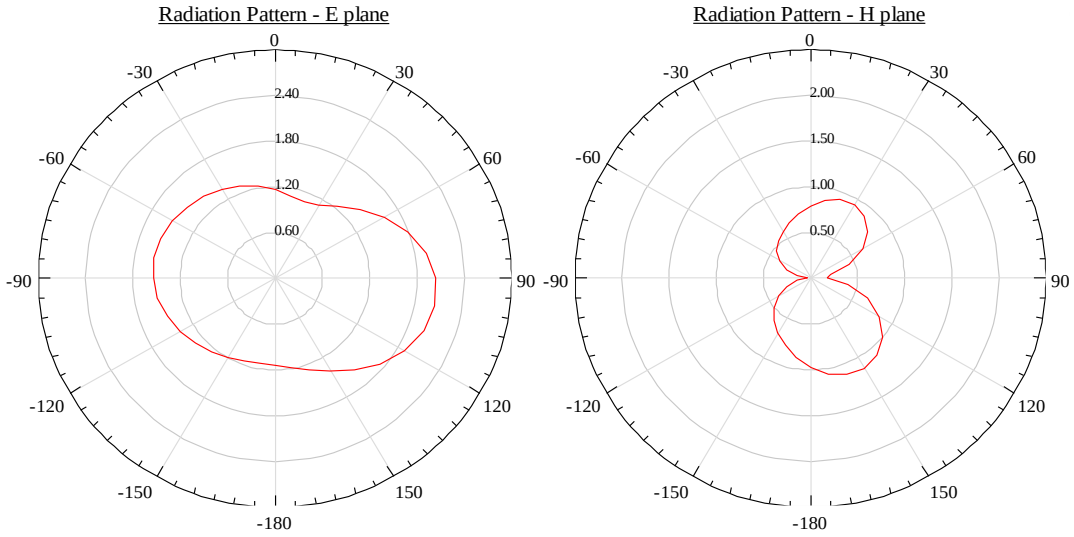

f_{0U} = 2.41 THz

(b)

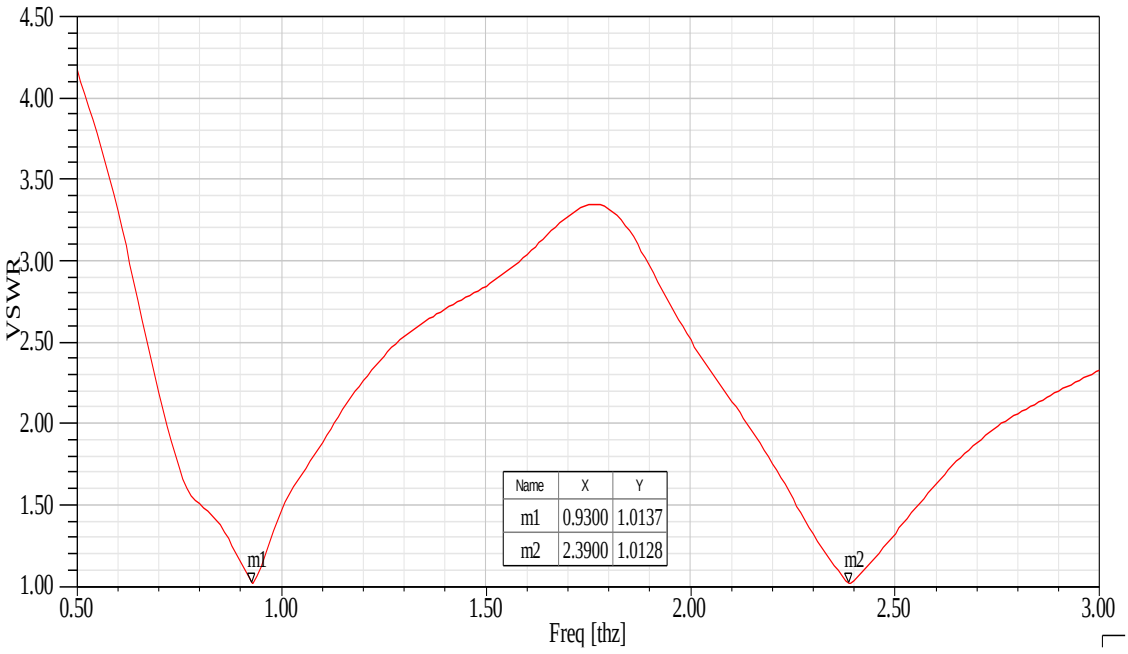

(c)

Figure 3.26 - Simulated RL (a), radiation pattern (b), and VSWR (c) graphs of the optimized THz MEMS pyramidal helix antenna using HFSS-based ANN modeling

As illustrated in figure 3.26, the new geometric characterization of the MEMS pyramidal helix antenna developed by ANN technique comes with very

low return losses with approximately -43dB, good directivity in both E-plane and H-plane, and excellent voltage standing wave ratios with closely 1.01 at the resonance frequencies. Details of the geometrical configuration of the new MEMS pyramidal helix antenna optimized in HFSS based on ANN modeling are presented in table 3.7.

Table 3.7 - Characterization of the THz MEMS pyramidal helix antenna optimized in HFSS using ANN modeling

Section	Parameter	Value (μm)
Helix form	Diameter (D)	17.2656
	Pitch (S)	16.0382
	Turn number (N)	11.1280
	Radius Change (R_A)	-2.5217
	Slent angle (α)	16.471^o
	Height (H_h)	178.4730
Antenna	Height (H_A)	187.7966

Finally, the ANN optimization strategy employed for investigating the MEMS pyramidal helix antenna characteristics shows high efficiency to achieve excellent performance and accuracy relying on high μm-level precision to support very good applications for communication and space areas like for radio astronomy and spectroscopy [8-10]. Therefore, it is very important to mention that global-function approximation capability and greater generalization capability of ANN technique facilitate the modeling phenomenon and can avoid the limitation encountered for objective-function formulation in the GA optimization [100].

General Conclusion

The investigation of compact THz helix antennas based on MEMS processing, has particularly reported major milestones to research in numerous applications, due to the encouraging results afforded by the real progress of the different computational electromagnetic optimization techniques employed in this research study, to provide a new class of integrated antennas for modern wireless systems to cover relevant areas including communication, biomedicine, spectroscopy, and other emerging fields.

This research work provides for the modern THz wireless systems novel integrated helix antenna designs using for conceiving such compact models, advanced silicon-based microelectronics processing as a relevant technique for preserving the advantages of micromachining technologies, and effective computational electromagnetic optimization techniques as significant tools for achieving optimal dimensions and uniform characteristics. Accordingly, this study has presented in details important technical concerns of integrated THz antennas in three main chapters:

- In the first chapter, important advances made in the designs of different integrated antennas have been described as an integral part for various modern wireless systems. This has offered insight into main antenna considerations being conducted at various steps of the design process to check that the antenna specifications meet the wireless system requirements. Interestingly, the key parameters that are often taken into consideration such as the radiation pattern, efficiency, gain, bandwidth and impedance are presented as main properties for antennas operating at different frequencies ranging from radio to terahertz.
- In the second chapter, main characteristics of THz waves have been exposed to understand the fundamental specifications to be considered when designing integrated antennas functioning in the electromagnetic THz gap. Many new manufacturing technologies have been used to stimulate interest in this unique spectral and provide high performance THz integrated antennas with um-level precision, accordingly chapter

two presents MEMS technology which is widely recommended for fabricating such a kind of antennas, particularly helix antennas by implementing silicon substrates to help enhancing their response and achieving excellent properties.

- In the third chapter, effective computational electromagnetic optimization techniques used for modeling a new class of high performance compact THz MEMS helix antennas have been described. The novel designs with different geometrical configurations and excellent responses are developed using 3D HFSS based on reliable evolutionary optimizers divided into Quasi-Newton and Sequential Non Linear Programming, effective stochastic solvers presented by Genetic Algorithm, and accurate automatic strategists which are Artificial Neural Networks. These computational processing methods used for optimization are very powerful and efficient to find solutions in a fast way due to their continuity and derivability in carrying out repeated electromagnetic simulations until retaining a good performance and accuracy. The proposed designs can be easily fabricated using MEMS technology, operate in different THz frequency bands and find several applications in numerous areas.

Finally, this research study has presented efficient computerized optimization strategies for investigating the proposed antenna characteristics demonstrating a high efficiency to achieve very low return loss properties, provide excellent voltage standing wave ratios, and maintain a good directivity, resulting in a high electromagnetic performance and excellent geometrical accuracy for the developed models for various THz frequency ranges extending from 0.5 to 4.5 THz, making the proposed MEMS helix antenna desings highly attractive for supporting different modern wireless systems.

As a perspective, it is very important to extend this research study through manufacturing the developed antenna designs in the future research works to

compare the measured results to the simulated results taking profit of the excellent performance for the proposed models for new wireless applications.

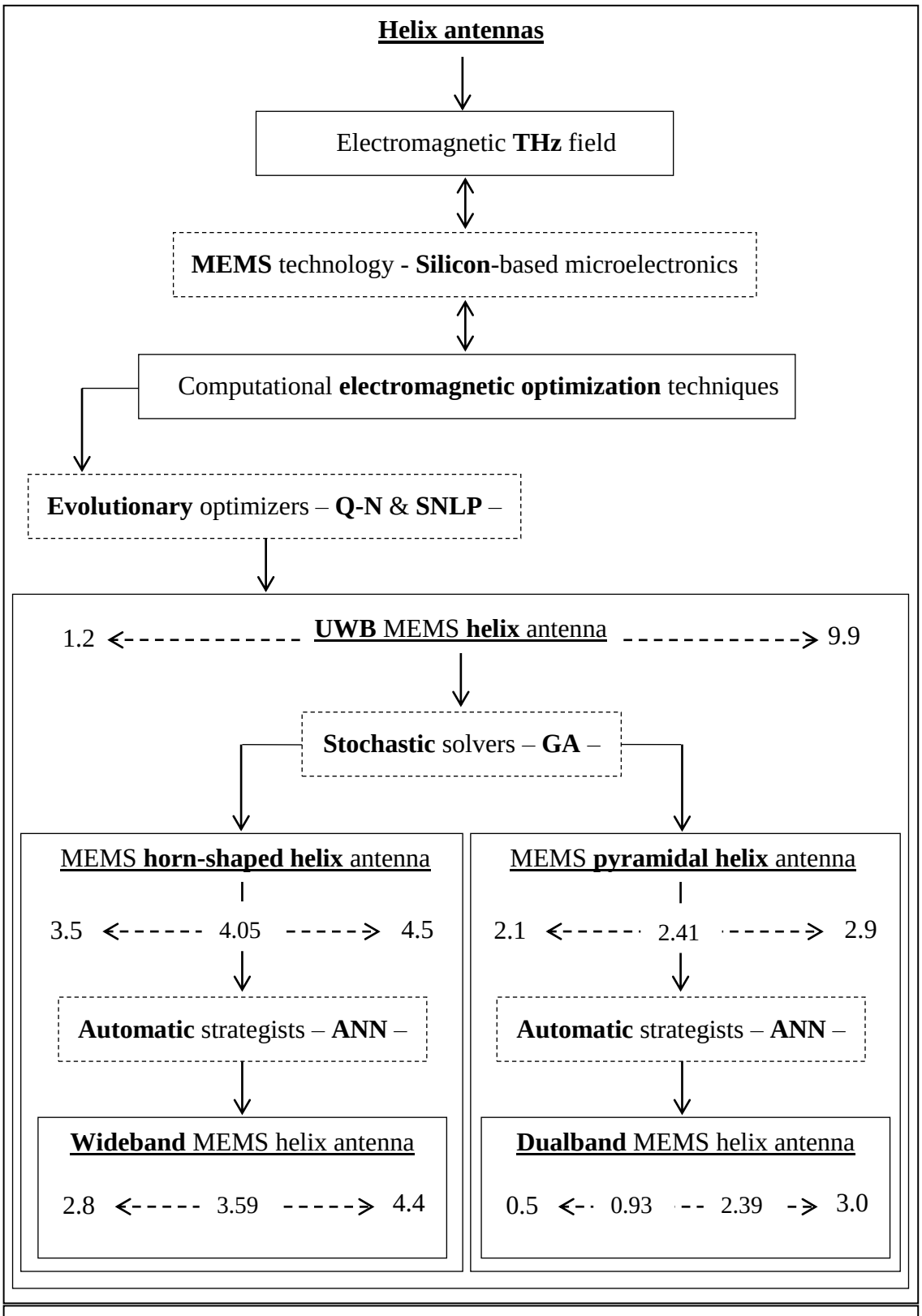

Synoptic scheme presenting the overall description of the performed study

List of Publications

I. International articles

1. **A. Boudkhil**, M. Chetioui, N. Benabdallah, and N. Benahmed, "Development and performance enhancement of MEMS helix antenna for THz applications using 3D HFSS-based efficient electromagnetic optimization," *TELKOMNIKA*, Vol. 16, Issue 1, pp. 210-216, Feb. 2018.

2. M. Chetioui, **A. Boudkhil**, N. Benabdallah, and N. Benahmed, "Design and analysis of Ku/K-band circular SIW patch antenna using 3D EM-based artificial neural networks," *TELKOMNIKA*, Vol. 16, Issue 2, pp. 594-599, Apr. 2018.

3. **A. Boudkhil**, M. Chetioui, N. Benabdallah, and N. Benahmed, "An optimal dualband pyramidal helix antenna based on MEMS technology for THz applications using GA and ANN techniques," submitted to *International Journal on Electrical Engineering and Informatics*, Apr. 2018.

4. M. Chetioui, **A. Boudkhil**, N. Benabdallah, and N. Benahmed, "A novel dualband coaxial-fed SIW cavity resonator antenna using ANN modeling," *Journal of Engineering Science and Technology Review*, Vol. 11, Issue 2, pp 82-87, May. 2018.

II. International communications

1. **A. Boudkhil**, M. Chetioui, N. Benabdallah, A. Ouzzani, and N. Benahmed, "A novel design of THz MEMS Λ-Helix antenna using HFSS-based effective stochastic solvers," in the 4th IEEE International Conference of Optimization Applications (ICOA), Apr. 26-27, Mohammedia, Morocco, 2018.

2. M. Chetioui, **A. Boudkhil**, N. Benabdallah, and N. Benahmed, "Design and optimization of SIW patch antenna for Ku band applications using ANN algorithms," in the 4th IEEE International Conference of Optimization Applications (ICOA), Apr. 26-27, Mohammedia, Morocco, 2018.

3. **A. Boudkhil**, N. Benabdallah, A. Ouzzani, M. Chetioui and N. Benahmed, "A highly miniaturized MEMS pyramidal helix antenna for THz applications using reliable evolutionary optimizers," in the International Conference on Applied Mathematics in Engineering (ICAME), Jun. 27-29, Balikesir, Turkey, 2018.

4. **A. Boudkhil**, M. Chetioui, N. Benabdallah, A. Ouzzani, and N. Benahmed, "A compact integrated THz horn-shaped helix antenna based on MEMS technology using accurate automatic strategists," accepted in the International Conference on Applied Mathematics in Engineering (ICAME), Jun. 27-29, Balikesir, Turkey, 2018.

References

1. J. Federici and L. Moeller, "Review of terahertz and subterahertz wireless communications," *Journal of Applied Physics*, Vol. 107, Issue 11, Jun. 2010.

2. Y. J. Cheng, *Substrate integrated antennas and arrays*, CRC Press Taylor & Francis, New York 2016.

3. D. Chicherin et al, "MEMS tunable metamaterials surfaces and their applications," in Proceeding of Asia Pacific Microwave Conference, Yokohama, Japan, Dec. 2010, pp. 239–242.

4. W. H. Ko, J. T. Suminto, G. J. Yeh, "Bonding techniques for microsensors," *Studies in Electrical and Electronic Engineering*, Vol. 20, pp. 41-61, Apr. 1985.

5. B. Pan, Y. Yoon, P. Kirby, J. P. Papapolymerou, M. M. Tenzeris, and M. Allen, "A W-band surface micromachined monopole for low-cost wireless communication systems," in IEEE MTT-S Int. Dig., Jun. 2004, G. T. pp. 1935–1938.

6. B. Liu et al., "An efficient method for antenna design optimization based on evolutionary computation and machine learning techniques," *IEEE Transactions on Antennas and Propagation*, Vol. 62, Issue 1, Jan. 2014.

7. HFSS online help. *Ansoft Corporation*, 2007.

8. Y. Yong, L. Yong, and L. Xin, "Novel 0.9 THz Integrated Horn Antenna Based on MEMS Technology," in International Symposium on Photoelectronic Detection and Imaging, 2009, Vol. 7385 738529-2.

9. B. Drouin, S. Yu, J. Pearson, and H. Gupta, "Terahertz spectroscopy for space applications: 2.5–2.7 THz Spectra of HD, H2O and NH3," *Journal of Molecular Structure*, Vol.1006, pp. 2-12, May 2011.

10. M. C. Gaidis, H. M. Pickett, C. D. Smith, S. C. Martin, R. P. Smith, and P. H. Siegel, "A 2.5-THz receiver front end for spaceborne applications," *IEEE Transactions on Microwave Theory and Techniques*, Vol. 48, Issue 4, pp. 733-739, Apr. 2000.

11. J. C. Maxwell, *A Treatise on Electricity and Magnetism*, London, U.K.: Oxford Univ. Press, 1873; 1904.

12. H. R. Hertz, *Electric Waves*, London: McMillian, 1893; New York, Dover, 1962.

13. J. D. Kraus, "Antennas since Hertz and Marconi," *IEEE Trans. Antennas and Propagat.*, Vol. AP-33, pp. 131–137, Feb. 1985.

14. S. Silver, *Microwave Antenna Theory and Design*, MIT Radiation Lab. Series, Vol. 12, New York: McGraw-Hill, 1949.

15. Special Issue on Wireless Communications, *IEEE Transactions on Antennas and Propagation*, Vol. 46, Issue 6, Jun. 1998.

16. E. Brown, "RF-MEMS switches for reconfigureable integrated circuits," *IEEE Trans. Microwave Theo. Tech.*, Vol. 46, Issue 11, pp. 1868, 1998.

17. J. Chiao, Y. Fu, I. M. Chio, M. DeLisio and L. Lin, "MEMS reconfigureable Vee antenna," *IEEE MTT Digest*, pp. 1515–1518, 1999.

18. B. Elmaran, I. Chio, L. Chen and J. Chiao, "A beam-steerer using reconfigureable PBG ground plane," *IEEE MTT Digest*, pp. 835-838, 2000.

19. S. A. Schelkunoff and H. T. Friis, *Antenna Theory and Practice*, New York: Wiley, 1952.

20. C. A. Balanis, *Antenna Theory: Analysis and Design*, New York: John Wiley and Sons, Inc., 2005.

21. J. D. Kraus and R. J. Marhefka, *Antennas for All Applications*, 3rd edition, McGraw Hill, Inc., 2002.

22. W. L. Pritchard and J. A. Sciulli, *Satellite Communications Systems Engineering*, New Jersey: Prentice-Hall, 1986.

23. S. D. Dorfman, “Satellite communications in the 21st century,” Strategies Summit, Telecom ’95 (IUT), Geneva, Switzerland, Oct. 10, 1995.

24. Jagoda and M. de Villepin, *Mobile Communications*, John Wiley and Sons, 1993.

25. G. W. Stimson, *Introduction to Airborne Radar*, Hughes Aircraft Company, Radar Systems Group, El Segundo, Calif., 1983.

26. C. T. Swift, “Passive microwave remote sensing of the ocean - a review,” *Boundary Layer Meteorology*, Vol. 18, pp. 25–54, 1980.

27. C. H. Durney, “Antennas and other electromagnetic applicators in biology and medicine,” Proc. IEEE, Vol. 80, Issue 1, Jan. 1992.

28. R. L. Magin and A. F. Perterson, “Non-invasive microwave phased arrays for local hyperthermia–a review,” *Int. J. Hyperthermia*, Vol. 5, pp. 429–450, 1989.

29. L. H. Van Tress, Ed., *Satellite Communication Systems*, New York: IEEE Press, 1979.

30. M. I. Skolnik, *Introduction to Radar Systems*, New York: McGraw-Hill. 1986.

31. D. K. Barton, *Radar Systems Analysis*, Dedham, Mass.: Artech House, 1976.

32. Wong, K. L., *Planar Antennas for Wireless Communications*, Wiley-Interscience, John Wiley & Sons, 2003.

33. G. Kandonian and W. Sichak, “Wide frequency range tuned helical antennas and circuits,” *IRE Conv Rec*. Part 2, pp. 42–47, 1953.

34. R. C. Johnson, *Antenna Engineering Handbook*, 3rd edition, McGraw Hill, Inc., 1993.

35. A. R. Clark, *A Study Guide for Electromagnetics*, Poynting Innovations (Pty) Ltd., 2004.

36. S. Adachi and Y. Mushiake, 'Studies of large circular loop antenna', *Science Report, Research Institute of Tohoko University*, B.9.2, pp. 79–103, 1957.

37. G. Kandonian and W. Sichak, 'Wide frequency range tuned helical antennas and circuits,' *IRE Conv Rec*. Part 2, pp. 42–47, 1953.

38. A.W. Love, *Reflector Antennas*, New York: IEEE Press, 1978.

39. R. Collin, and F. J. Zucker, *Antenna Theory Part II*, McGraw-Hill, 1969.

40. R. L. Li, V. Fusco and H. Nakano, 'Circularly polarized open-loop antenna,' *IEEE Trans. Antennas Propagat*., Vol. 51, Issue 9, pp. 2475–2477, 2003.

41. M. Sumi, K. Hirasawa and S. Shi, 'Two rectangular loops fed in series for broadband circular polarization and impedance matching,' *IEEE Trans. Antennas Propagat*., Vol. 52, Issue 2, 551–554, 2004.

42. A.W. Love, *Electromagnetic Horn Antennas*, IEEE Press, 1976.

43. P. J. B. Clarricoats and A. D. Olver, *Corrugated Horns for Microwave Antennas*, London: Peter Peregrinus Press, 1984.

44. K. R. Carver, *Microstrip Antenna Technology*, Vol. 29, Issue 1, Jan. 1981.

45. D. M. Pozar, *Microstrip Antennas*, Proc. IEEE, Vol. 80, Issue 1, pp. 79–91, Jan. 1987.

46. P. Bhartia, K. Rao, and R. S. Tomar, *Millimeter-Wave Microstrip and Printed Circuit Antennas*, Artech House, 1st edition, Boston, 1991.

47. K. L. Wong, *Planar Antennas for Wireless Communications*, Wiley-Interscience, John Wiley & Sons, 2003.

48. T. Taga, and K. Tsunekawa, "Performance Analysis of a Built-In Planar Inverted F Antenna for 800 Mhz Band Portable Radio Units," *IEEE Journal on Selected Areas in Communications*, Vol. 5, pp. 921–929, June 1987.

49. J. S. McLean, "A Re-Examination of the Fundamental Limits on the Radiation Q of Electrically Small Antennas," *IEEE Transactions on Antennas and Propagation*, Vol. 44, pp. 672–676, May 1996.

50. A. D. Yaghjian, and S. R. Best, "Impedance, Bandwidth and Q of Antennas," *IEEE Transactions on Antennas and Propagation*, Vol. 53, Issue 4, pp. 1298–1324, Apr. 2005.

51. K.R. Jha, and G. Singh, "Terahertz planar antennas for future wireless communication: a technical review," *Infrared Phys. Technol.*, Vol. 60, Issue 9, pp. 71–80, 2013.

52. M. Koch, *Terahertz communication: a vision 2020. In: NATO Security through Science Series: Terahertz Frequency Detection and identification of Materials and Objects*. Springer, Germany, pp. 325–338, 2000.

53. K.C. Huang, and Z. Wang, "Terahertz terabit wireless communication," *IEEE Microw. Mag.*, Vol. 41, Issue 3, pp. 108–116, 2011.

54. R.C. Daniels, and R. W. Heath, "60 GHz wireless communications: emerging requirements and design recommendations," *IEEE Veh. Tech. Mag.*, Vol. 2, Issue 3, pp. 41–50, 2007.

55. R. C. Daniels, J. N. Murdock, T. S. Rappaport, and R. W. Heath, "60 GHz wireless: Up close and personal," *IEEE Microw. Mag.*, Vol. 11, Issues 7, pp. 44–50, 2010.

56. I. Frigyes, J. Bito, B. C. Hedler, and L. Horvath, "Applicability of the 50–90 GHz frequency bands in feeder networks," In Proc.: Eur. Antennas Propag. Conf. Berlin, Germany, March 23–27, pp. 336–340, 2009.

57. D. L. Woolard, R. Brown, M. Pepper, M. Kemp, "Terahertz frequency sensing and imaging: Time of reckoning future applications?" IEEE Proc. Vol. 93, Issue 10, pp. 1722–1743, 2005.

58. J. Federici, L. Moeller, “Review of terahertz and sub-terahertz wireless communications, “ *J. Appl. Phys.*, Vol. 107, Issue 11, 111101-1-21, 2010.

59. M. Matsuura, M. Tani, and K. Sakai, “Generation of coherent terahertz radiation by photomixing in dipole photoconductive antennas,” *Appl. Phys. Lett*., Vol. 70, pp. 559–561, 1997.

60. S. Schiller, B. Roth, F. Lewen, O. Ricken, M. C. Wiedner, “Ultra-narrow-line width continuous-wave THz source based on multiplier chains,” *Appl. Phys. B*., Vol. 95, Issue 1, pp. 55–61, 2009.

61. J. D. Kraus and R. J. Marhefka, *Antennas for all applications*, McGraw Hill, New York, 2002.

62. E. R. Brown, “Fundamentals of terrestrial millimeter-wave and THz remote sensing,” *Int. J. High Speed Electron. Systems*, Vol. 13, Issue 4, pp. 995–1097, 2003.

63. A. Karttunen, J. Ala-Laurinaho, R. Sauleau, and A. V. Raisanen, “A study of extended hemispherical lenses for a high gain beam-steering antenna,” In Proc: European Conference on Antennas and Propagation, Barcelona, Spain, Apr. 12–16, 2010, pp. 1–5.

64. C. Jastrow, K. Munter, R. Piesiewicz, T. Kurner, M. Koch, and T. Kleub-Ostman, “300 GHz transmission system,” *Elect. Lett.*, Vol. 44, Issue 3, pp. 213–214, 2008.

65. M. Koch, “Terahertz communication: a vision 2020,” In: NATO Security through Science Series: Terahertz Frequency Detection and identification of Materials and Objects. Ed., Springer, Germany, pp. 325–338, 2000.

66. A. Sharma, V. K. Dwivedi, and G. Singh, “THz rectangular patch microstrip antenna design using photonic crystal as substrate,” Prog. in Electromagn. Res. Symp., Cambridge, USA, Jul. 2–6, 2008, pp. 161–165.

67. G. Singh, “Design consideration for rectangular microstrip patch antenna on electromagnetic crystal substrate at terahertz frequency,” *Infrared Physics and Technology,* Vol. 53, Issue 1, pp. 17–22, 2010.

68. Y. Munemassa, M. Mitra, T. Takanao, and M. Sano, “Lightwave antenna with a small aperture manufactured using MEMS processing technology,” *IEEE Trans. Antennas Propag.,* Vol. 55, Issue 11, pp. 3046–3051, 2007.

69. M. Rebiez, “Millimeter-wave and terahertz integrated circuit antennas,” Proc. of the IEEE, Vol. 80, pp. 1748–1770, Nov. 1992.

70. D. S. Hernandez and I. Robertson, “Integrated antennas for terahertz circuits,” IEE Colloquium on Terahertz Technology, pp. 1–7, 1995.

71. T. Li, M. Mastro, and A. Dadgar, *III–V Compound semiconductors - Integration with silicon-based microelectronics*, 1st edition, CRC Press, Inc., 2011.

72. G. T. Kovacs, N. L. Maluf, K. E. Petersen, “Bulk micromachining of silicon,” in Proceedings of IEEE, Aug. 1998, Vol. 86, Issue 8, pp. 1536-1551.

73. R. N. Dean, Jr., P.C. Nordine and C. G. Christodoulou, “ 3-D helical THz antennas”, *Microwave and Optical Technology Letters*, pp. 106–111, Jan. 2000.

74. N. Chong and H. Ahmed, “Antenna-coupled polycrystalline silicon airbridge thermal detector for mid-infrared radiation,” *Appl. Phys. Lett.,* Vol. 71, Issue 12, pp. 1607–1609, 1997.

75. D. P. Neikirk et al, “Imaging antenna array at 119 μm,” *Appl. Phys. Lett.,* Vol. 41, Issue 4, pp. 329–331, Aug. 1982.

76. G. M. Rebeiz et al, “Monolithic millimeter-wave two-dimensional horn imaging array,” *IEEE Trans. Antennas Propagat.,* Vol. 28, pp. 1473–1482, Sept. 1990.

77. R. A. York and Z. B. Popovic, Ed., *Active and Quasi-Optical Arrays for Solid-State Power Combining,* New York: John Wiley & Sons, 1997.

78. G. M. Rebeiz, “Millimeter-wave and terahertz integrated circuit antennas,” in Proceedings on the IEEE, 1992, Vol. 80, pp. 1748-1770.

79. L. Guo, F. Huang, and X. Tang “A novel integrated MEMS helix antenna for terahertz applications,” *Optik*, pp. Vol. 125, Issue 1, pp. 101-103, Jan. 2014.

80. L. Guo, F. Huang, and X. Tang, “Design of MEMS on-chip helical antenna for THz application,” in IEEE MTT-S International MWS-AMP for RF and THz Application, Chengdu, China. Oct. 2016, Vol. 56, Issue 8, pp. 15-18.

81. P.H. Siegel, P. de Maagt, and A. I. Zaghloul, “Antennas for terahertz applications,” in IEEE Antennas and Propagation Society International Symposium, Albuquerque, NM, USA, Jul. 2006, pp.2383–2386.

82. A. F. Morabito, A. R. Lagana, and T. Isernia, “Isophoric array antennas with a low number of control points: a 'size tapered' solution,” *Progress In Electromagnetics Research Letters*, Vol. 36, pp. 121-131, 2013.

83. X. H. Lai et al, “Suspended nanoscalesolenoid metal inductor with tens-nH level inductance,” in IEEE 21st International Conference on MEMSYS, Wuhan, China, Jan. 2008, pp. 1000–1003.

84. C. Li, K. Ding, W.G. Wu, and J. Xu, “Ultra-fine nanofabrication by hybrid of energeticion induced fluidization and stress,” in IEEE 24th International Conference on MEMSYS, Cancun, Mexico, Mar. 2011, pp. 340–343.

85. G. T. Kovacs, N. L. Maluf, K. E. Petersen, “Bulk micromachining of silicon,” in Proceedings of IEEE, Aug. 1998, Vol. 86, Issue 8, pp. 1536-1551.

86. A. Boudkhil, M. Chetioui, N. Benabdallah, and N. Benahmed, “Development and performance enhancement of MEMS helix antenna for THz applications using 3D HFSS-based efficient electromagnetic optimization,” *TELKOMNIKA*, Vol. 16, Issue 1, pp. 206-210, Feb. 2018.

87. D. E. Goldberg, *Genetic Algorithms in Search, Optimization, and Machine Learning. Reading*, Addison-Wesley, 1989.

88. K. E. Kinnear, *Advances in Genetic Programming*, Cambridge: MIT Press. 1994.

89. D. S. Weile and E. Michielssen, "Genetic algorithm optimization applied to electromagnetics: A review," *IEEE Trans Antennas Propag.*, Vol. 45, pp. 343–353, 1997.

90. A. Boudkhil, M. Chetioui, N. Benabdallah, A. Ouzzani, and N. Benahmed, "A novel design of THz MEMS Λ-Helix antenna using HFSS-based effective stochastic solvers," in the 4th IEEE International Conference of Optimization Applications (ICOA), Apr. 26-27, Mohammedia, Morocco, 2018.

91. S. Haykin, *Neural Networks: A comprehensive Foundation*, Prentice Hall of India, July 1998.

92. Q. Zhang, C. K. Gupta, and K. Devabhaktuni, "Artificial Neural Networks for RF and microwave design—From theory to practice" *IEEE Transactions on Microwave Theory and Technique*, Vol. 51, Issue 4, Apr. 2003.

93. M. Chetioui, A. Boudkhil, N. Benabdallah, and N. Benahmed, "Design and analysis of Ku/K-band circular SIW patch antenna using 3D EM-based artificial neural networks," *TELKOMNIKA*, Vol. 16, Issue 2, pp. 594-599, Apr. 2018.

94. M. Chetioui, A. Boudkhil, N. Benabdallah, and N. Benahmed, "Design and optimization of SIW patch antenna for Ku band applications using ANN algorithms," in the 4th IEEE International Conference of Optimization Applications (ICOA), Apr. 26-27, Mohammedia, Morocco, 2018.

95. M. Chetioui, **A.** Boudkhil, N. Benabdallah, and N. Benahmed, "A novel dualband coaxial-fed SIW cavity resonator antenna using ANN modeling," *Journal of Engineering Science and Technology Review*, Vol. 11, Issue 2, pp. 82 – 87, May. 2018.

96. T. Y. Kwok and D. Y. Yeung, "Constructive algorithms for structure learning in feedforward neural networks for regression problems," *IEEE Trans. Neural Networks*, Vol. 8, pp. 630–645, May 1997.

97. Q. J. Zhang and K. C. Gupta, *Neural Networks for RF and Microwave Design*. Norwood, MA: Artech House, 2000.

98. A. Boudkhil, M. Chetioui, N. Benabdallah, A. Ouzzani, and N. Benahmed, "A compact integrated THz horn-shaped helix antenna based on MEMS technology using accurate automatic strategists," accepted in the International Conference on Applied Mathematics in Engineering (ICAME), Jun. 27-29, Balikesir, Turkey, 2018.

99. A. Boudkhil, M. Chetioui, N. Benabdallah, and N. Benahmed, "An optimal dualband pyramidal helix antenna based on MEMS technology for THz applications using GA and ANN techniques," submitted to *International Journal on Electrical Engineering and Informatics*, Jun. 2018.

100. B. Khuntia, S. S. Pattnaik, D. C. Panda, D. K. Neog, S. Devi, and M. Dutta, "Genetic Algorithms with Artificial Neural Network as its Fitness Function to Design Rectangular Microstrip Antenna on Thick Substrate", Microwave and Optical Technology Letters, Vol. 44 (2), Jan 2005.

Abstract

This research work provides for the THz wireless access systems novel designs of highly miniaturized helix antennas based on MEMS technology with particular emphasis on major optimization challenges facing the device structure complexity. The different antenna geometrical structures are developed using 3D high frequency structure simulator (HFSS) based on efficient computational techniques for modal analysis and active optimization. Each time, the optimization strategy aims to vary the antenna geometric structure and maximize its EM response with a high accuracy for the selective frequency band by training the samples and minimizing the error from Finite Element Method- (FEM) based simulation tool. Excellent antenna performance and high structure precision are finally achieved by modifying and rectifying different parameters embedded in silicon platform including the helix and feeding variables using reliable evolutionary optimizers, effective stochastic solvers and accurate automatic strategists for conceiving high-performance THz MEMS helix antennas.

Key words: Integrated antennas, Terahertz (THz) applications, Micro-electromechanical system (MEMS) technology, computational electromagnetic (EM) optimization, evolutionary/stochastic/automatic strategists.

ملخص

يقدم هذا البحث لأنظمة تيراهيرتز اللاسلكية تصميمات مبتكرة عالية الدقة لهوائيات حلزونية (لولبية) باستعمال تكنولوجيا الأنظمة الكهروميكانيكية الجزئية و التركيز على تحديات التحسين الأساسية التي تواجه هيكلة الجهاز المعقدة، مختلف الهياكل الهندسية للهوائيات تم تصميمها باستخدام برنامج ثلاثي الأبعاد لمحاكاة الهياكل عالية التردد اعتمادا على تقنيات حوسبة كهرومغناطيسية فعالة من أ جل تحليل نشط و تحسين أمثل، في كل مرة، تهدف إستراتيجية التحسين المتبعة لتغيير بنية الهوائي الهندسية وزيادة استجابته الكهرومغناطيسية بدقة عالية حسب نطاق التردد المختار من خلال تدريب العينات وتقليل الأخطاء باستعمال طريقة العناصر المحددة، و في الأخير تم الحصول على أداء ممتاز ودقة بنية عالية للهوائي عن طريق تعديل وتصحيح عدةأبعاد مختلفة متضمنة في قاعدة السليكون بما في ذلك مقاييس اللولب و الإمداد باستخدام أدوات تحسين تطورية،معالجات ستوكاستيكية فعالة، و استراتيجيات أوتوماتيكية دقيقة

الكلمات المفتاحية: الهوائيات المتكاملة، تطبيقات تيراهيرتز، تكنولوجيا الأنظمة الكهروميكانيكية الجزئية، التحسين الكهرومغناطيسي الحاسوبية،لاستراتيجيات التطورية / الستوكاستيكية / الأوتوماتيكية.

Résumé

Ce travail de recherche fournit aux systèmes d'accès sans fil térahertz de nouveaux modèles d'antennes hélicoïdales hautement miniaturisées basées sur la technologie des systèmes micro-électromécaniques (SMEM), avec un accent particulier sur les principaux défis d'optimisation face à la complexité de la structure du dispositif. Les différentes structures géométriques d'antennes ont été développées en utilisant un 3D simulateur de structure haute fréquence (SSHF) basé sur des techniques de calcul efficaces pour une analyse modale et une optimisation active. A chaque fois, la stratégie d'optimisation vise à faire varier la structure géométrique de l'antenne et à maximiser sa réponse électromagnétique avec une grande précision pour la bande de fréquences sélective en entraînant les échantillons et en minimisant l'erreur par l'utilisation de la méthode des éléments finis. Une excellente performance et une grande précision de structure pour l'antenne sont finalement obtenues en modifiant et rectifiant plusieurs paramètres intégrés dans la plate-forme de silicium y compris les variables d'alimentation et d'hélice en utilisant des optimiseurs évolutionnaires fiables, des solveurs stochastiques efficaces et des stratèges automatiques précis pour concevoir des antennes hélices à haute performance.

Mots clés: Antennes intégrées, Applications térahertz (THz), Technologie des systèmes micro-électromécaniques (SMEM), Optimisation électromagnétique (EM), Stratégistes évolutionnaire/stochastiques/automatiques.